

STRUCTURAL GEOLOGY OF THE SOUTHWESTERN SHORE  
OF CONCEPTION BAY, EASTERN AVALON ZONE,  
NEWFOUNDLAND APPALACHIANS

CENTRE FOR NEWFOUNDLAND STUDIES

**TOTAL OF 10 PAGES ONLY  
MAY BE XEROXED**

(Without Author's Permission)

CLAUDIA PAZ RIVEROS



## INFORMATION TO USERS

This manuscript has been reproduced from the microfilm master. UMI films the text directly from the original or copy submitted. Thus, some thesis and dissertation copies are in typewriter face, while others may be from any type of computer printer.

**The quality of this reproduction is dependent upon the quality of the copy submitted.** Broken or indistinct print, colored or poor quality illustrations and photographs, print bleedthrough, substandard margins, and improper alignment can adversely affect reproduction.

In the unlikely event that the author did not send UMI a complete manuscript and there are missing pages, these will be noted. Also, if unauthorized copyright material had to be removed, a note will indicate the deletion.

Oversize materials (e.g., maps, drawings, charts) are reproduced by sectioning the original, beginning at the upper left-hand corner and continuing from left to right in equal sections with small overlaps. Each original is also photographed in one exposure and is included in reduced form at the back of the book.

Photographs included in the original manuscript have been reproduced xerographically in this copy. Higher quality 6" x 9" black and white photographic prints are available for any photographs or illustrations appearing in this copy for an additional charge. Contact UMI directly to order.

# UMI

A Bell & Howell Information Company  
300 North Zeeb Road, Ann Arbor MI 48106-1346 USA  
313/761-4700 800/521-0600





**STRUCTURAL GEOLOGY OF THE  
SOUTHWESTERN SHORE OF CONCEPTION BAY,  
EASTERN AVALON ZONE, NEWFOUNDLAND APPALACHIANS**

by

**Claudia Paz Riveros**

**A thesis submitted to the School of Graduate Studies in partial fulfillment of the requirements  
for the degree of Master of Science**

**Department of Earth Sciences, School of Graduate Studies / Faculty of Science  
Memorial University of Newfoundland**

**© Claudia P. Riveros**

**March, 1998**

**St. John's**

**Newfoundland**



**National Library  
of Canada**

**Acquisitions and  
Bibliographic Services**

**395 Wellington Street  
Ottawa ON K1A 0N4  
Canada**

**Bibliothèque nationale  
du Canada**

**Acquisitions et  
services bibliographiques**

**395, rue Wellington  
Ottawa ON K1A 0N4  
Canada**

*Your file Votre référence*

*Our file Notre référence*

**The author has granted a non-exclusive licence allowing the National Library of Canada to reproduce, loan, distribute or sell copies of this thesis in microform, paper or electronic formats.**

**The author retains ownership of the copyright in this thesis. Neither the thesis nor substantial extracts from it may be printed or otherwise reproduced without the author's permission.**

**L'auteur a accordé une licence non exclusive permettant à la Bibliothèque nationale du Canada de reproduire, prêter, distribuer ou vendre des copies de cette thèse sous la forme de microfiche/film, de reproduction sur papier ou sur format électronique.**

**L'auteur conserve la propriété du droit d'auteur qui protège cette thèse. Ni la thèse ni des extraits substantiels de celle-ci ne doivent être imprimés ou autrement reproduits sans son autorisation.**

**0-612-34221-2**

## ABSTRACT

The Newfoundland Avalon Zone of the eastern Appalachians has, for many years, been affected by two major tectonic events: the late Proterozoic Avalonian Orogeny, which occurred prior to the final collision of the Gondwanan and Laurentian continents, and the mid-Paleozoic Acadian Orogeny, associated with the final accretion of the Gondwanan to Laurentian continents. Recent geochronological data show, however, that the Avalon Zone was affected by multiple late Proterozoic thermal events (ca. 760 Ma, ca. 680 Ma, ca. 630-600 Ma and ca. 575-550 Ma) and by the Paleozoic Salinic and Alleghenian-Hercynian orogenies.

Systematic constraints on the structural characteristics of these tectonic events are lacking in the Avalon Zone. The present study addresses this problem via a detailed investigation of the structural and stratigraphic relationships observed along the southwestern shore of the Conception Bay, eastern Avalon Zone. The cross-cutting relationships between a pervasive regional ( $S_2$ ) cleavage and structures truncated by the sub-Cambrian unconformity are used to distinguish between  $D_1$  Proterozoic and  $D_2$  post-Cambrian structures. Distinctive structural characteristics observed through the study site are used, further, to identify four distinctive styles and relative ages of deformation;  $D_{1a}$ ,  $D_{1b}$ ,  $D_{2a}$  and  $D_{2b}$ .

$D_{1a}$  and  $D_{1b}$  reflect two phases of deformation associated with the Avalonian Orogeny. Both appear to have occurred in a late period of this prolonged and diachronous orogenic event.  $D_{1a}$  is a block faulting extensional event that produced north-trending block faults. These have produced the north-trending Brigus and Holyrood horsts. This "brittle" deformational event produced few identifiable mesoscale features and no cleavage.

$D_{1b}$  was a north-south shortening event.  $D_{1b}$  structures include northwest-trending dextral kink band sets and northeast-trending sinistral kink band sets, northwest- and northeast-trending open to isoclinal  $F_1$  folds, and regional dome and basin and periclinal structures. Some of the faults that underwent normal displacement during  $D_{1a}$  were reactivated as strike-slip faults during  $D_{1b}$ . North- to north-northeast-trending faults (e.g., Brigus, Marysvalle and Topsail faults) underwent apparent sinistral strike slip and north-northwest-trending faults (e.g., Bacon Cove, Duffs and Holyrood faults) underwent apparent dextral

strike slip during  $D_{1b}$ . A cleavage ( $S_1$ ) is commonly developed in discrete zones in tight to isoclinal  $F_1$  folds, but is regionally non-penetrative. This restricted development of  $S_1$  reflects the semi-brittle deformational regime of  $D_{1b}$  (moderate to low temperature and mean stress conditions).

$D_{2a}$  represents a mid-Paleozoic contractional event related to the Acadian and/or Salinic orogenies.  $D_{2a}$  is characterized by a pervasive, generally upright cleavage ( $S_2$ ) that indicates east-west contraction. Upright, open, north- to north-northeast-trending folds ( $F_2$ ) overlie east- and west-directed thrust and reverse faults. Some of these  $D_{2a}$  faults are inverted  $D_1$  structures. Cambrian beds preserved in the core of  $F_2$  synclines and in inverted  $D_{1a}$  horsts provide the only direct age constraint (post early Cambrian) on the  $D_{2a}$  structures.  $S_2$  can transect the  $F_2$  axial traces by up to 15° in plan view. It is inferred that the  $F_2$  fold trends are strongly influenced by the orientation of the associated faults (formed during earlier deformational events), whereas the  $S_2$  cleavage more directly reflects the  $D_{2a}$  east-west shortening.

The bedding of Cambrian rocks and  $S_2$  display similar rotations adjacent to some of the north-trending faults. Cambrian rocks are preserved in  $D_{2b}$  down-faulted blocks. These features are interpreted to indicate post- $S_2$  normal fault separation on reactivated  $D_{1a}$  and/or  $D_{2a}$  faults. There is also post- $S_2$  apparent sinistral and dextral strike-slip along minor northwest-trending faults in Cambrian rocks. Collectively, these fault movements are interpreted to indicate northwest-southeast oriented extension during  $D_{2a}$ . These structures could be associated with the mid-Devonian to early Permian Alleghenian-Hercynian orogeny and/or opening of the North Atlantic during the Mesozoic.

*Dedicated to Benjamin and Sylvia*



## **ACKNOWLEDGMENTS**

I am grateful to my supervisors Jamie Jamison and Peter Cawood, who provided me with this study opportunity and whose constructive criticism and unquestionable patience guided this study to existence. Funding for this study came from their NSERC operating grants.

I am also thankful to Adam Szybinski and Hank Williams for their meticulous review of a draft of the thesis, as well as to Art King, Jeroen van Gool, John Ketchum, Dave Corrigan and Kate MacLachlan for insightful discussions on various aspects of the study. Gitte Aage and Alan Cull are thanked for their assistance and companionship in the field.

I am grateful to Lyla Riveros for a grammatical review of the thesis. I also thank Michael Settingerton for his dynamic and withstanding support.

## TABLE OF CONTENTS

ABSTRACT .....	i
ACKNOWLEDGMENTS .....	iv
TABLE OF CONTENTS .....	v
LIST OF TABLES .....	viii
LIST OF FIGURES .....	viii
1. INTRODUCTION .....	1
1.1 Preamble .....	1
1.2 Regional Geology of the Avalon Zone .....	3
1.3 Geological Setting of the Avalon Peninsula .....	7
1.4 Tectonic Expression of the Avalon Zone .....	9
1.4.1 Unconformities in the Avalon Zone: Relationships and Problems .....	11
1.5 Study Objectives .....	15
1.6 Study Site .....	16
2. STRUCTURAL GEOLOGY OF THE STUDY SITE .....	20
2.1 Introduction .....	20
2.2 Geology of the Study Site .....	21
2.2.1 Brigus Area .....	25
2.2.2 Marysvale Area .....	29
2.2.3 Bacon Cove Area .....	29

2.2.4 Salmon Cove Area .....	35
2.2.5 Chapels Cove Area .....	41
2.3 The Sub-Cambrian Unconformity Used as an Age Control for Deformation.....	41
2.3.1 D <sub>1</sub> Pre-Cambrian Structures.....	45
2.3.1.1 F <sub>1</sub> Folds and Associated Faults .....	45
2.3.1.2 D <sub>1</sub> Normal Faults.....	56
2.3.2 D <sub>2</sub> Post-Cambrian Structures.....	60
2.3.2.1 F <sub>2</sub> Folds and Associated Faults .....	60
2.3.2.2 D <sub>2</sub> Reverse, Oblique-slip and Thrust Faults .....	65
2.3.2.3 D <sub>2</sub> Normal Faults.....	68
2.3.3 Criteria Established to Distinguish D <sub>1</sub> from D <sub>2</sub> Structures.....	74
2.4 Zones Without the Sub-Cambrian Unconformity as an Age Control for Deformation.....	75
2.4.1 D <sub>1</sub> Pre-Cambrian Structures.....	75
2.4.1.1 F <sub>1</sub> Folds and Associated Faults .....	75
2.4.1.2 D <sub>1</sub> Strike-slip Faults .....	81
2.4.1.3 D <sub>1</sub> Kink Bands .....	84
2.4.2 D <sub>2</sub> Post-Cambrian Structures.....	93
2.4.2.1 F <sub>2</sub> Folds and Associated Faults .....	93
2.4.2.2 D <sub>2</sub> Strike-Slip Faults.....	95
3. STRUCTURAL EVOLUTION OF THE STUDY SITE — A MODEL.....	97
3.1 Introduction .....	97
3.2 Model.....	103

3.2.1 D <sub>1a</sub> Block Faulting Extensional Event.....	103
3.2.2 D <sub>1b</sub> Conjugate Kink Band Contractional Event.....	104
3.2.3 D <sub>2a</sub> S <sub>2</sub> Cleavage Contractional Event.....	106
3.2.4 D <sub>2b</sub> Block Faulting Extensional Event.....	108
3.3 Validity of Model — A Discussion.....	109
4. DISCUSSION AND CONCLUSIONS .....	115
4.1 Discussion .....	115
4.2 Conclusions.....	117
LITERATURE CITED .....	119

## **LIST OF TABLES**

Table 1.1 Summary table of the rocks of the onland Newfoundland Eastern Avalon Zone, and the orogenies that have affected them.....	6
---	---

## **LIST OF FIGURES**

Figure 1.1 Sketch map of the North Atlantic Avalonian-Cadomian-Pan African belt and Appalachian-Caledonian orogenic belt.....	2
Figure 1.2 Simplified geological map of the Newfoundland Avalon Zone.....	4
Figure 1.3 Simplified geological map of the southwestern shore of Conception Bay and the study site.....	17
Figure 2.1 A typical section of lower Cambrian and earliest middle Cambrian sequences, Brigus area.....	22
Figure 2.2 Harbour Main Group lapilli tuffs, Brigus area.....	23
Figure 2.3 Lower Conception Group turbidite sequence, Brigus area.....	24
Figure 2.4 Geological map of the Brigus area.....	26
Figure 2.5 Cross-section of the Brigus area.....	28
Figure 2.6 Geological map of the Marysvale area.....	30
Figure 2.7 Cross-section of the Marysvale area.....	31
Figure 2.8 Geological map of the Bacon Cove area. ....	32
Figure 2.9 Cross-section of the Bacon Cove area. ....	34
Figure 2.10 Geological map of the Salmon Cove area.....	36
Figure 2.11 Cross-section of the Salmon Cove area.....	38
Figure 2.12 Intra-Harbour Main Group erosional surface. ....	40



Figure 2.13 Geological map of the Chapels Cove area.....	42
Figure 2.14 Cross-section of the Chapels Cove area.....	43
Figure 2.15 The sub-Cambrian unconformity at Seal Head, Brigus area. ....	44
Figure 2.16 The sub-Cambrian unconformity in the Bacon Cove area. ....	46
Figure 2.17 Geological map of the Seal Head area, Brigus area.....	47
Figure 2.18 Cross-section of the Seal Head area, Brigus area.....	48
Figure 2.19 Overturned, east-verging $F_1$ anticline pair in the Harbour Main Group, Seal Head, Brigus area. ....	50
Figure 2.20 Summary stereo plots and sketch of $F_1$ folds in the Harbour Main Group, Seal Head, Brigus area. ....	51
Figure 2.21 $F_1$ and axial plane $S_1$ cleavage in the Harbour Main Group, Seal Head, Brigus area. ....	53
Figure 2.22 Open, box-style, west-verging and south-plunging $F_1$ folds in the Conception Group, Bacon Cove area. ....	54
Figure 2.23 Summary stereo plots of $F_1$ and $F_2$ folds in the Bacon Cove area. ....	55
Figure 2.24 Detailed map of $F_1$ folds and the Brigus fault zone in the Brigus area. ....	57
Figure 2.25 Harbour Main Group and Conception Group horses along the Brigus fault zone.....	58
Figure 2.26 $F_2$ folds and $S_2$ axial plane relationships at North Head, Brigus area. ....	61
Figure 2.27 The Salmon Cove fault and adjacent deformation in Cambrian beds. ....	64
Figure 2.28 Photomicrographs of $S_2$ in a conglomerate of the Conception Group adjacent to the Bacon Cove fault. ....	66
Figure 2.29 The Long Pond normal fault in the Brigus area. ....	69
Figure 2.30 The North Head shallow normal fault at North Head, Brigus area. ....	70

Figure 2.31 A photomicrograph of a c-s shear fabric of the North Head normal fault showing east-directed movement on the fault. ....	72
Figure 2.32 The Pebble normal fault in the Chapels Cove area.....	73
Figure 2.33 Summary stereo plots of $F_1$ folds in Domain II and Zone C in the Brigus area. ....	77
Figure 2.34 Sketches illustrating the cross-cutting relationships between $F_1$ , $S_1$ and $S_2$ in the Conception Group, Bacon Cove area.....	79
Figure 2.35 $F_1$ flexural slip fold, Bacon Cove area. ....	80
Figure 2.36 Sketch showing kink band relationships and morphologies. Summary stereo plots of an $F_1$ syncline and a dextral kink band set, Zone A, Brigus area. ....	86
Figure 2.37 Dextral kink band set in argillaceous Conception Group units, Zone A, Brigus area. ....	87
Figure 2.38 Dextral kink band set in argillaceous Conception Group units, Zone B, Brigus area. ....	89
Figure 2.39 Sinistral kink band set in argillaceous Conception Group units, Zone D, Marysvale area. ....	91
Figure 2.40 Conjugate kink band set in argillaceous Conception Group units, Zone D, Marysvale area. ....	92
Figure 3.1 Structural evolution model of the study site and Avalon Peninsula.....	99
Figure 3.2 Schematic diagram showing the relative stratigraphic, tectonic and time relationships between the pre- $D_{1a}$ , $D_{1a}$ and $D_{1b}$ deformational events. ....	102

# **1. INTRODUCTION**

## **1.1 Preamble**

The Avalon Zone (Williams 1976, 1978), also known as the Avalon terrane (Williams and Hatcher 1982) and Avalon composite terrane (Keppie 1985), is the most extensive and widest tectonostratigraphic division of the Appalachian Orogen. It was once part of the late Proterozoic Avalonian-Cadomian-Pan African orogenic belt in the offshore of the Gondwanan supercontinent (D'Lemos et al. 1990). It presently extends up to 700 km to the edge of the Grand Banks, southeast of Newfoundland (Lilly 1966; Haworth and Lefort 1979), southwestward to the eastern United States and to correlatives in northwest France, Spain and parts of Britain and Morocco (Rast et al. 1976; Rast and Skehan 1983; Dallmeyer et al. 1983) (Fig. 1.1).

In much of the northeastern Appalachians, rocks of the Avalon Zone are separated along major ductile transcurrent shear zones from rocks of the adjacent Gander Zone to the west and the Meguma Zone to the east (Irving 1979; van der Voo et al. 1979; Gibbons 1990). The north-northeast-trending Dover-Hermitage Bay fault zone separates the low metamorphic grade Avalon Zone from the medium to high metamorphic grade Gander Zone, which underwent ductile deformation in the Silurian and brittle deformation in the Devonian (Blackwood and Kennedy 1975; Blackwood and O'Driscoll 1976; Dallmeyer et al. 1981; Kennedy et al. 1982) (Fig. 1.2). The Dover-Hermitage Bay fault zone has been modeled seismically as a vertical structure that penetrates the entire crust (Marillier et al. 1989).

The Newfoundland Avalon Zone has continental chemical affinities (Papezik 1970; King 1990; Williams et al. 1995). The little known about an underlying basement block comes from mainly isotopic data (Krogh et al. 1988) and partly from the composition of the late Proterozoic volcanic sequences of the Harbour Main Group and equivalents, which ranges from basaltic to rhyolitic (Nixon and Papezik 1979; King 1990; O'Brien et al. 1992).

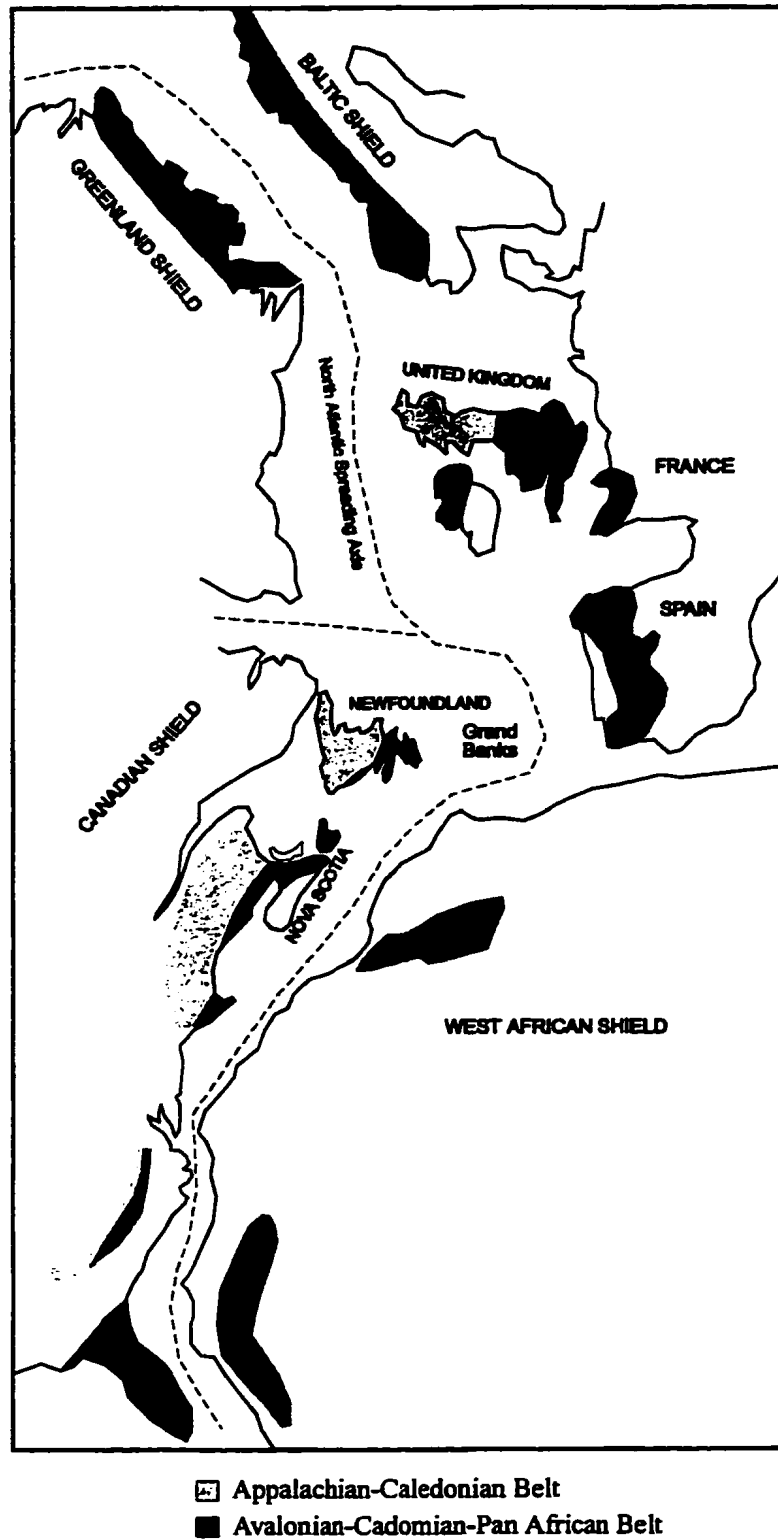


Fig. 1.1 An early Mesozoic pre-drift reconstruction sketch map of the North Atlantic borderlands showing the approximate extent of the Avalonian-Cadomian-Pan African belt and Appalachian-Caledonian orogenic belt (modified from Williams 1984 and Skehan 1988).

Late Proterozoic rocks (685–670 Ma) are part of a complex that is basement to Dunnage Zone strata in the Hermitage Flexure (Fig. 1.2 inset map), and basement to rocks of equivalent age and facies to the Harbour Main Group in the Connaigre Peninsula (Fig. 1.2) (O'Brien and O'Brien 1990; O'Brien et al. 1991; 1996).

Devonian and possibly early Silurian sedimentary and volcanic facies of the Avalon Zone resemble those formed across the Appalachians, suggesting that by this time, the Avalon and Gander zones were connected (O'Brien et al. 1983). The Ackley Granite (dated at  $\geq 410$  Ma, 378 – 374 Ma and 355 Ma by Kontak et al. 1988) intrudes across the Avalon and Gander zones, which further suggests that collision between the two zones occurred at least prior to 410 Ma. In addition, late Proterozoic fluvial/alluvial deposits, characteristic to the Avalon Zone, were not formed in the adjacent Gander Zone, indicating that both zones were two distinctive blocks that were juxtaposed after late Proterozoic time.

## **1.2 Regional Geology of the Avalon Zone**

The geology of the Avalon Zone is characterized by late Proterozoic activity of bimodal vulcanism and associated plutonism and sedimentation; deep marine and terrestrial sedimentation and associated igneous activity; and the unconformable onlap of a regional Cambrian-Ordovician transgressive platformal sequence.

Cambrian-Ordovician sequences comprise mainly mudstones, siltstones, shales, limestones and sandstones, with body and trace fossils of the Acado-Baltic province (Hutchinson 1962). The Cambrian miogeosynclinal sequence varies in thickness from 300 metres to 1.2 kilometres and occurs in synclinal or down-faulted scattered exposures across the Avalon Zone, mainly on the Avalon and Burin peninsulas, to the west of Trinity Bay and north of Fortune Bay (Fig. 1.2). Early Ordovician rocks occur in basins on the north shore of Fortune Bay and in Conception Bay (Fig. 1.2).

The earliest and most distinctive late Proterozoic tectonic unit is the Burin Group (U-Pb zircon date of about 763 Ma, Krogh et al. 1988) that crops out in a fault-bounded region



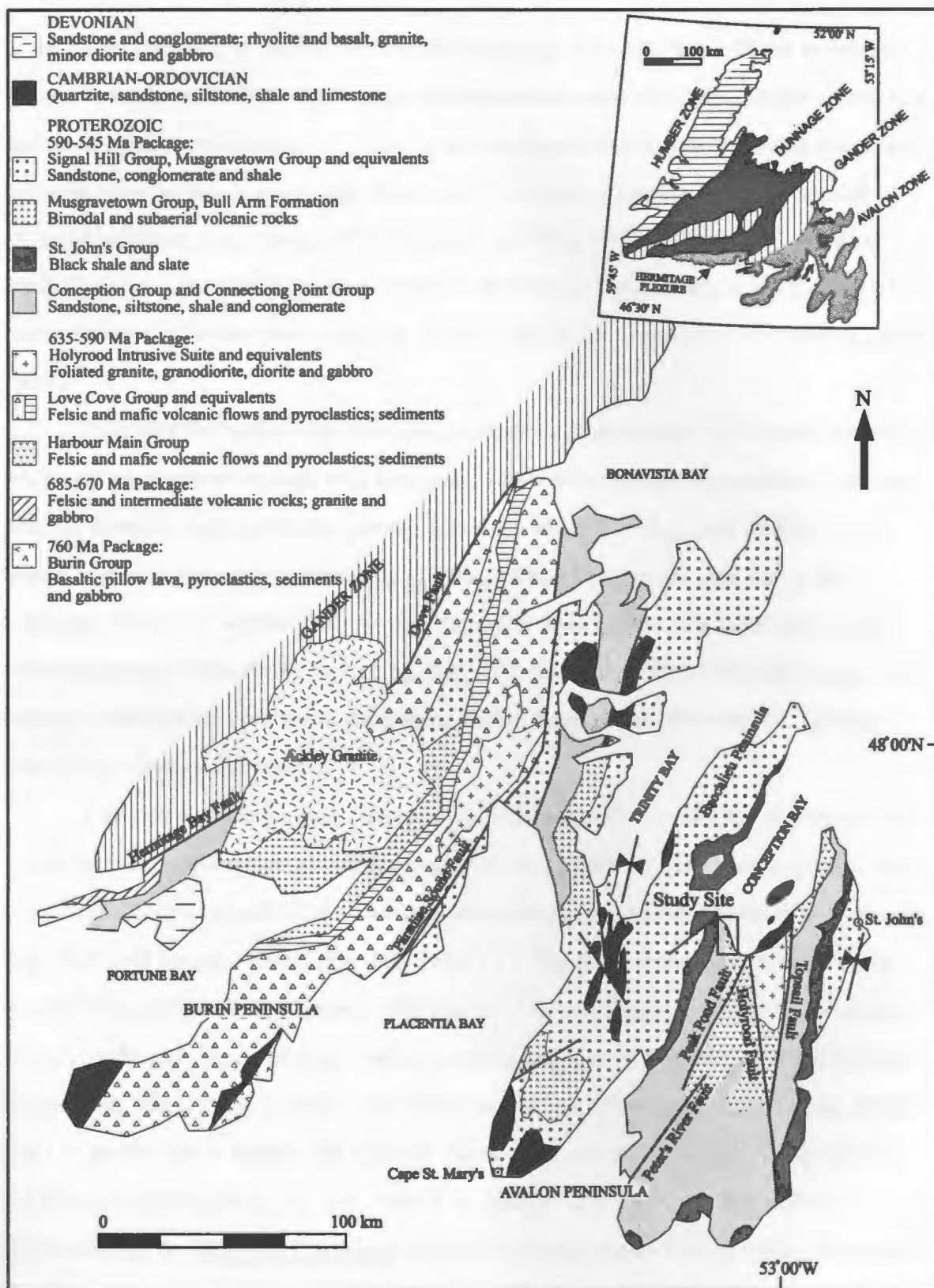


Fig. 1.2 Simplified geological map of the Avalon Zone in Newfoundland (taken from King 1990). Box shows location of the study site in the Avalon Peninsula. The inset map shows the location of the tectonostratigraphic zones of the Newfoundland Appalachians.

in the Burin Peninsula of the western Avalon Zone (Fig. 1.2). The Burin Group comprises submarine mafic volcanic rocks, oceanic gabbro intrusions and associated unique clastic and carbonate olistostromal sequences. These rocks are about 130 my older than and chemically different from the rest of the Avalon Zone late Proterozoic sequences, showing oceanic chemical affinities (e.g., Greene 1973; Strong et al. 1978a; 1978b). The older age of the Burin Group indicates that it is not correlative with the rest of the Avalon Zone, however, it is correlative with ophiolite units in the Pan African belts of the Gondwanan continent (LeBlanc 1981).

Following the earliest late Proterozoic tectonomagmatic event, a low-grade, arc-related felsic and intermediate volcanic rock formation (685 – 670 Ma) and an associated arc-root plutonic complex and amphibolite gneisses (dated at about 673 Ma) were formed in an overall contractional setting (O'Brien et al. 1992, 1996). These rocks crop out in the Connaigre Peninsula, southwestern Avalon Zone, and form a basement to unconformably overlying younger Proterozoic rocks (Fig. 1.2) (O'Brien et al. 1992). Rock packages of the first two events do not crop out in the eastern Avalon Zone and in the study site, and are therefore not further discussed.

The third tectonic package reflects a period between 635 to 590 Ma of widespread late Proterozoic, predominantly bimodal vulcanism (e.g., Harbour Main Group, part of the Love Cove Group and equivalents), marine sedimentation and coeval calc-alkaline plutonism (e.g., Holyrood Intrusive Suite) (Fig. 1.2, Table 1.1). The latest Proterozoic suite of rocks formed over a period of time between 590 and 545 Ma, and comprise peralkaline granites, volcanic rocks and associated deep marine to deltaic and to terrestrial siliciclastic sequences (King 1990). These rocks comprise the Conception Group, Connecting Point Group, deltaic rocks of the St. John's Group, and subaerial clastic rocks of the Signal Hill, Long Harbour and Musgravetown groups (Fig. 1.2, Table 1.1). Igneous activity during this period is represented by the Bull Arm Formation, part of the Musgravetown Group, which comprises bimodal volcanic rocks and associated Swift Current granite, with radiometric age dates ranging from about 548 Ma to 580 Ma (Dallmeyer et al. 1981).

Table 1.1 A summary table of the geology in the onland Avalon Zone, and the orogenies that have affected them (modified after Hutchinson 1962, McCartney 1967, and King 1988). Shaded areas depict rocks that occur in the study site.

Era	Period	Group & Thickness (m)	Formation & Thickness (m)	Lithology	
Meso- zoic	Triassic			diabase dykes	
LATE PALEOZOIC	Permian			absent in onland eastern Avalon Zone	HERCYNIAN
	Carboniferous			absent in onland eastern Avalon Zone	
	Devonian			Clarendville biotite granite; Powder Horn Complex & Iona Islands Suite-diorite, gabbro, minor granite	
	Silurian			diabase, diorite and gabbro sills	
EARLY PALEOZOIC	Mid- to Late-Ordovician			absent in onland eastern Avalon Zone	ACADIAN OROGENY
	Early Ordovician	Wabana Group 305 +		shale, sandstone, oolitic hematite black shale	
	minor disconformity				
	Late Cambrian- Early Ordovician	Bell Island Group 1200 +		sandstone, shale, oolitic hematite, quartzite	
	base not exposed				
	Middle-Late Cambrian	Harcourt Group 730+		grey-black shale, siltstone, limestone concretions, mafic pillow lava and pyroclastic rocks	
	disconformity				
	Early-Middle Cambrian	Adeyton Group 270+	Chamberlains Brook Formation 107+	grey-green slate and shale, thin limestone beds, manganiferous basal beds, spilitic cherty pillow lava	
	minor disconformity				
			Brigus Formation 23-130+	limestone nodular red and green shale and slate, thin limestone beds, basal conglomerate (if directly on Pre-cambrian rock)	
		Smith Point Formation 10 +	pink algal limestone, red limy argillite laminae		
		Bonavista Formation 0-28 +	red and green shale and slate, thin pink limestone beds, basal conglomerate		
		Random Formation 0-200+	orthoquartzite, green and red arkose and siltstone, minor conglomerate		
disconformity					
unconformity with the Musgravetown Group					

(continued)

Group & Thickness (m)		Formation & Thickness (m)	Lithology		
unconformity with the Harbour Main and Conception groups nonconformity with the Holyrood Intrusive Suite					
LATE PROTEROZOIC	UPPER UNITS			AVALONIAN OROGENY	
	Signal Hill & Musgravetown (up to 5000)		red, grey and green sandstone, conglomerate and shale		
		unknown			"Lilly unconformity"
		Swift Current granite			
		intrusive			
		Bull Arm Formation	felsic & mafic flows & pyroclastics, clastic sedimentary rocks		
		conformity/ disconformity			
	MIDDLE UNITS				
	St. John's Group (up to 2000)		black shale and slate		
		conformity			
	Conception & Connecting Point groups 3000+	Mistaken Point Formation 400+	green-grey shale & purple tuffaceous siltstone, shale & sandstone, fossiliferous beds towards the top		
		Briscall Formation	grey coarse sandstone, argillaceous siltstone & shale, red arkosic sandstone		
		Drook Formation 1500+	green argillaceous chert, siliceous siltstone & sandstone, silicified tuff		
		Gaskiers Formation 300+	grey tillite, red mixtite & mudstone		
		Mall Bay Formation	green siliceous siltstone, quartzose sandstone		
	LOWER UNITS				
	conformable and unconformable with the HMO nonconformable with the Holyrood Intrusive Suite				
		Holyrood Intrusive Suite- granite, diorite, gabbro			
Intrusive into Harbour Main Group					
Harbour Main & Love Cove groups 2000+		red, pink and grey ignimbrites, volcanogenic sedimentary rocks, dark green-purple massive amygdaloidal basal, pink and red rhyolite			
	unknown				

The tectonic setting for these suite of rocks may represent either a volcanic arc in a contractional regime or an intracratonic rift in an extensional regime (e.g., O'Brien et al. 1996).

### **1.3 Geological Setting of the Avalon Peninsula**

The Avalon Peninsula in the eastern Avalon Zone is the type area to the late 635 to 590 Ma Proterozoic rock package of the Harbour Main Group and associated Holyrood Intrusive Suite. The Avalon Peninsula is also the type area to the 590 to 545 Ma suite of rocks comprising the Conception, Connecting Point, St. John's, Signal Hill and Musgravetown groups.

The Harbour Main Group (Rose 1952) represents a complex suite of typically bimodal volcanic rocks and minor volcanoclastic sedimentary rocks. Vulcanism was emplaced over a wide area with ages ranging from about 635 to 590 Ma (Krogh et al. 1988), demonstrated by the change from subaerial to submarine conditions (e.g., Nixon and Papezik 1979). The nature of the basement of the Harbour Main Group is unknown.

The Holyrood Intrusive Suite (McCartney 1954) is a high-level intrusion (Hughes 1971), dominantly calc-alkaline granite and granodiorite, with minor quartz monzonite and gabbro (Table 1.1) that intrudes both volcanic and minor sedimentary rocks of the Harbour Main Group and reportedly intrudes into basal Conception Group sediments (Rose 1952). The Holyrood Intrusive Suite regionally contains a wide range of plutons, of which the Type Holyrood has an U/Pb zircon age of about 620 Ma (Krogh et al. 1988).

The Holyrood Intrusive Suite is interpreted as comagmatic with the volcanic rocks it intrudes (Hughes and Brückner 1971; Strong et al. 1978b; O'Driscoll and Strong 1979; O'Brien et al. 1990), with an unknown associated tectonic setting. Some workers argue that mineralogical and chemical data and petrochemical trends indicate that these rocks (635-590 Ma) formed in a continental, extensional tectonic environment, similar to the Basin and Range province, dominated by block faulting (Papezik 1970; Nixon and Papezik 1979). Others

argue that the intrusion is chemically similar to Andean-type granitoids (Hughes 1970, O'Driscoll and Strong 1979) and transitional between orogenic and non-orogenic environments.

The Conception Group (Rose 1952) typically comprises a thick succession of shales, siltstones and sandstones, and less abundant conglomerate, pyroclastic rocks, tillite, rare mafic pillow lavas and mafic dykes (Table 1.1). The youngest rocks of the Conception Group are 565 Ma in age (Benus *in* King 1990; from the top of the Ediacaran fossil-bearing Mistaken Point Formation). An absolute age within the base of the Conception Group is lacking. The abundance of tuff and other volcanic detritus throughout the Conception Group suggests that sedimentation was contemporaneous with vulcanism (O'Brien and Knight 1988, Knight and O'Brien 1988), possibly associated with the Harbour Main Group (Hughes and Brückner 1971).

The lower Conception Group proximal turbiditic rocks are interpreted to have been deposited in a basin margin, while upper Conception Group deep marine units are interpreted to have been deposited in an extensive deep marine basin floor (Gardiner and Hiscott 1988). Upper Conception Group deep marine rocks and pro-deltaic to shallow marine units of the St. John's Group reflect conformable deposition in a subsiding marine basin during a period of quiescence, followed by the deposition of the Signal Hill Group molasse-like clastic sequences (Table 1.1) (King 1990). The Conception, St. John's and Signal Hill groups and Bull Arm Formation show characteristics of a modern volcanic arc-marginal basin setting (Knight and O'Brien 1988). The source for basinal clastic deposits of the Conception, St. John's and Signal Hill groups are interpreted to have been derived from a "provinance high" to the north of the Avalon Peninsula (King 1979).

The Harbour Main Group and Holyrood Intrusive Suite occur in an elongate, north-trending structural high referred to as the Harbour Main Massif or Holyrood Horst (e.g., McCartney 1967, 1969), bounded to the east by the north-trending Topsail fault zone and to the west by a series of north-northeast-trending faults, including the Peter's River and Peak-Pond faults (Fig. 1.2). The Holyrood Intrusive Suite crops out in the Harbour Main Massif or



Holyrood Horst (McCartney 1967). Layered late Proterozoic rocks deformed to regional elongate domes and basins across the Avalon Peninsula (King 1988), in which the Bull Arm Formation crops out in one of these regional domes near Cape St. Mary's (Fig. 1.2).

## **1.4 Tectonic Expression of the Avalon Zone**

The juxtaposition of the Avalon and Gander zones during the closure of the Iapetus Ocean, and subsequent collision of the Gondwanan and Laurentian blocks (Humber Zone and adjacent Notre Dame subzone) in the Paleozoic Appalachian Orogen (Fig. 1.2 inset map), have traditionally been interpreted to reflect the accretionary event (Dallmeyer et al. 1981, 1983) of the mid-Paleozoic (Silurian-Devonian) Acadian Orogeny in Newfoundland (Williams and Hatcher 1982, Doig et al. 1990; Williams 1993), in which the peak low-grade metamorphic conditions occurred between 370-390 Ma (Dallmeyer et al. 1983). Recent data show that collision of the Avalon and Gander zones initiated during the Silurian Salinic Orogeny, which was dominated by sinistral accretion along the Hermitage Bay-Dover fault zone, based on paleomagnetic data (Doig et al. 1990), and was later reactivated by Acadian brittle deformation (O'Brien et al. 1996).

The Acadian Orogeny is recognized by undeformed late Devonian conglomerates unconformably overlying latest Proterozoic and Cambrian sequences with an angular discordance in the western Avalon Zone (Williams 1971). Carboniferous granites intrude late Devonian rocks and the Ackley Batholith (410-355 Ma) (Dallmeyer et al. 1983). Devonian rocks are absent in the eastern Avalon Zone. Acadian deformation has been interpreted to decrease in intensity eastward from central Newfoundland to the offshore Avalon Zone (Williams 1993).

Documentation of Salinic deformation in eastern Newfoundland is restricted to the Gander-Avalon zone boundary and is not well controlled in age across the Avalon Zone (Dunning et al. 1990; O'Brien et al. 1996). Silurian (440 Ma) magmatism is restricted to the emplacement of alkali basalt sills in the southwestern Avalon Peninsula (Greenough et al.

1993). These youngest strata on the Avalon Peninsula may have been deformed by the main Silurian events recorded farther west, and/or by Devonian deformation.

The mid-Devonian to early Permian Alleghenian-Hercynian Orogeny affected the maritime Avalon Zone (Rast and Grant 1973) with minimal effects in the Newfoundland Avalon Zone. The Alleghenian-Hercynian Orogeny is characterized by narrow fault-bounded areas bordered by broad areas of little or no deformation, associated with a strike-slip tectonic system (Williams 1995). The Alleghenian-Hercynian and Appalachian belts in North America are parallel and partly superimposed, and are therefore difficult to distinguish from each other in many areas.

Evidence for Triassic extension continuing at least until the early Cretaceous, in the Canadian maritime provinces is widespread (e.g., Roberts and Williams 1993; Wyn and Williams 1993; Greenough 1995) and is dominated by rift facies vertical tectonics of older high angle faults that have been reactivated (Roberts and Williams 1993). Mesozoic deformation is pervasive in the offshore Avalon Zone (e.g., Cutt and Laving 1977; Grant 1987), represented by diabase dykes and mafic volcanism (Papezik and Barr 1981), and is associated with the early rifting and drifting that led to the opening of the present Atlantic Ocean. Northeast-trending Triassic mafic dykes are the only known post-Carboniferous rocks in the onland Newfoundland Avalon Zone (Hodych and Hayatsu 1980) and are parallel to early Jurassic dykes that occur in the maritime provinces and eastern U.S. (Greenough 1995). These dykes indicate that the maximum extensional stress direction was oriented approximately northwest-southeast in the upper crust at the time of intrusion.

The late Proterozoic Avalonian Orogeny in the Newfoundland Avalon Zone is unrelated to the Paleozoic Appalachian orogenic event (e.g., O'Brien et al. 1990) and has been broadly correlated with the Cadomian Orogeny east of the Atlantic Ocean (e.g., D'Lemos et al. 1990). The Avalonian Orogeny has traditionally been recognized as a low metamorphic grade tectonostratigraphic event which affected late Proterozoic sedimentary and volcanic rocks over a poorly defined period of 50 to 100 Ma (Rose 1952; Lilly 1966; Poole 1967, McCartney 1967, 1969; Rodgers 1967, Brückner 1969; Hughes 1970). The

Avalonian Orogeny has been interpreted to be associated with a Proterozoic accretionary event (Williams et al. 1995). The Avalonian Orogeny is most obviously expressed by the sub-Cambrian unconformity across the Avalon Zone.

Late Proterozoic rocks have undergone a complex, prolonged and episodic geologic history in the Avalon Zone. In western Avalon Zone of the Hermitage Bay Peninsula, at least four Proterozoic depositional and tectonomagmatic events have been recognized: ca. 760 Ma, ca. 680 Ma, ca. 630-600 Ma, and ca. 575-550 Ma (O'Brien et al. 1990, 1992, 1996). These events occurred over a 200 Ma period, between the Grenvillian Orogeny and the onset of the Appalachian Orogenic Cycle, and are represented by unconformities or a hiatus within the late Proterozoic package. Whether these four distinctive events are part of the prolonged and heterogeneous Avalonian Orogeny is inconclusive.

#### **1.4.1 Unconformities in the Avalon Zone: Relationships and Problems**

Unconformities commonly represent a hiatus of erosion or non-deposition reflecting episodes of tectonism. Relevant to the study are the late Proterozoic 635-590 Ma and 590-545 Ma rock packages and therefore unconformities between and within these rock packages are discussed below. They include the sub-Conception Group unconformity, the sub-Signal Hill Group and equivalent sub-Musgravetown Group unconformity, and the sub-Cambrian unconformity.

The sub-Conception Group unconformity is manifest in a number of areas in the Avalon Peninsula (e.g., Rose 1952, McCartney 1967, Williams and King 1979, O'Brien 1972, O'Brien et al. 1997) with a marked angular discordance. Near Woodsford's, McCartney (1967) identified a folded angular unconformity between Conception Group sediments and underlying Harbour Main Group sedimentary and mafic volcanic rocks. West of Colliers Bay, in the southwestern shore of Conception Bay, Conception Group sequences of up to 2 metre thick unconformably overlie Harbour Main Group mafic volcanic flows (Rose 1972).

The unconformable contact between the Harbour Main and Conception groups has been interpreted to represent terminal Neoproterozoic Avalonian events (O'Brien et al. 1996).

However, the time span of at least 50 Ma to the end of deposition of the molasse facies Signal Hill Group implies that the Avalonian Orogeny must have been a prolonged sequence of events (e.g., Rice 1996).

The age of the basal Conception Group is unknown and could be older than 620 Ma (Krogh et al. 1983). In the Colliers Bay area, the (620 Ma) Type Holyrood Intrusive Suite would have unlikely intruded Conception Group rocks because they overlie post-610 Ma Harbour Main Group rocks. With this in mind, the oldest Conception Group rocks must be younger than the 610 Ma Harbour Main Group on which they unconformably overlie in the Avalon Peninsula. Yet, there is probably a significant hiatus between the Harbour Main Group and Conception Group deposition. The angular unconformity mapped between the two groups, along with the presence of Holyrood Intrusive Suite detritus in the Conception Group (King 1990), argues for pre-Conception Group tectonism affecting the Harbour Main Group and Holyrood Intrusive Suite, associated with the 630-600 Ma tectonic event.

The Harbour Main Group has also been reported to interdigitate with lower units of the Conception Group, of unknown age (Hughes and Brückner 1971, Williams and King 1979) (Table 1.1). An interdigitating contact implies that the deposition of the Conception Group was coeval with an active, adjacent magmatic arc for more than 30 Ma, manifest by tuffaceous interlayers in the volcanoclastic sediments, the petrography of sedimentary facies and the composition of detrital phases in the Conception Group (Dec et al. 1992).

This may further imply that the volcanic rocks of the 635 – 590 Ma package may represent a basement to the younger (590-545 Ma) sedimentary package. Both an unconformable and interdigitating contact between the Harbour Main and Conception groups reflects on the present lack of understanding of the nature of the contact.

Rocks of the 590–545 Ma package, were affected by inhomogeneous deformation and low-grade metamorphism across the Avalon Zone, reflecting a complex tectonic setting, in which magmatism began between 590 Ma and 580 Ma and continued until near the end of the Proterozoic (O'Brien et al. 1996). Angular unconformities within this rock package are locally exposed across the Avalon Zone. In the Avalon Peninsula, the Lilly Unconformity

(Anderson et al. 1975) developed between red breccia beds of the Piccos Brook Member of the upper Signal Hill Group and underlying, folded rocks of the Mannings Hill Member of the upper Drook Formation, Conception Group (Table 1.1).

In the western Avalon Zone, several other well defined late Proterozoic unconformities occur in sequences with broadly similar facies as the Signal Hill Group (Dallmeyer et al. 1983; O'Brien and Knight 1988). The sub-Musgravetown Group unconformity is expressed by the unconformable onlap of Musgravetown Group basal conglomerate-breccia over mafic volcanic rocks of the Love Cove Group (Fig. 1.2) (O'Brien and Knight 1988) and felsic volcanic flows of the Connecting Point Group (Christie 1950, Jenness 1963). Elsewhere, the Musgravetown Group conformably overlies the Connecting Point Group (Jenness 1963).

The sub-Musgravetown Group and sub-Signal Hill Group unconformity represents orogenesis within the 590-545 Ma rock package. This unconformity may represent heterogeneities within or a distinctive phase of the Avalonian event, or may reflect progressive, Avalonian syntectonic deposition (e.g., Rice 1996, O'Brien et al. 1996). As a result of the contemporaneous relationship between deformation and sedimentation during contraction, progressive syntectonic unconformities are commonly generated within the onlapping, synrotational sequences (e.g., Rice 1996) in which a fold propagation pattern is deduced from the relative age of the syntectonic unconformities (e.g., Espina et al. 1996).

In the Avalon Peninsula, Cambrian-Ordovician sequences unconformably overlie highly irregular, erosional surfaces of folded Harbour Main and Conception group rocks with an angular discordance in the southwestern shore of Conception Bay, and nonconformably overlie Holyrood granite at Duffs, and Holyrood granite and Harbour Main Group volcanic rocks at Manuels in the southern shore of Conception Bay (e.g., McCartney 1967). These relationships reflect a period of significant late Proterozoic deformation and erosion, at least locally in the Harbour Main Massif in the Avalon Peninsula (e.g., McCartney 1967).

Farther west in the Avalon Zone, Cambrian rocks conformably overly the Eocambrian Random Formation (Williams et al. 1972), while the Random Formation unconformably overlies the Musgravetown Group with a minor discordance (e.g., southeastern shore of

Trinity Bay, Hutchinson 1953, Fletcher 1972). Elsewhere on the Avalon Zone, the sub-Random Formation contact is conformable and gradational, while the contact between the Random Formation and overlying basal Cambrian beds is disconformable (McCartney 1967). These relationships represent a relatively stable tectonic environment from the latest Proterozoic onwards, in areas outside the Harbour Main Massif in the Avalon Zone (e.g., Smith and Hiscott 1984; O'Brien et al. 1996).

A relatively stable tectonic environment in the latest Proterozoic is demonstrated by Smith and Hiscott (1984). They suggest that the latest Proterozoic terrestrial to shallow marine Recontre and Chapel Island formations of the Long Harbour Group, and Eocambrian macrotidal facies of the Random Formation were deposited in the Fortune Bay Basin, associated with either a (syntectonic) rift or pull-apart basin, controlled by crustal thinning, stretching and fault-bounded subsidence.

The pull-apart basin model is consistent with the model proposed by O'Brien and others (1983) which suggests that latest Proterozoic Avalonian rocks underwent extension with insignificant spreading. Faulting and the formation of the Fortune Bay Basin ceased with the onset of the extensive Cambrian transgression and deposition of upper Random Formation sequences (Smith and Hiscott 1984), marked by an unconformity with minor discordance, suggesting that the basin and associated structures are late Proterozoic in age and formed during relatively stable tectonic environments.

The Recontre Formation may be time equivalent to upper units of the Signal Hill Group which are not exposed in the Avalon Peninsula (O'Brien and Taylor 1983). Growth folds in the Signal Hill Group may represent a prolonged Avalonian event which may have developed in a relatively stable tectonic environment into the Cambrian, similar to the western Avalon Zone. The lack of Cambrian rocks over the Signal Hill Group does not permit for this postulated relationship to be tested on the Avalon Peninsula.

The relationship between the 635-590 Ma rock package underlying the sub-Cambrian unconformity with an angular discordance in the Harbour Main Massif, versus the 590-545 Ma rock package underlying the sub-Cambrian unconformity with a minor or no discordance

elsewhere in the Avalon Zone, suggests that i), the 630-600 Ma tectonic event was more intense than the 575-550 Ma tectonic event, and ii) heterogeneities associated with late Proterozoic tectonism may reflect exposure at different structural levels of sedimentary sequences, changes in fault trends and dips, and/or significant contrasts in rock rheologies. These relationships are supported by the sub-Musgravetown Group and sub-Signal Hill Group unconformity and their non-extensive occurrence across the Avalon Zone, which further implies that the nature and relative timing of late Proterozoic tectonism in the Avalon Zone is unclear.

## **1.5 Study Objectives**

As discussed above, the Avalon Zone was affected by at least a late Proterozoic and a mid-Paleozoic tectonic event. The late Proterozoic event in the Avalon Peninsula has traditionally been recognized as the Avalonian Orogeny, while the mid-Paleozoic event has traditionally been recognized as the Acadian Orogeny.

The timing and nature of the Proterozoic tectonic event(s) is ambiguous in the Avalon Zone. A local age control on Proterozoic deformation in the study site is provided by the unconformable surface (or sub-Cambrian unconformity) between relatively undeformed lower Paleozoic strata and underlying tilted and folded Proterozoic rocks. Based on structural and stratigraphic observations, certain criteria can be established to differentiate between the Proterozoic and Paleozoic tectonic events. The criteria may then be applied to areas where the sub-Cambrian unconformity is absent in the Avalon Zone. Thus, the primary objective of this study is to determine whether field-based structural and stratigraphic criteria can be used to distinguish between pre-Cambrian and post-Cambrian deformations.

Another important question is whether Proterozoic rocks were affected by a single Proterozoic tectonic event or multiple Proterozoic tectonism, and whether Paleozoic rocks were affected by a single post-Cambrian tectonic event or multiple post-Cambrian tectonism. For example, O'Brien and others (1990, 1992, 1996) suggest that in the western Avalon Zone, at least four late Proterozoic orogenic events were recognized: ca. 760 Ma, ca. 680 Ma, ca.

630-600 Ma, and ca. 575-550 Ma. Similarly, the main Paleozoic tectonism in the Avalon Zone has traditionally been shown to be Devonian in age (Acadian tectonism). However, as discussed above, Silurian (Salinic) tectonism, as well as the mid-Devonian to early Permian Alleghenian-Hercynian Orogeny and early Mesozoic deformation have also been documented in the Avalon Zone.

Unconformities are absent within Proterozoic and Paleozoic rocks in the study site, and therefore cannot be used to control the ages of different tectonism. However, structural and stratigraphic cross-cutting relationships in Proterozoic and Paleozoic rocks can be used to differentiate between more than one tectonic event. Thus, a second objective of this study is to determine whether each of the Proterozoic and Paleozoic rocks were affected by multiple tectonism, a single tectonic event, or different phases of a single event.

Based on structural and stratigraphic relationships documented in this study, the nature and relative age of the tectonic events affecting the study site can be developed into a structural evolution model of the study site. The model may then be discriminately applied to regions in the Avalon Zone, outside the study site. Thus, the final objective of this study is to develop a model of the structural evolution of the study site.

## **1.6 Study Site**

The study site is located in the western margin of the Harbour Main Massif, on the southwestern shore of Conception Bay, in the Avalon Peninsula. Rocks in the study site include Cambrian formations overlying the late Proterozoic 635-590 Ma rock package which includes the Harbour Main Group and minor granitic dykes of the Holyrood Intrusive Suite that intrude the Harbour Main Group (Fig. 1.3). Lower units of the Conception Group which are part of the 590-545 Ma rock package, are also found in the study site. The study site is separated into five distinctive geographic areas: Brigus, Marysvale, Bacon Cove, Salmon Cove and Chapels Cove (Fig. 1.3), where both Proterozoic and Cambrian rocks are exposed.




Fig. 1.3 Regional geological map of the southwestern shore of Conception Bay (modified after McCartney 1967 and King 1988). The five study areas are designated by the dashed boxes: A- Brigus, B- Marysvale, C- Bacon Cove, D- Salmon Cove, and E- Chapels Cove.

## LEGEND

### EARLY-MIDDLE CAMBRIAN

#### ADEYTON GROUP




-  CHAMBERLAIN'S BROOK FORMATION  
Grey-green shale and siltstone, thin green limestone beds, manganiferous basal beds

-  BONAVIDA, SMITH POINT and BRIGUS FORMATIONS  
Red and green shale and siltstone, thin pink limestone beds, limestone nodules, basal conglomerate


### LATE PROTEROZOIC

-  LOWER CONCEPTION GROUP  
Green siliceous siltstones and sandstones, argillaceous cherts, silicified tuffs







#### HARBOUR MAIN GROUP (not in stratigraphic order)

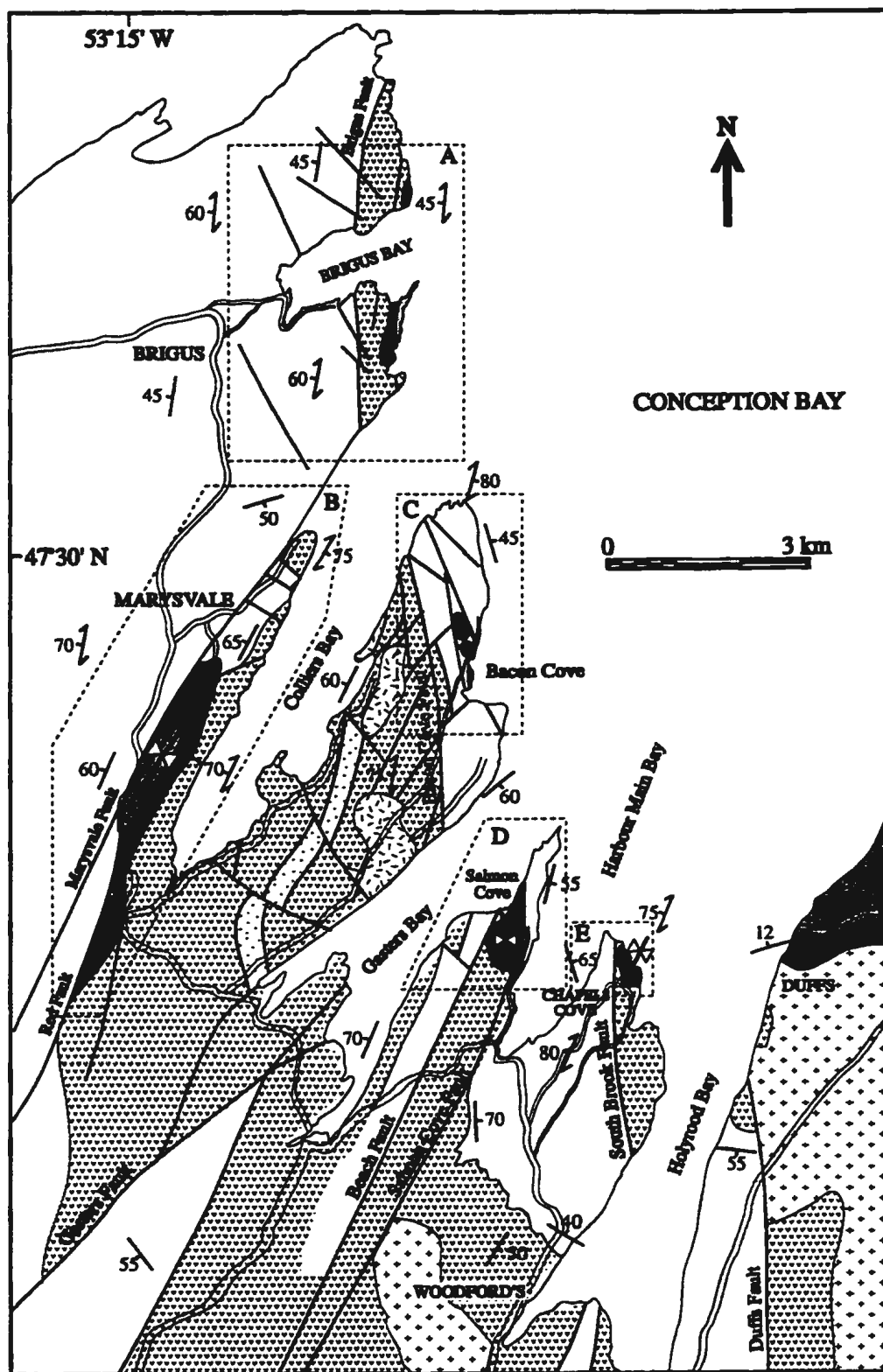
-  Basic intrusions
-  Undivided volcanic and sedimentary rocks
-  Sandstones, conglomerates, shales, tuff interlayers

#### HOLYROOD INTRUSIVE SUITE

-  Granite, diorite, gabbro

## SYMBOLS

-  Geological contact (defined, assumed)
-  Bedding
-  S<sub>2</sub> cleavage
-  F<sub>2</sub> syncline
-  High angle fault
-  Paved road



Unique to the study site is the sub-Cambrian unconformity, particularly spectacular at Seal Head in the Brigus area and in the Bacon Cove area. The unconformity surface provides an age control between deformed Proterozoic rocks and overlying, relatively undeformed Paleozoic rocks. The study site also shows Proterozoic rocks and structures with relatively insignificant amount of overprinting of younger deformation, thus making possible the differentiation between Proterozoic and Paleozoic deformation and the implementation of the study objectives.

## **2. STRUCTURAL GEOLOGY OF THE STUDY SITE**

### **2.1 Introduction**

The primary objective of this study is to determine whether field-based structural and stratigraphic criteria can be used to distinguish between pre-Cambrian (or Proterozoic) and post-Cambrian deformations. The first portion of this chapter addresses this question by using the sub-Cambrian unconformity as a control to differentiate between pre-Cambrian and post-Cambrian structures. Pre-Cambrian structures are denoted by  $D_1$  and post-Cambrian structures by  $D_2$ . As mentioned above, the sub-Cambrian unconformity is exposed in all of the areas of the study site, however, the best relationships come from exposures at the Brigus (Seal Head), Marysvale and Bacon Cove areas.

Based on the characterization of fold styles, cross-cutting relationships and apparent stratigraphic offsets along faults, certain criteria were established to distinguish between pre- and post-Cambrian structures. In this chapter, these criteria were tested in zones without the control of the sub-Cambrian unconformity in the study site.

The study site is located in the western margin of the Harbour Main Massif. Based on the wide range of age dates available for the Conception Group (610 to 565 Ma) and recent mapping results from O'Brien and others (1997), the Conception Group rocks that crop out in the study site may be part of the sub-Drook Formation, here assigned to the 590-545 Ma rock package. It is assumed that these lower Conception Group rocks blanketed the study site, covering the Harbour Main Group and Holyrood Intrusive Suite. It is also assumed here that the St. John's and Signal Hill groups were not deposited in the study site or on the Harbour Main Massif.

Terms used to identify the scale of the structures include macroscopic (hundreds of metres), mesoscopic (tens of metres) and microscopic (less than 1 centimetre). The conventions used for orientation are dip direction / dip magnitude (e.g., 225°/35°) for planar data and plunge magnitude → plunge direction (e.g., 35°→225°) for linear data.

Stereographic data were plotted on a lower hemisphere, equal area projection using the

program QuickPlot (van Everdingen et al. 1992). All photomicrographs were cut perpendicular to the main foliation and fold axis or parallel to the lineation (where applicable). The geographic areas in the study site are divided into sub-regions, zones and domains (e.g., Seal Head, Zone A, Domain I, etc.) to facilitate discussion of structures.

## **2.2 Geology of the Study Site**

Cambrian rock exposures include the Adeyton Group: the Bonavista Formation of mudstone, siltstone and shale-rich units with thin nodular limestone interlayers and local quartz-pebble basal conglomerate; the Smith Point Formation of massive algal limestone and thin mudstone, siltstone and shale interlayers, the Brigus Formation of mudstone, siltstone and shale and thin limestone interlayers; and the Chamberlain's Brook Formation of mudstones, siltstones and shales with thin limestone interlayers and a manganiferous unit near the base (e.g., Fig. 2.1).

Basal Cambrian beds vary in thickness from absent to about 50 centimetres in the study site, and comprise conglomerates, sandstones, arkosic argillites and limestones in a muddy limestone matrix, with sub-rounded pebbles. Pebbles are composed mainly of shales, dacitic tuffs and quartz. A regional cleavage is strongly developed in the more argillaceous units, typically showing slaty cleavage, and weakly developed in the limestones (e.g., Fig. 2.1). A weak cleavage is observed in some volcanic clasts in the basal conglomerate unit.

The Harbour Main Group largely comprises dacitic flows and associated tuff and breccia, volcanoclastic sedimentary sequences of red sandstone, greywacke and siltstone, and basaltic flows and associated tuff and breccia (e.g., Papezik 1970; Nixon and Papezik 1979), dated at 610 Ma and up. A regional cleavage in these rocks is commonly absent (e.g., Fig. 2.2A), or weak and patchy (e.g., Fig. 2.2B).

The Conception Group comprises primarily a thick sedimentary succession of green argillaceous cherts, siliceous siltstones, sandstones, silicified tuffs, slates and shales typical of lower turbiditic units (Fig. 2.3). A regional cleavage is well developed in argillaceous units of

A



B

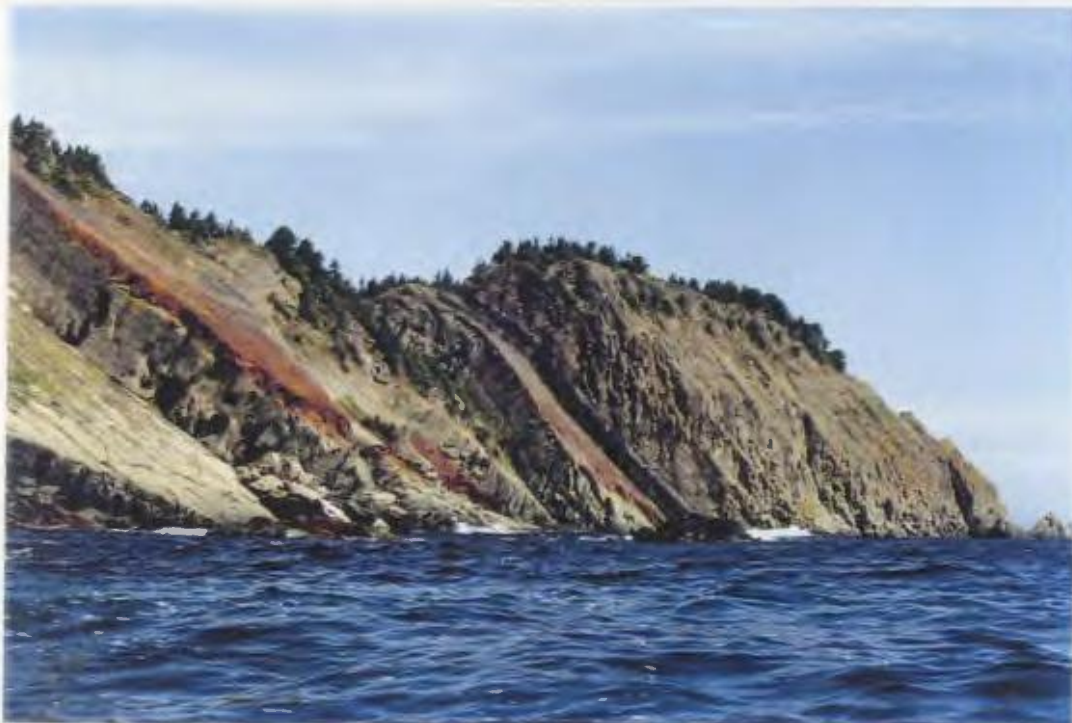


Fig. 2.1 A typical section of lower Cambrian and earliest middle Cambrian sequences. Well-bedded, red and green limestone, nodular shale and limestone units are typically gently dipping (A) and less commonly steeply dipping (B). The black manganiferous shaley unit (A and B) marks the base of the Chamberlain's Brook Formation. The regional  $S_1$  cleavage is generally steep and penetrative in shales. Looking northwest in the Brigus area.



A



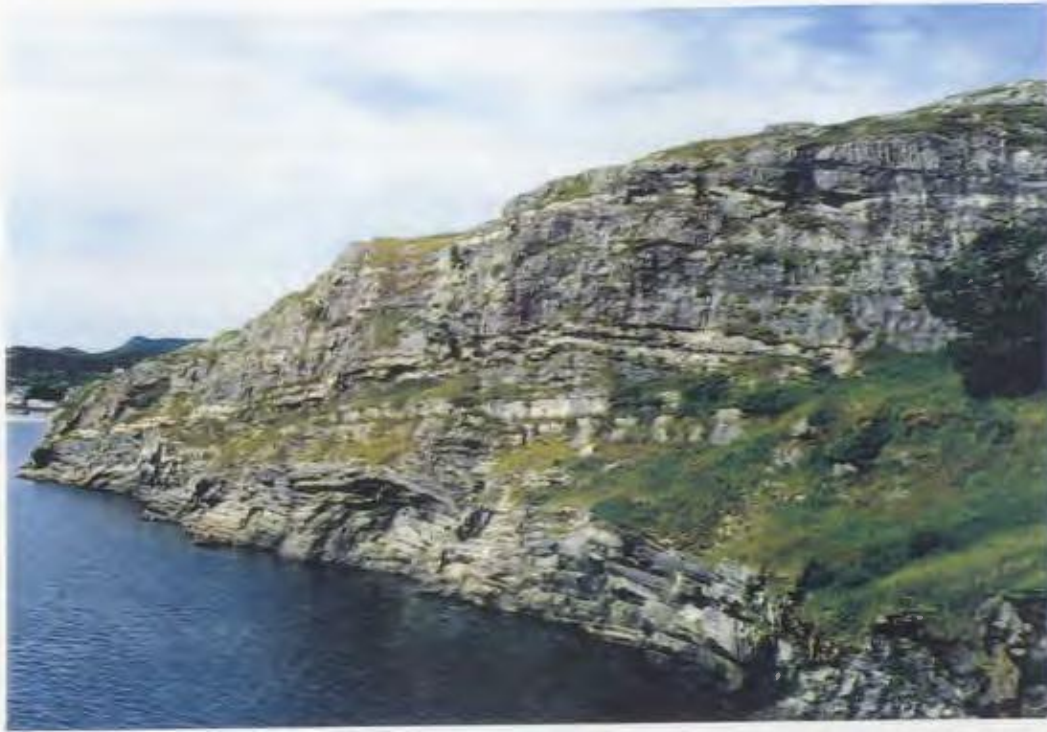
B



Fig. 2.2. The Harbour Main Group felsic and intermediate lapilli tuffs in the Brigus area. A) Tuffs are typically massive, with a weak and variably oriented regional  $S_2$  cleavage (B).



A



B



Fig. 2.3 A) A typical section of the lower Conception Group turbidite sequence of medium-to-thickly-well-bedded, green siltstone, fine sandstone, greywacke and shale, Brigus area. B) The regional  $S_1$  cleavage is commonly weak in thicker and more massive sandstone units and strong in argillaceous units, with a refracted morphology at their interface.

the Conception Group, and is commonly refracted on the contact with, and weak or absent in, more competent sandstone layers within the stratigraphic sequence (Fig. 2.3B).

The common element most of the Proterozoic and Paleozoic rocks share across the study site is a regional, steep, generally north-trending cleavage. The intensity of the cleavage appears to reflect the rock rheology, where shales and layered argillaceous units developed a stronger, more pervasive cleavage, while massive volcanic flows and tuffs, granitic dykes and thick sandstone layers lacked a penetrative cleavage. This cleavage shows no more than a mild refraction across the sub-Cambrian unconformity surface in the study site. Based on this observation, combined with its regionally consistent orientation and penetrative nature, the regional cleavage is referred to as  $S_1$ .

### **2.2.1 Brigus Area**

The Brigus area is segmented into three broad regions by the north-trending Brigus and Long Pond faults (Figs. 2.4, 2.5). Outcrops west of the Brigus fault consist exclusively of the Conception Group. The region east of the Long Pond fault consists predominantly of massive volcanic flows and tuffs and layered sedimentary facies of the Harbour Main Group that are unconformably overlain by lower to middle Cambrian strata. The region bounded by the Brigus and Long Pond faults consists mainly of the Harbour Main Group, divisible into a generally west-dipping belt of volcanic flows and tuffs, along with horses (or fault-bounded lenses of rock mass) of pyroclastic breccias, basaltic flows and sedimentary units. The stratigraphic sequences of the Harbour Main and Conception groups are generally westward younging, with a minor faulted angular discordance between the two groups.


Northeast- to north-trending folds are common through this region. Northwest-trending faults are well developed in Conception and Harbour Main group rocks west of the Long Pond fault.

**Fig. 2.4 Geological map of the Brigus area. SF- Sparrow fault, LPF- Long Pond fault, QF- Quidi fault, LF- Lobster fault. The inset map shows the location of the Brigus area relative to the other map areas.**

## LEGEND


### EARLY-MIDDLE CAMBRIAN

- ADEYTON GROUP**  
**CHAMBERLAIN'S BROOK FORMATION**  
 Grey-green shale, thin green limestone beds, manganiferous basal beds

-  **BONAVISTA, SMITH POINT and BRIGUS FORMATIONS**  
 Red and green shale, thin pink limestone beds, limestone nodules, basal conglomerates

### LATE PROTEROZOIC

-  **LOWER CONCEPTION GROUP**  
 Green siltstones and sandstones, argillaceous cherts, silicified tuffs














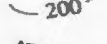

-  **HARBOUR MAIN GROUP ( not in stratigraphic order)**  
 Dacitic lava flows and lapilli tuffs, siliceous tuffs, basaltic lapilli tuffs

-  Basaltic lava flows

-  Pyroclastic breccias

-  Shales, sandstones, conglomerates, tuff interlayers

## SYMBOLS

-  Geological contact (defined, assumed)
-  Bedding
-  S<sub>1</sub> cleavage
-  S<sub>2</sub> cleavage
-  F<sub>1</sub> syncline, anticline
-  F<sub>2</sub> syncline
-  Mesoscopic F<sub>1</sub> fold axis, F<sub>1</sub> kink fold axis
-  Mesoscopic F<sub>2</sub> fold axis
-  Structural trend
-  High angle fault
-  Thrust fault
-  Normal fault
-  Paved road, trail
-  Elevation contour (in 100 feet intervals)
-  Profile section location





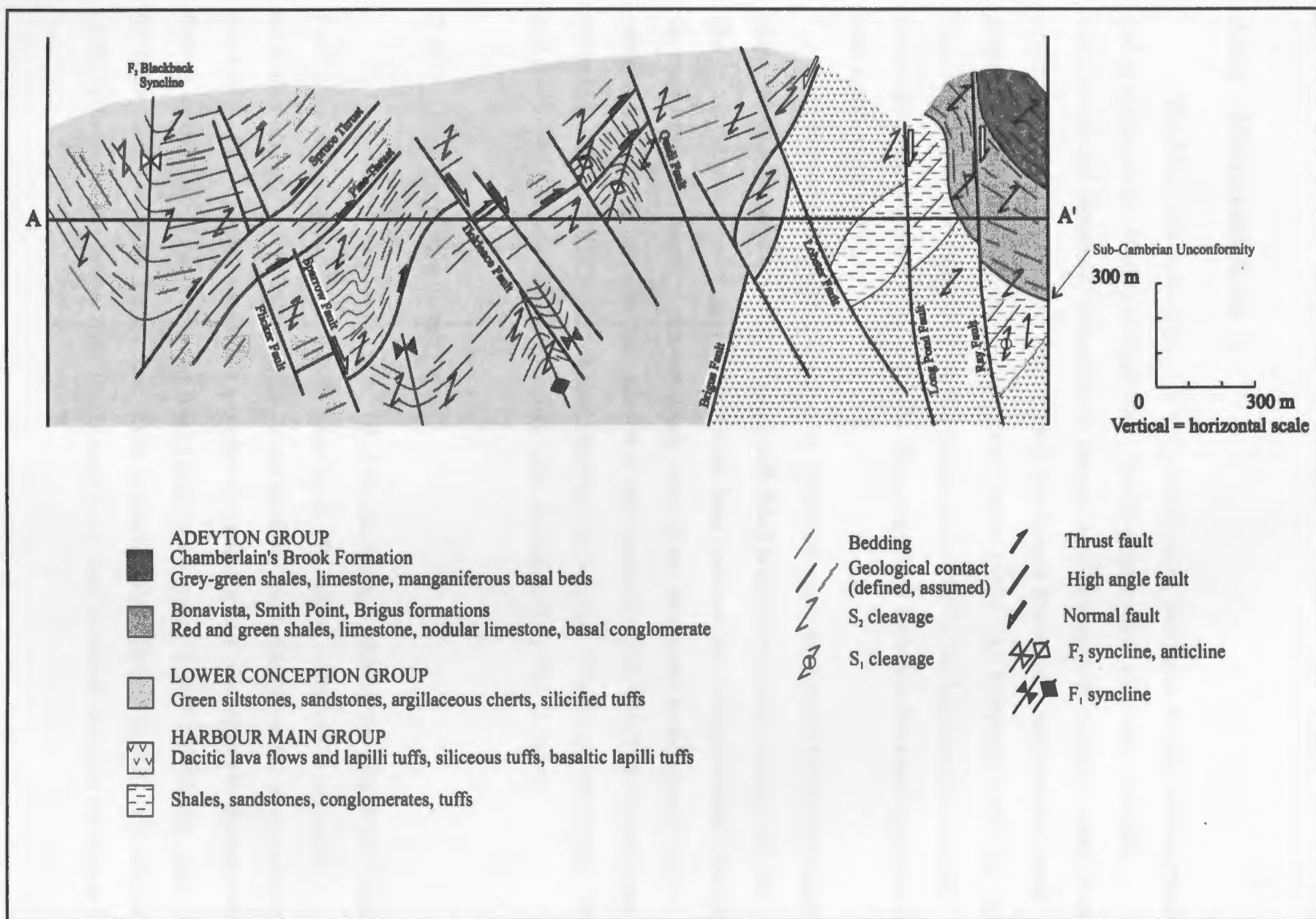


Fig. 2.5 Cross-section AA' across the southern Brigus area, projected along the plunge of the F<sub>1</sub> Blackback Syncline.

### **2.2.2 Marysvale Area**

The Marysvale area (Figs. 2.6, 2.7) encompasses structures that are formed parallel to, and at angles to, the Marysvale fault zone. The Marysvale fault zone has a braided morphology and separates moderately to steeply west-dipping and younging strata of the Conception Group on the west from folded and faulted Conception and Harbour Main groups and Cambrian rocks on the east (McCartney 1967). The Marysvale fault does not align with any of the major faults in the Brigus area to the north, but projects along the Brigus-southern shoreline (Fig. 1.3). The Marysvale fault truncates the east-dipping Red and Park faults to the south.

In the southern portion of the area, Cambrian strata are bounded by the Red and Park faults, which coalesce to one fault to the north (Red fault) before they connect with the Marysvale fault. It appears that the Marysvale fault truncates the coalesced faults. Elsewhere in the area, lower and middle Cambrian strata occur in the Marysvale syncline and in a subordinate anticline, adjacent and parallel to the Marysvale fault. Basal Cambrian strata unconformably overlie Conception and Harbour Main group rocks (e.g., McCartney 1967) and the faulted contact between these two units (Junction fault, Fig. 2.7BB').

### **2.2.3 Bacon Cove Area**

In the Bacon Cove area (Figs. 2.8, 2.9), the north-northwest-trending Bacon Cove fault is a steeply-dipping braided fault zone, up to 200 metres wide, which separates northwest-dipping and younging rocks of the Harbour Main Group on the west from folded and faulted Conception Group and Cambrian rocks to the east. Although the Bacon Cove fault is approximately parallel to the Brigus fault to the north, it does not directly align with the latter fault, and it has the opposite sense of stratigraphic offset (e.g., Fig. 1.3). McCartney (1967) referred to the Brigus fault- and Bacon Cove fault-bounded block as the Brigus Horst.



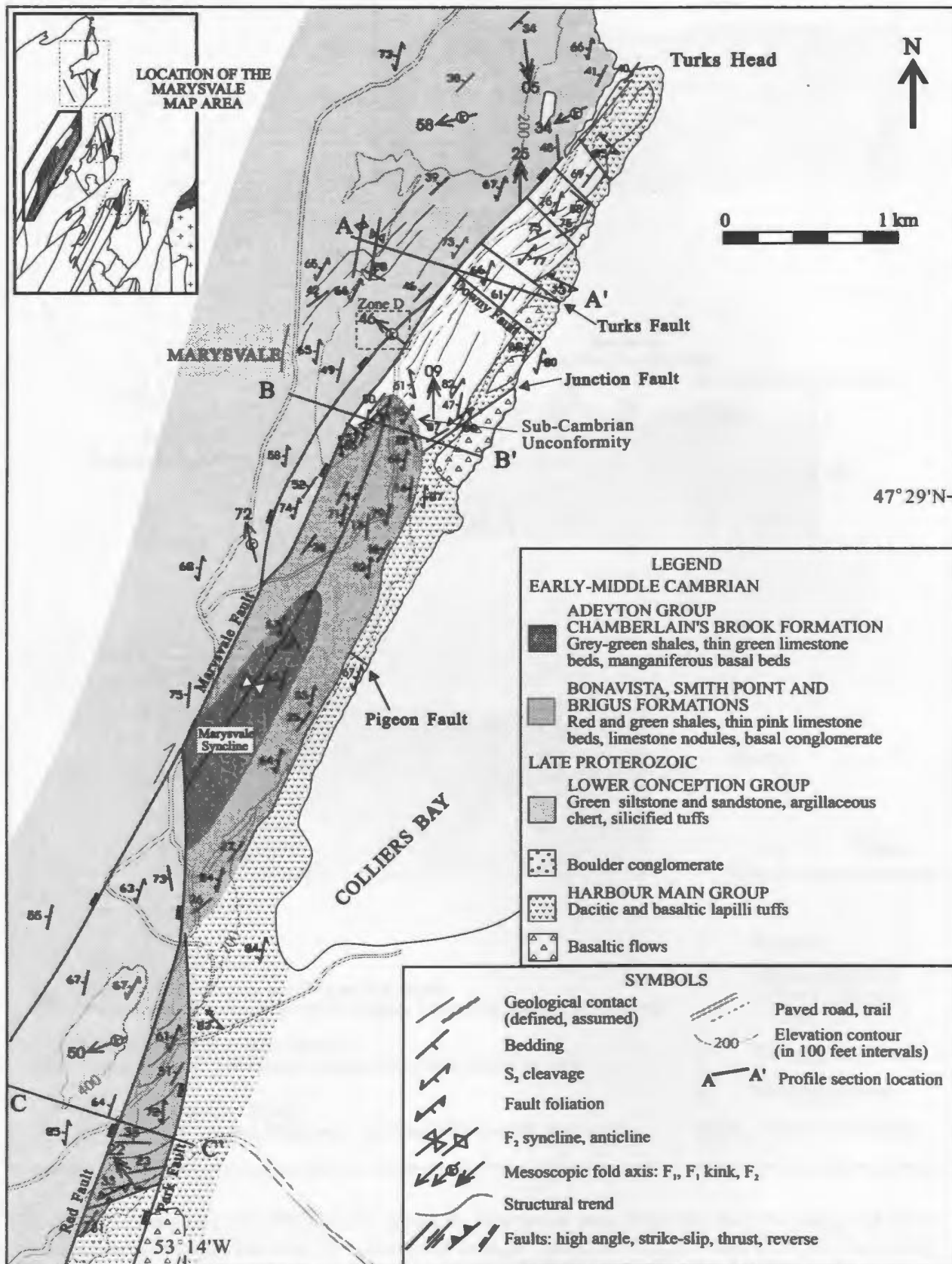


Fig. 2.6 Geological map of the Marysville area. Inset map shows the location of the Marysville area relative to the other map areas.



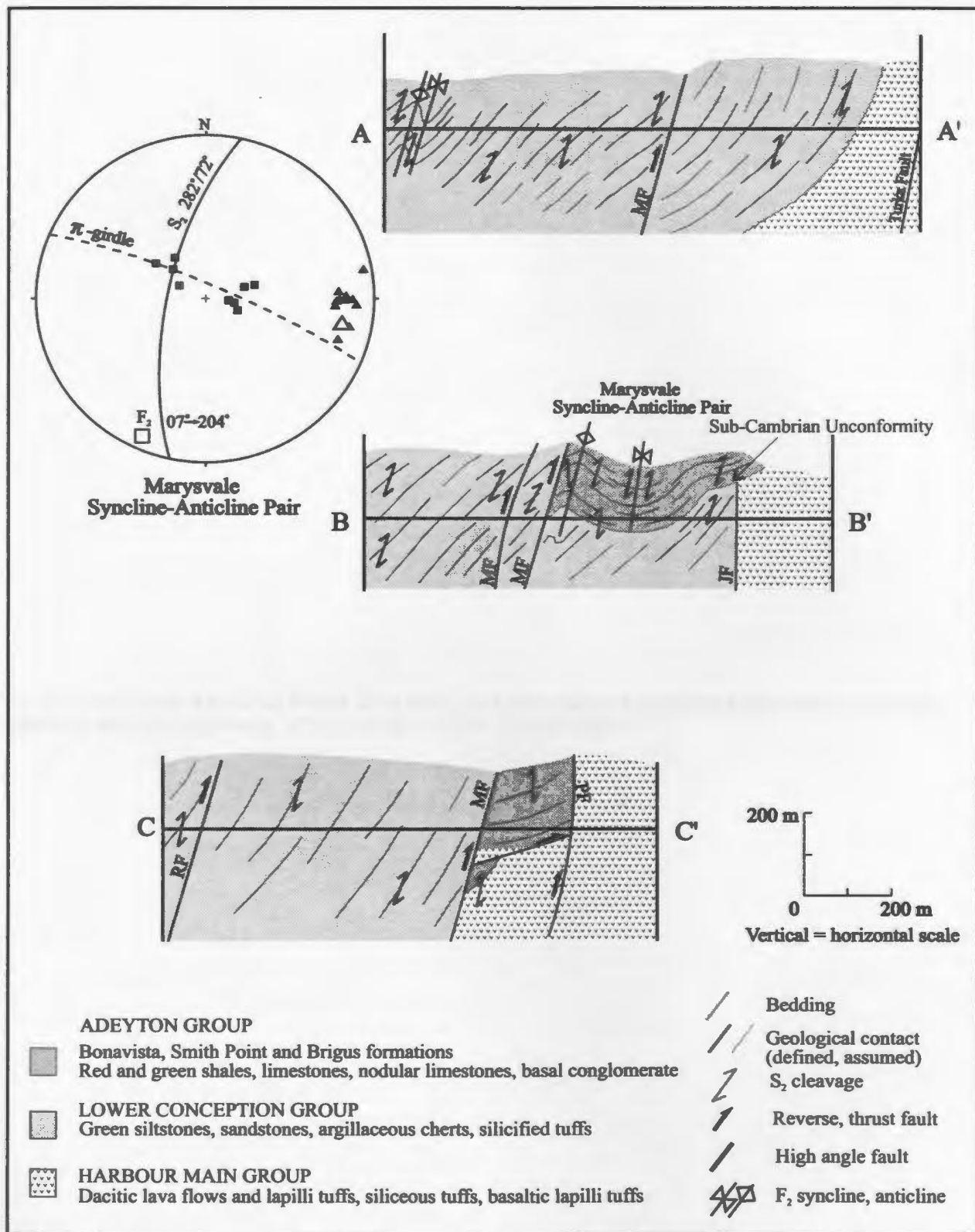



Fig. 2.7 Cross-sections AA', BB' and CC' across the Marysvale area, projected along the plunge of the  $F_2$  Marysvale syncline-anticline pair. MF- Marysvale fault, JF- Junction fault, RF- Red fault, PF- Park fault. Summary stereo plots show the sub-cylindrical, fault-parallel Marysvale syncline-anticline pair.

□ pole to  $\pi$ -girdle (poles to  $S_0$ ),  $\Delta$  mean to  $S_2$  poles,  $\triangle$ .


**Fig. 2.8 Geological map of the Bacon Cove area. Inset map shows the location of the Bacon Cove area relative to the other map areas. AT- Aspen thrust, HF- Humber fault.**

## LEGEND

### EARLY-MIDDLE CAMBRIAN

-  **BONAVISTA & SMITH POINT FORMATIONS**  
Red and green shales, thin pink limestone beds, limestone nodules, basal conglomerate

### LATE PROTEROZOIC



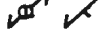








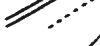
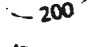

-  **LOWER CONCEPTION GROUP**  
Green siltstone and sandstone, argillaceous chert, silicified tuffs

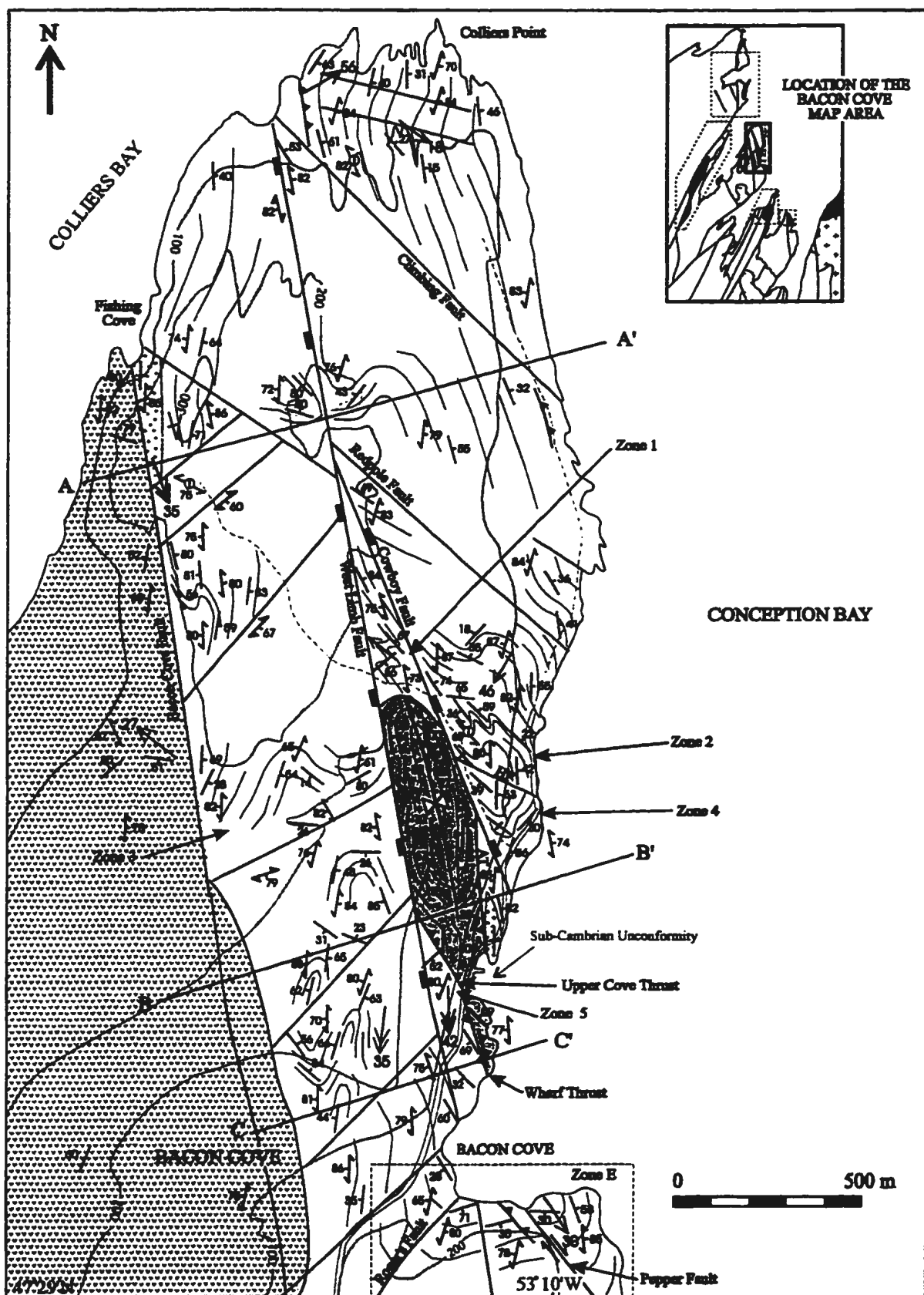
-  Red and green cobble conglomerate

-  Red mixtite (Gaskiers Formation?)

-  **HARBOUR MAIN GROUP**  
Undivided basaltic and rhyolitic lapilli tuffs, tuff breccias and lava flows, sedimentary units

## SYMBOLS

-  Geological contact (defined, assumed)
-  Bedding (inclined, vertical)
-  Cleavage ( $S_1$ ,  $S_2$ )
-   $F_2$  syncline
-  Mesoscopic  $F_1$ ,  $F_2$  fold axis
-  Structural trend
-  High angle fault
-  Strike-slip fault
-  Thrust fault
-  Reverse fault
-  Fault-parallel foliation
-  Paved road, trail
-  Elevation contour (in 100 feet intervals)
-  Profile section location



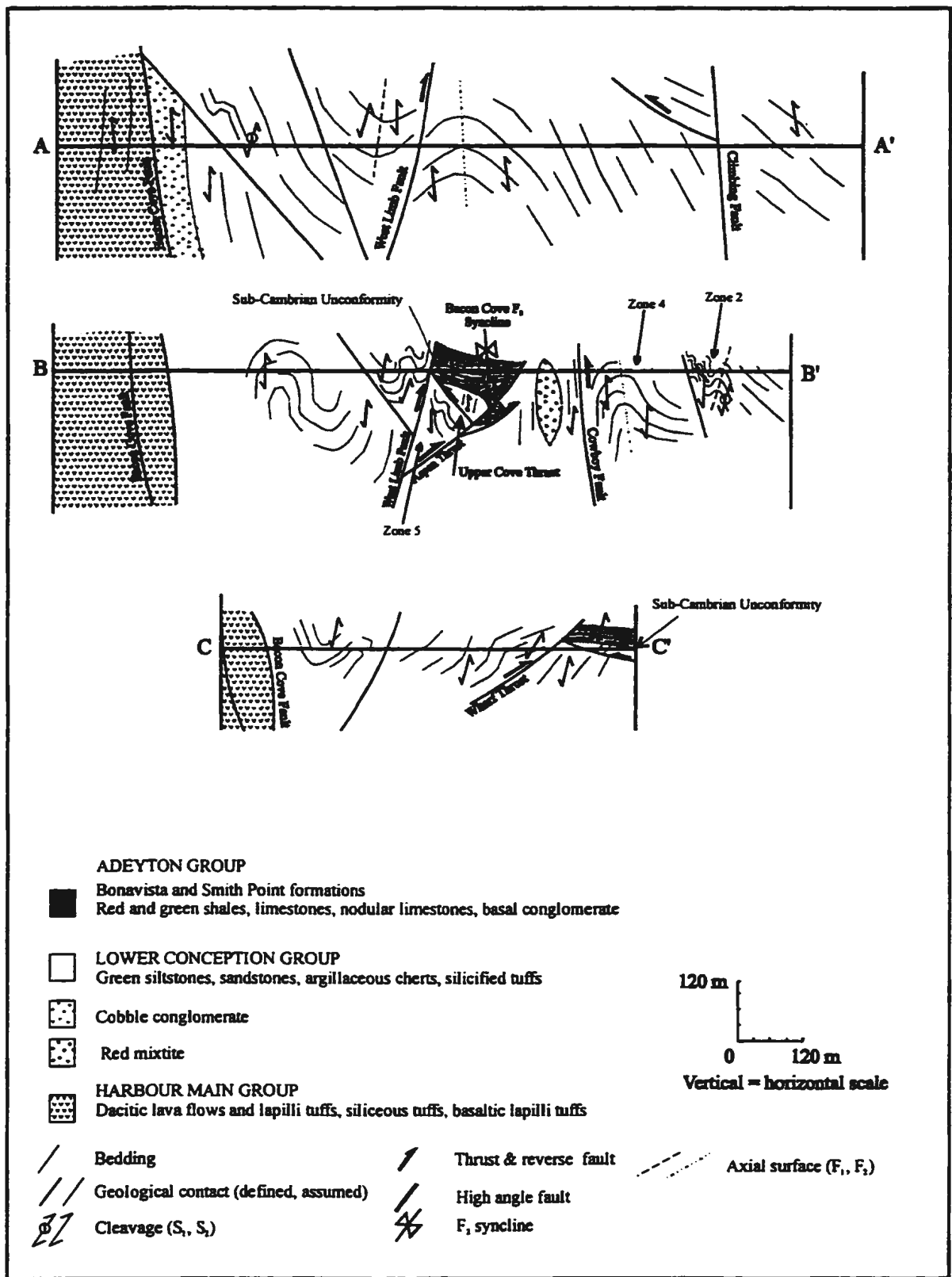


Fig. 2.9 Cross-sections AA', BB' and CC' across the Bacon Cove area, projected along the plunge of the Bacon Cove  $F_1$  syncline.

East of the Bacon Cove fault, tilted and folded strata of the Conception Group are overlain with an angular unconformity by lower Cambrian strata (e.g., King et al. 1974). Exposures of Cambrian beds are bounded by the north-northwest-trending West Limb and Cowboy faults and the Wharf thrust (Fig. 2.9). A series of northwest- and northeast-trending faults segment the Conception Group. Most of these faults terminate against various north-northwest-trending faults. The angular discordance across the sub-Cambrian unconformity in the area unequivocally demonstrates the occurrence of Proterozoic deformation in the Conception Group. The unconformity is cross-cut by  $S_2$  with only minor refraction.

The periclinal open Bacon Cove syncline was developed in Cambrian strata between, and parallel to, the West Limb and Cowboy faults, unconformably overlying red tillite in a fault-bounded block. This unit of mixtite and glaciomarine deposits may be correlative of the Gaskiers Formation (Table 1.1), stratigraphically below the Drook Formation of the Conception Group, which elsewhere contains granitic boulders and pebbles derived from the (620 Ma) Holyrood Intrusive Suite (Williams and King 1979).

Throughout the central part of the Bacon Cove area, the Conception Group is deformed into a complex fold system which is poorly constrained due to spotty outcrop across the region. In general, however, strata of the Conception Group are east-dipping and younging. In contrast, Conception Group strata in the Brigus and Marysvalle areas are generally west-dipping and younging, aside from local perturbations.

#### **2.2.4 Salmon Cove Area**



In the Salmon Cove area (Figs. 2.10, 2.11), the north-northeast-trending Beach and Salmon Cove faults bound Cambrian rocks and isolate them from generally east-dipping and younging Conception Group rocks on the east, and structurally complex Conception and Harbour Main group strata on the west. Both faults are interpreted to extend to the southwest for several kilometres from this area (Fig. 1.3). In this fault-bounded block, lower and middle Cambrian strata crop out in the Salmon Cove syncline which trends parallel to the Salmon

Fig. 2.10 Geological map of the Salmon Cove area. Conception Group rocks of zones i) and ii) are summarized in stereo plots. PF- Point fault, TF- Teal fault, SF- Shore fault. Inset map shows the location of the Salmon Cove area relative to the other map areas.


□  $\pi$ -pole to  $\pi$ -circle (poles to  $S_0$ ), ▣,  $\Delta$  mean of poles to  $S_1$ , ▲, ☆ mean of poles to  $S_0$ .

## LEGEND




### ADEYTON GROUP

-  Chamberlain's Brook Formation  
Grey-green shales, limestones, manganiferous basal beds
-  Bonavista, Smith Point and Brigus Formations  
Red and green shales, pink limestones, nodular limestones





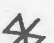





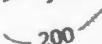


### LOWER CONCEPTION GROUP

-  Green siltstone, sandstone, argillaceous chert, silicified tuffs

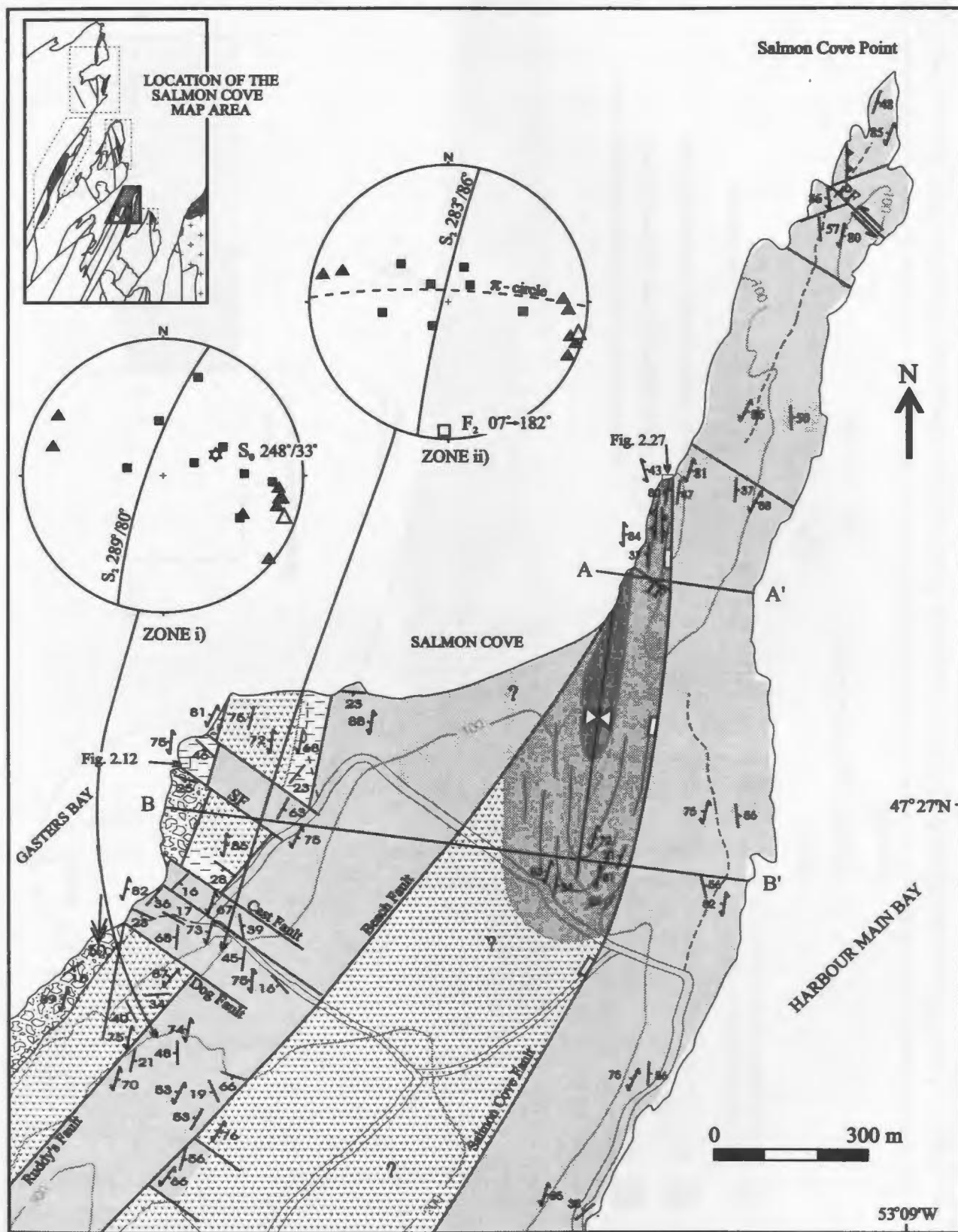
### HARBOUR MAIN GROUP (not in stratigraphic order)

-  Shale, sandstone, siltstone, conglomerate, tuffs
-  Dacitic and basaltic lava flows and lapilli tuffs
-  Dacitic and basaltic pyroclastic breccias

## SYMBOLS

-  Geological contact (defined, assumed)
-  Bedding
-   $S_2$  cleavage
-  Mesoscopic fold axis ( $F_1$ ,  $F_2$ )
-   $F_2$  syncline
-  Structural trend
-  High angle fault
-  Strike-slip fault
-  Thrust fault
-  Fault: reverse, normal
-  Paved road, trail
-  Elevation contour (in 100 feet intervals)
-  Profile section location





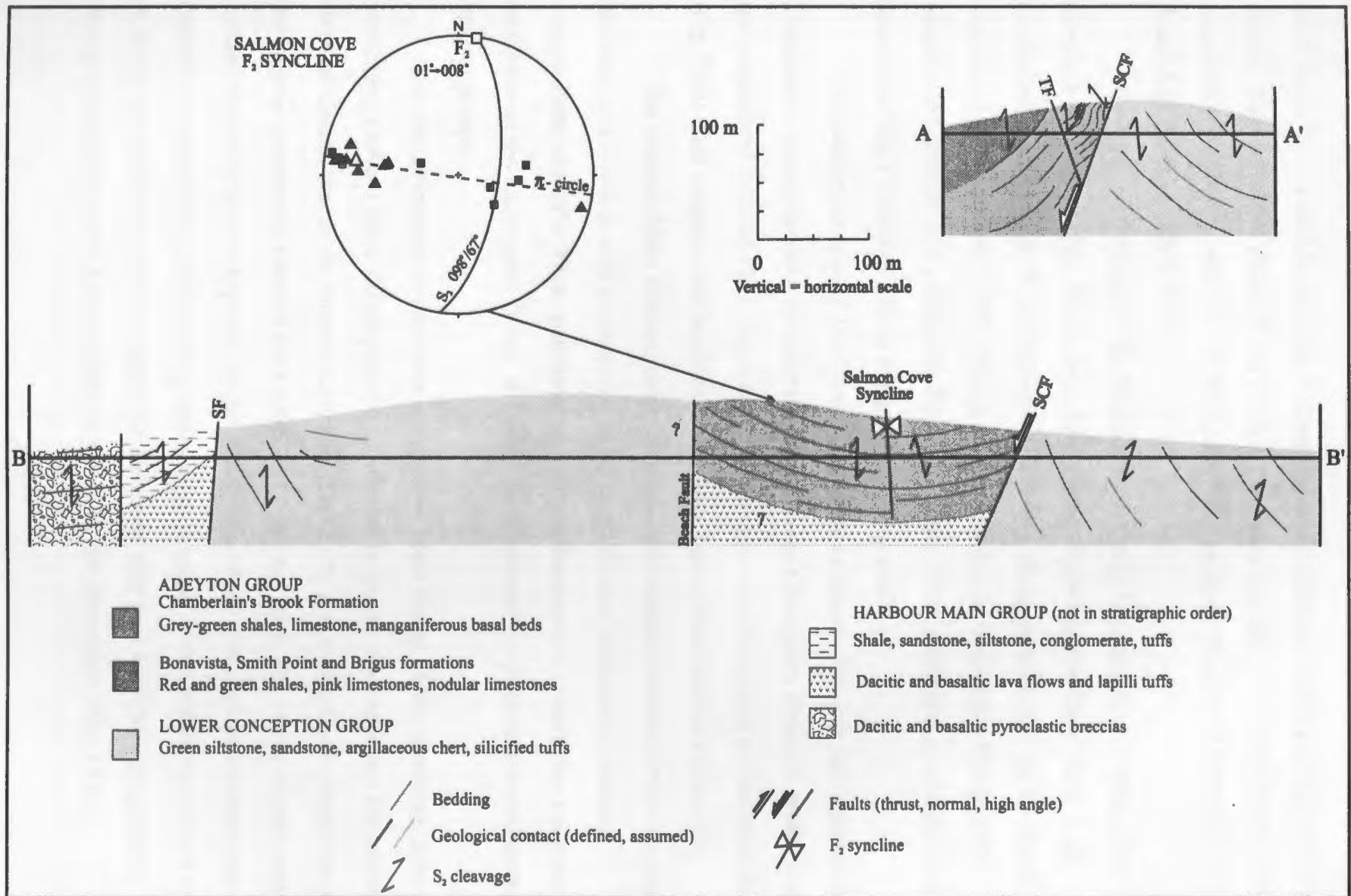


Fig. 2.11 Cross sections AA' and BB' across the Salmon Cove area projected along the plunge of the Salmon Cove F<sub>2</sub> syncline. SCF- Salmon Cove Fault, TF- Teal fault, SF- Shore fault.

Cove fault. The regional  $S_2$  cleavage is steep and north-northeast-trending across the area in all rock types and axial planar to the Salmon Cove syncline (Fig. 2.11). McCartney (1954) extrapolated Cambrian rocks west of the Beach fault, however, the lack of outcrop west of the Beach fault cannot confirm this.

There are no outcrops of the Harbour Main Group between the two faults. The existence of Harbour Main Group rocks stratigraphically below Cambrian rocks is an extrapolation of outcrops of the Harbour Main Group along strike farther south, outside the map area (e.g., McCartney 1954). Similarly, the existence of Conception Group rocks adjacent to Cambrian rocks along the Beach fault (near Salmon Cove) is an extrapolation of outcrops of the Conception Group along strike farther south.

The western portion of the mapped area shows complex fold and fault patterns in Proterozoic strata. Exposures of structural fabrics in the Conception Group in zones i) and ii) are summarized in stereo plots, where  $S_0$  poles are scattered while  $S_2$  data plot in tight clusters (Fig. 2.10). This suggests that these rocks may have been affected by both  $D_1$  and  $D_2$ .

The Harbour Main Group comprises dacitic and basaltic pyroclastic breccias, lapilli tuffs and lava flows, as well as sequences of red to green shale, sandstone, siltstone, conglomerate and tuffs. These sediments are less argillaceous and coarser than the green sediments of the Conception Group. A faulted nonconformable contact is exposed between the two groups.

A disconformable contact between Harbour Main Group cherty sandstone units and underlying Harbour Main Group pyroclastic breccias is locally exposed along the western shore of Gasters Bay in the Salmon Cove area (Fig. 2.12). It is an erosional contact based on the angular relationship between the contact and overlying beds. The extent of this contact is unclear due to the lack of exposure of the contact elsewhere. The erosional surface may represent a channel-fill, cross-bedding sedimentary structure within the Harbour Main Group, in which the angle between the contact and sandstone beds may have been exaggerated during post-Cambrian ( $D_2$ ) deformation as shown by the stereo plot (Fig. 2.12).

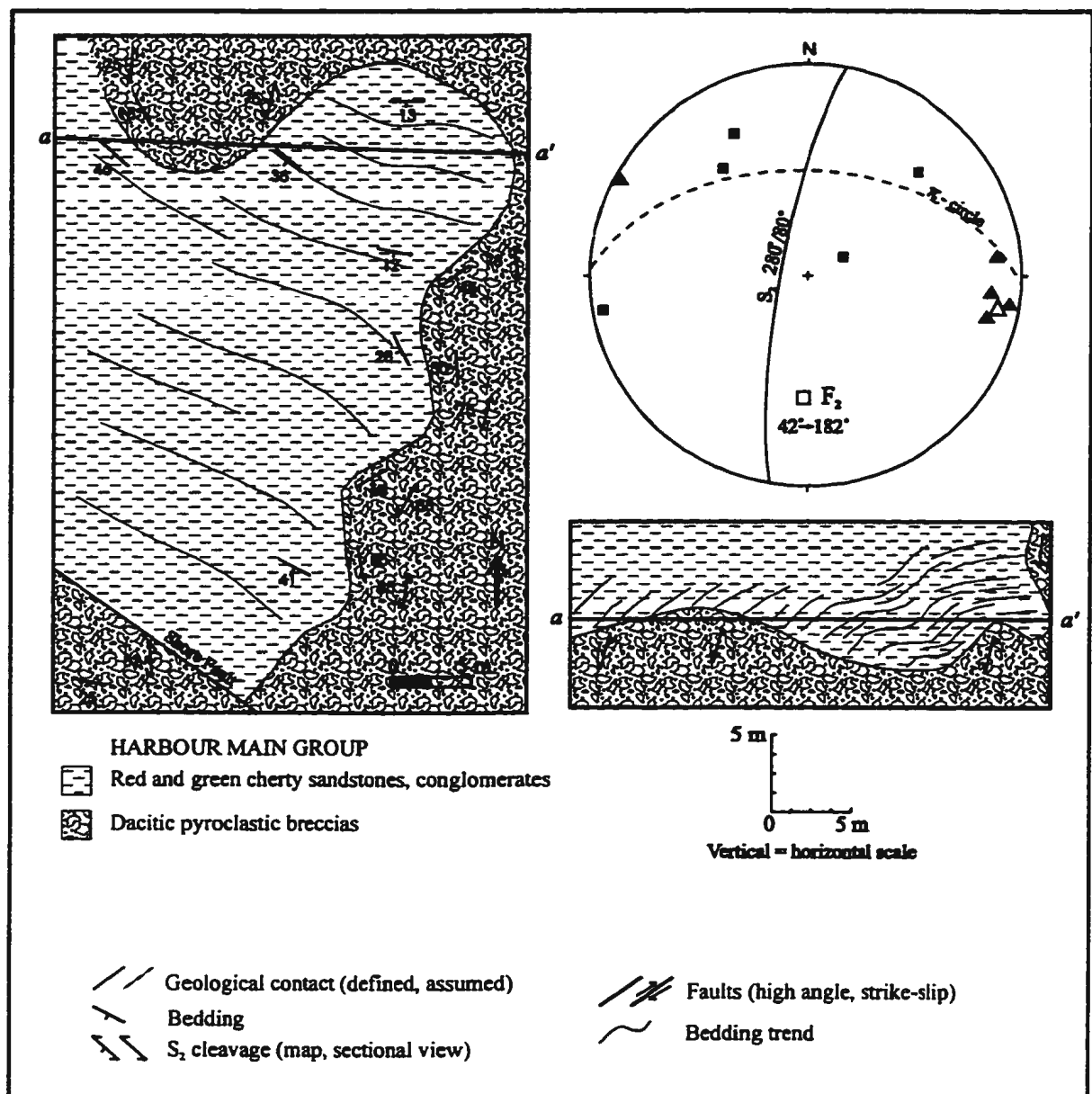


Fig. 2.12 Sketch and cross-section aa' of an  $F_1$  folded erosional surface between Harbour Main Group clastic sedimentary rocks and underlying Harbour Main Group pyroclastic breccia. Eastern Gasters Bay, Salmon Cove area.

$\square$   $\pi$ -pole to  $\pi$ -circle (poles to  $S_0$ ,  $\Delta$ ),  $\Delta$  mean of poles to erosional surface,  $\Delta$ .

### **2.2.5 Chapels Cove Area**

In the Chapels Cove area (Figs. 2.13, 2.14), the north-trending South Brook fault separates steeply east-dipping and younging Conception Group strata to the west of the fault from Harbour Main Group and unconformably overlying Cambrian rocks to the east of the fault (McCartney 1967). The South Brook fault represents a nonconformable faulted contact between the Harbour Main and Conception groups.

The South Brook fault is parallel to, but does not align with, the Bacon Cove and Brigus faults (e.g., Fig. 1.3). Rocks of the Harbour Main Group here are intruded by northeast-trending quartz monzonite dykes of the Holyrood Intrusive Suite, which is exposed to the east of the map area (e.g., Fig. 1.3). Cambrian strata occur in the northeast-trending Chapels Cove syncline-anticline pair. The regional north-northeast-trending steep  $S_2$  cleavage is relatively consistent in orientation across the area, with a local, yet significant shift in orientation to the northeast on the west side of Red Rock Cove (Fig. 2.13).

Cambrian strata terminate against both the Little Brook fault and the north-northeast-trending Red Rock fault, the latter being one of a series of parallel faults that segment Cambrian rocks in the map area. The Little Brook fault aligns with the Duffs fault, which lies farther south, outside the map area (e.g., Fig. 1.2) and marks the western margin of the Holyrood Intrusive Suite.

## **2.3 The Sub-Cambrian Unconformity Used as an Age Control for Deformation**

Exposures of the sub-Cambrian unconformity at Bacon Cove, Marysvale area and Seal Head in the Brigus area, provide the best field relationships in the study site. At Seal Head (Fig. 2.15), folded sedimentary units of the Harbour Main Group along with associated northwest-trending faults are overlain by the sub-Cambrian angular unconformity. This location is spectacular and significant in that it provides the most definitive temporal control

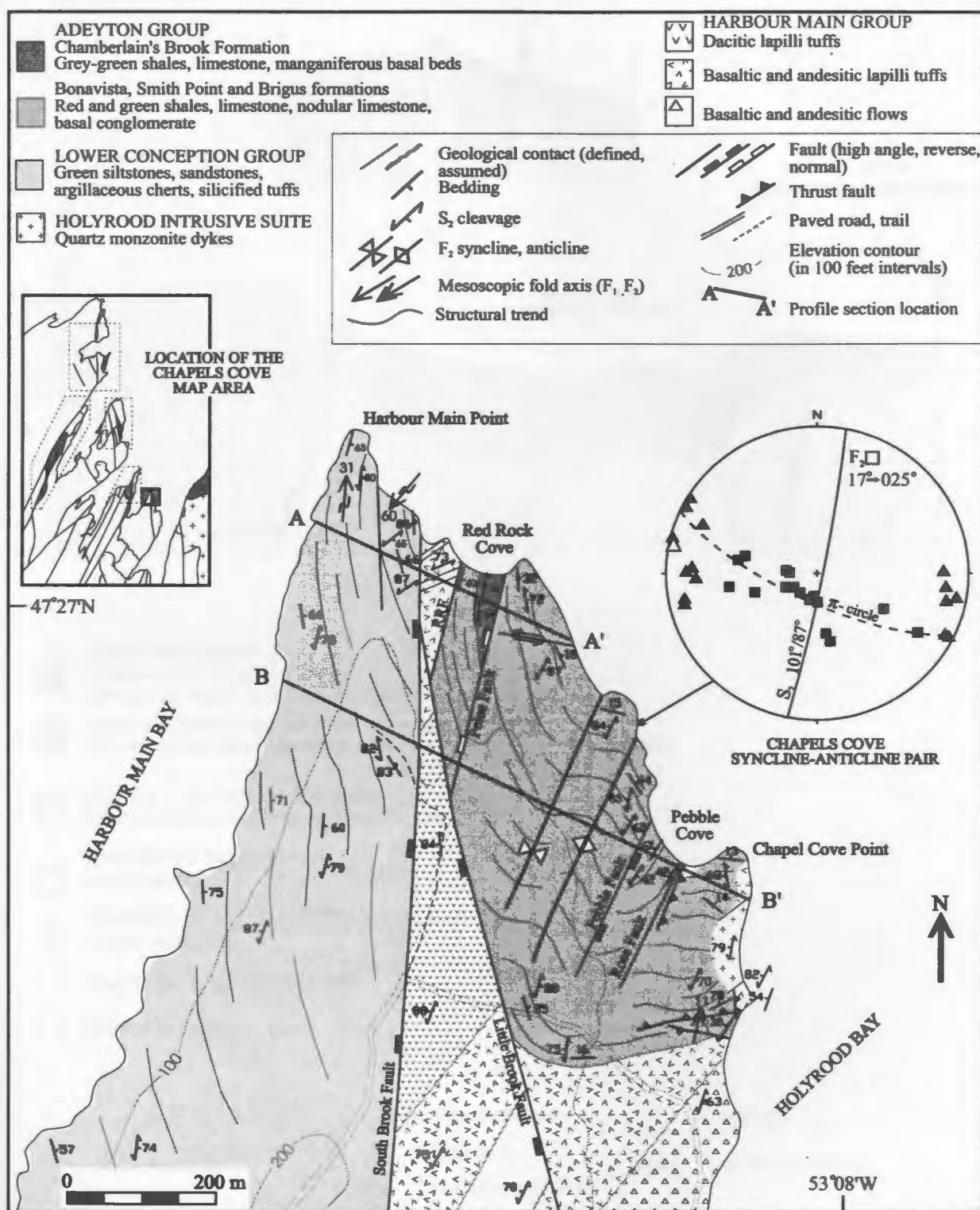


Fig. 2.13 Geological map of the Chapels Cove area.  $\square$   $\pi$ -pole to  $\pi$ -circle (poles to  $S_0$ ,  $\blacksquare$ ),  $\Delta$  mean of poles to  $S_2$ ,  $\blacktriangle$ . RRF- Red Rock fault. The inset map shows the location of the Chapels Cove area relative to the other map areas.

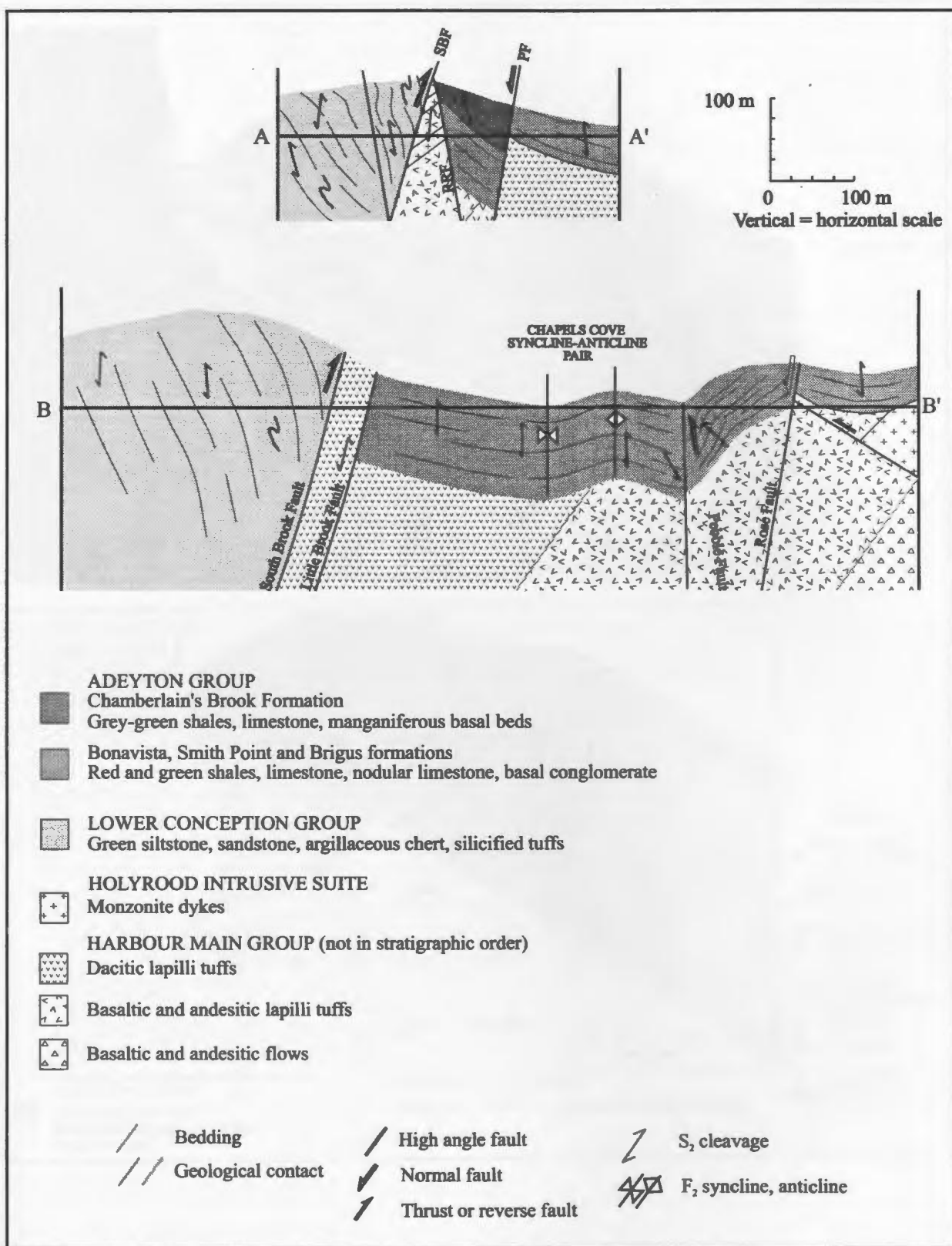


Fig. 2.14 Cross-sections AA' and BB' across the Chapels Cove area. SBF- South Brook fault, PF- Pelee fault, RRF- Red Rock fault.



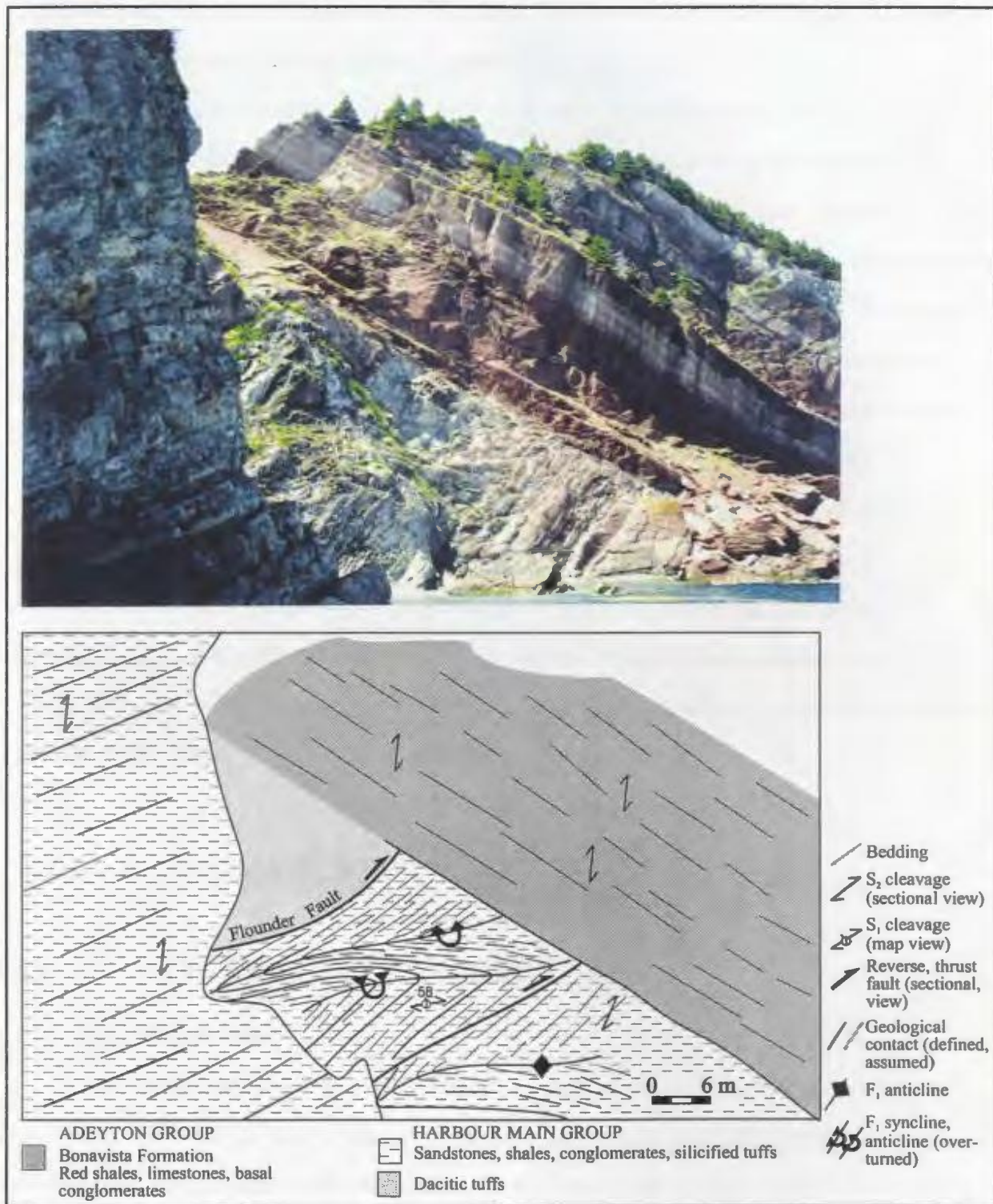


Fig. 2.15 Sketch of photograph showing the sub-Cambrian unconformity at Seal Head, Brigus area. The Cambrian Bonavista Formation unconformably overlies tightly F<sub>1</sub> folded sedimentary units of the Harbour Main Group and associated faults with an angular discordance. Looking northwest. Note that both apparent map and sectional views are shown.



on pre-Cambrian,  $F_1$  fold structures and is, thus, used as a basis for identifying some of the fundamental characteristics of the early phase(s) of deformation.

At Bacon Cove (Fig. 2.16), exposures of the sub-Cambrian angular unconformity overlying folded Conception Group sediments are also spectacular and informative. The marked contrast between the sub-Cambrian unconformity here and at Seal Head lies in the stronger intensity of the Proterozoic deformation that affected the underlying Harbour Main Group rocks at Seal Head versus the less intense deformation that affected the Conception Group in the Bacon Cove area. In the Marysvale area (e.g., Fig. 2.6), the sub-Cambrian unconformity overlies the faulted contact between tilted Conception Group sediments and massive Harbour Main Group volcanic rocks, east of the town of Marysvale. This area provides a temporal control on the tilted Conception Group units and nonconformable faulted contact between the two rock groups.

Elsewhere in the study site, exposures of basal Cambrian units nonconformably overlie massive volcanic rocks of the Harbour Main Group or granitic dykes of the Holyrood Intrusive Suite, and do not provide structures that so clearly establish a temporal control on structures formed by pre-Cambrian deformation.

## **2.3.1 $D_1$ Pre-Cambrian Structures**

### **2.3.1.1 $F_1$ Folds and Associated Faults**

#### ***Seal Head, Brigus Area***

At Seal Head (Fig. 2.17), basal Cambrian units dipping moderately to the east, unconformably overlie steeply southwest-dipping and younging folded interlayers of clastic sedimentary units, dacitic tuffs and pyroclastic breccias of the Harbour Main Group with an angular discordance (Fig. 2.18). The Flounder and Pike faults and folded strata of the Harbour Main Group are truncated by, and terminate against, the sub-Cambrian unconformity (Figs. 2.17, 2.18), which clearly establishes these to be pre-Cambrian structures.

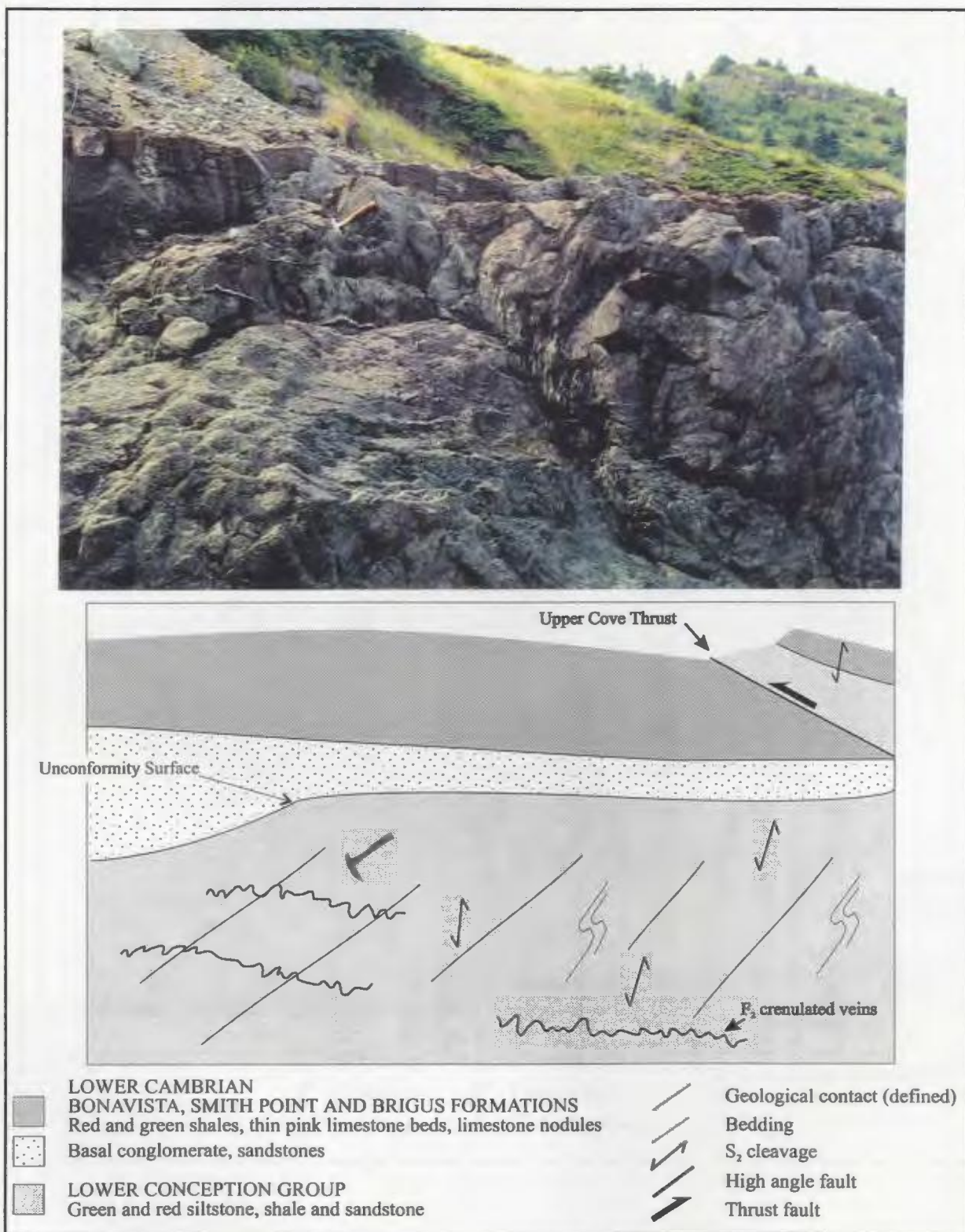


Fig. 2.16 Photograph and sketch show the sub-Cambrian unconformity in the Bacon Cove area marked by the onlap of Cambrian basal conglomerate of the Bonavista Formation onto steeply tilted and F<sub>1</sub> folded lower Conception Group rocks. Looking north-northeast.

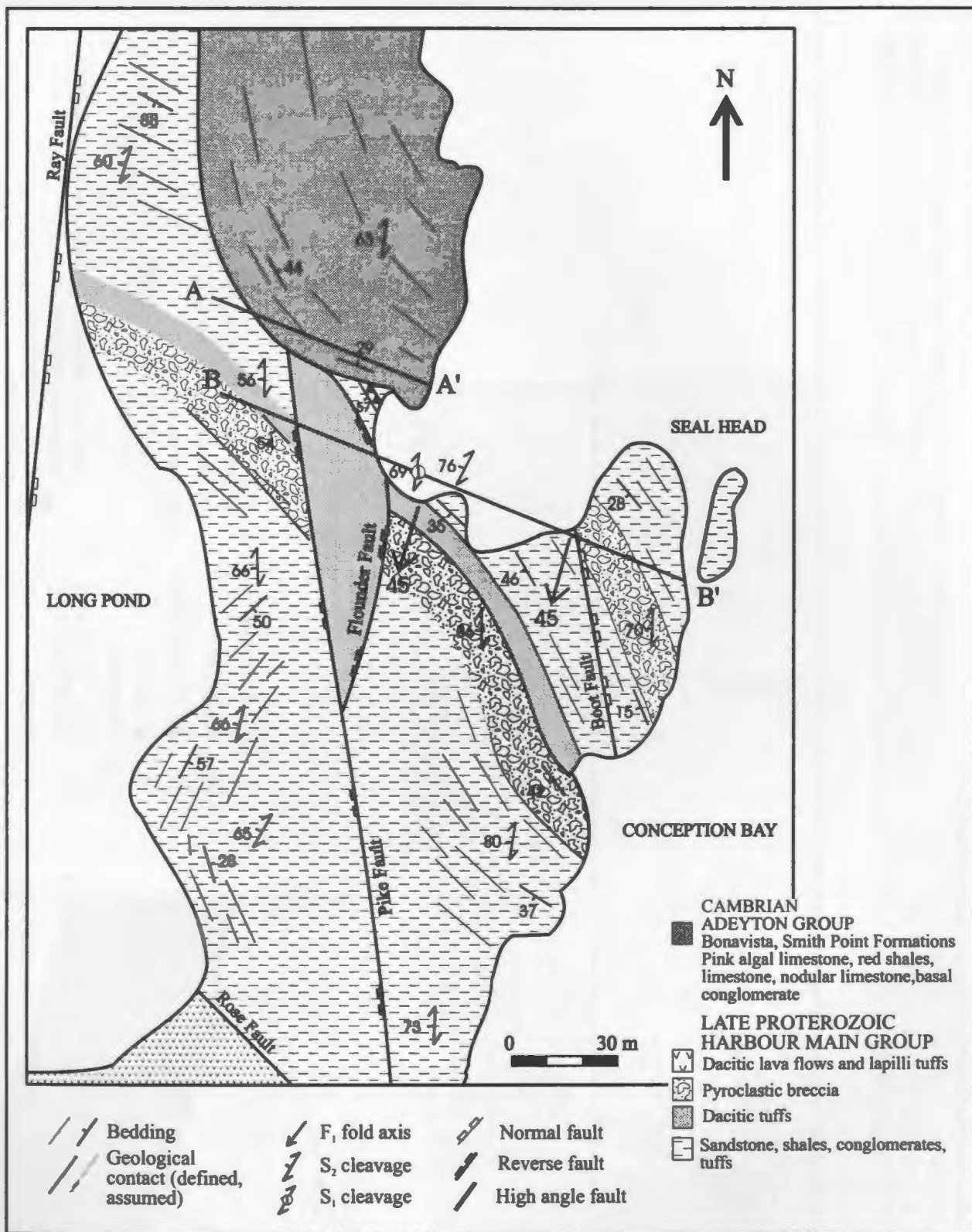


Fig. 2.17 Detailed geological map of the Seal Head area, Brigus area, showing the angular unconformity between moderately east-dipping Cambrian rocks and underlying steeply southwest-dipping Harbour Main Group sedimentary rocks.



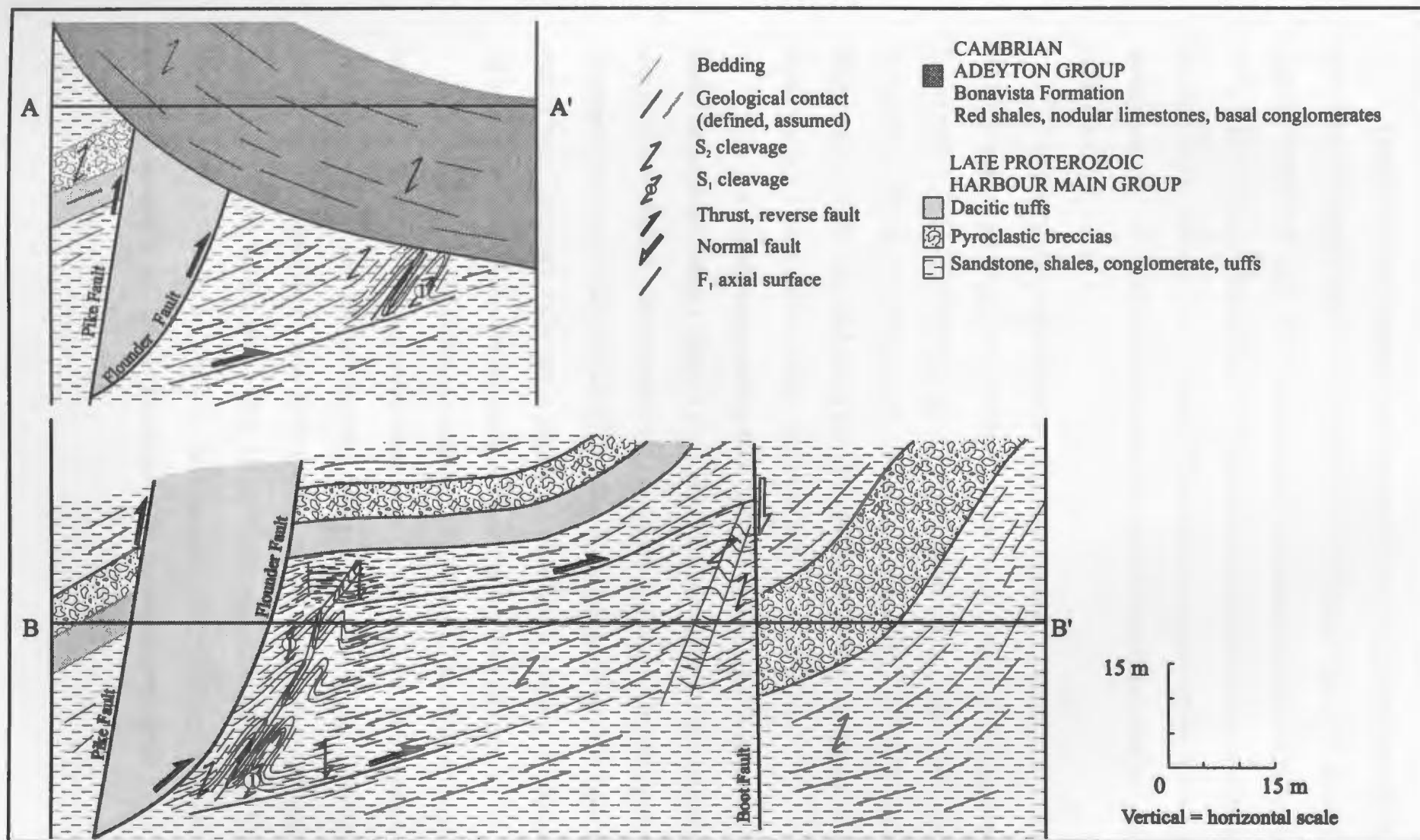


Fig. 2.18 Cross-sections across the Seal Head area, Brigus area, projected along the mean plunge of the F<sub>1</sub> anticline pairs. Section AA' shows the angular unconformity between the Cambrian rocks and underlying, locally isoclinally F<sub>1</sub> folded Harbour Main layered units. Section BB' shows the east-verging, tight F<sub>1</sub> anticline pair that formed in layered Harbour Main Group rocks. These folds decrease in amplitude and become more open and box-style up-stratigraphic-section towards massive dacitic tuffs and breccia interlayers.

Dacitic tuffs are thrust up against layered units of the Harbour Main Group along the east-directed Flounder fault. In the footwall of the Flounder fault there are two east-verging, slightly overturned, north-northeast-trending  $F_1$  mesoscopic anticlines in the layered sequence of the Harbour Main Group (Fig. 2.19), which are truncated by the sub-Cambrian unconformable surface (Fig. 2.18AA'). These folds have structurally thinned short limbs, quartz and sulphide filled extension fractures through their hinges and are south-southwest-plunging (Fig. 2.20).

The folds locally develop an axial plane cleavage ( $S_1$ ) preserved in chlorite schists in the fold hinge zones (Fig. 2.21). A more pervasively developed  $S_2$  cleavage clearly cross-cuts  $S_1$  and their fold axial surfaces by up to  $20^\circ$  in plan view (e.g., Figs. 2.17, 2.19, 2.20B, 2.21). In sectional view,  $S_2$  is approximately parallel to  $S_1$  (e.g., Figs. 2.18, 2.19). Up-section, the folds become more open and box-style, diminish in amplitude and die out completely at the contact with a 5 metres thick dacitic tuff layer (Fig. 2.18BB', 2.19).

The north-northwest-trending Boot fault is a brittle, steep zone up to 3 metres wide of quartz and tectonic breccia (Figs. 2.17, 2.18BB'). It partitions the Harbour Main Group comprising dominantly finer-grained volcanoclastic sequences in the footwall from dominantly coarser-grained volcanoclastic units in the hangingwall. The Boot fault terminates against basal Cambrian rocks and is therefore a Proterozoic structure. Slickensides rake  $55^\circ$  to the south-southeast on the steeply, east-northeast dipping fault surface.

If the Boot fault formed in relation to the folding in the adjacent layered sequences, the fault dip-direction would indicate west-vergence on the fault. This would be inconsistent with the postulated east-directed Flounder fault and associated  $F_1$  folds. However, a possible solution to this inconsistency may lie in the fact that the fault is steep and may have rotated during more recent deformation. Thus, based on the adjacent contractional features and brittle features in fold hinges, the Boot fault probably underwent east-directed,  $D_1$  reverse separation, consistent with the development of the  $F_1$  folds at Seal Head.

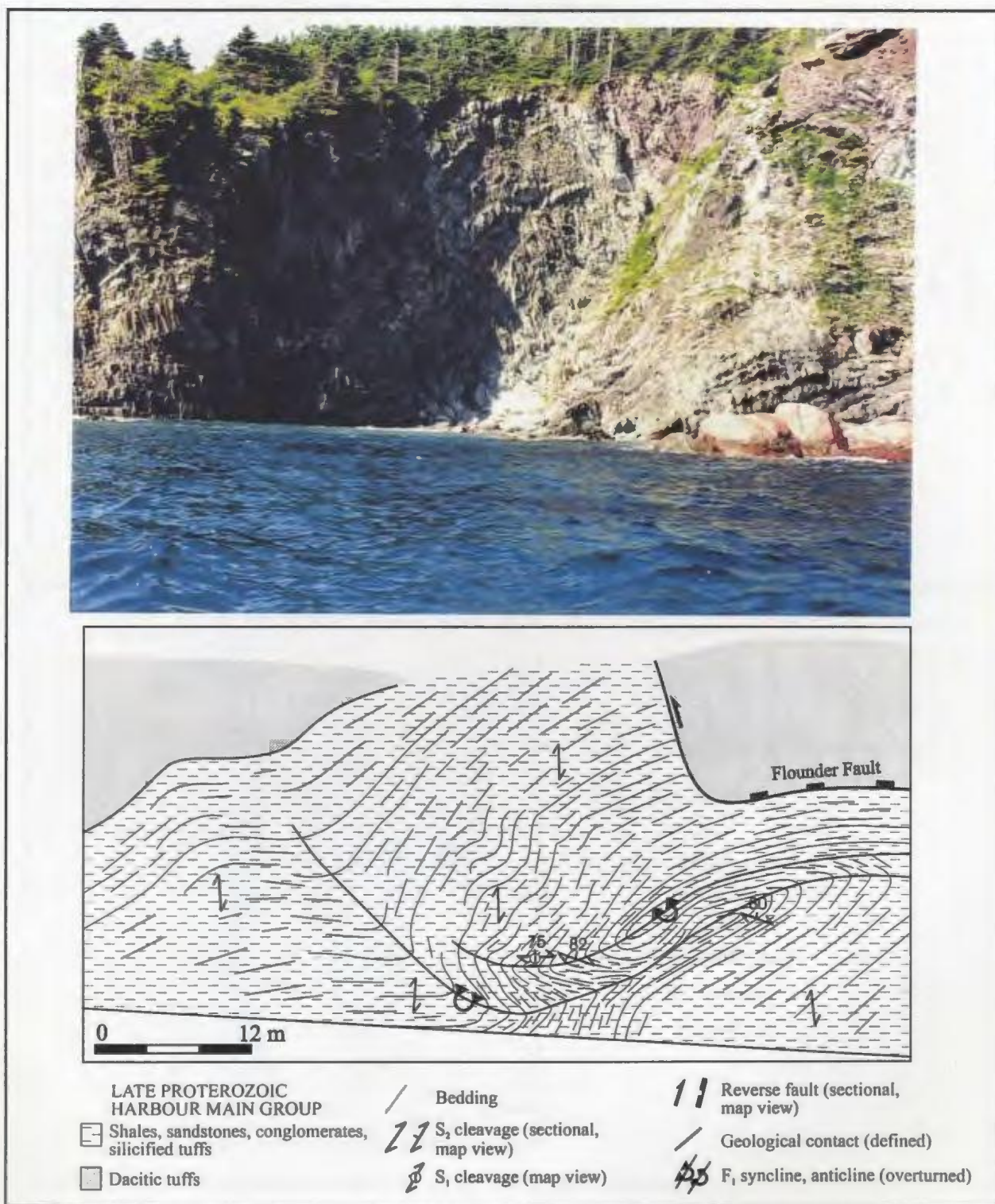


Fig. 2.19 Sketch of photograph showing an overturned, east-verging F<sub>1</sub> anticline pair in layered Harbour Main Group rocks which terminate into open, box-style folds against the massive dacitic tuff layer of the Harbour Main Group. Looking south-southwest, Seal Head, Brigus area. Note that both map and sectional apparent views are shown.

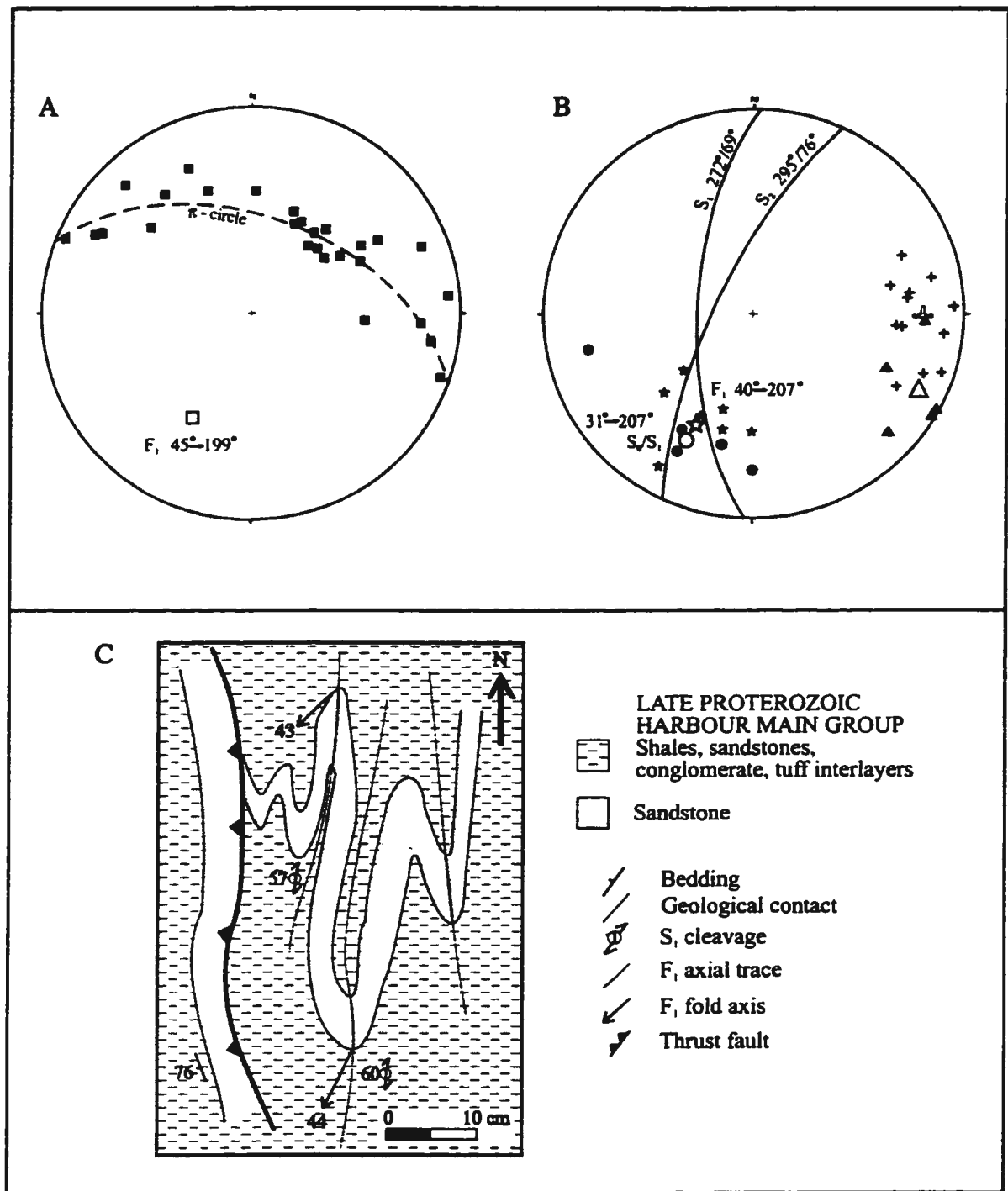


Fig. 2.20 Summary stereo plots from measurements made in Harbour Main Group rocks at Seal Head, Brigus area. A) shows sub-cylindrical  $F_1$  folds and B) shows that  $S_2$  cross-cuts  $S_1$  by more than 20 degrees. C) is a sketch of a tightly  $F_1$  folded sandstone layer, showing the slightly reclined nature of the folds. □  $\pi$ -pole to  $\pi$ -circle (poles to  $S_0$ ,  $\Rightarrow$ ,  $+$  mean of poles ( $\rightarrow$ ) to  $S_1$ ,  $\Delta$  mean of poles ( $\blacktriangle$ ) to  $S_2$ ,  $\star$  mean to measured  $F_1$  fold axes ( $*$ ),  $\odot$  mean to  $S_0/S_1$  intersection lineations ( $\bullet$ ).



### ***Bacon Cove***

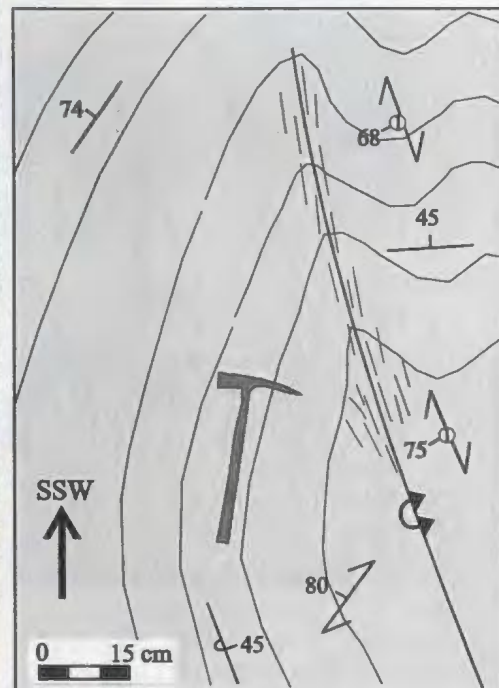
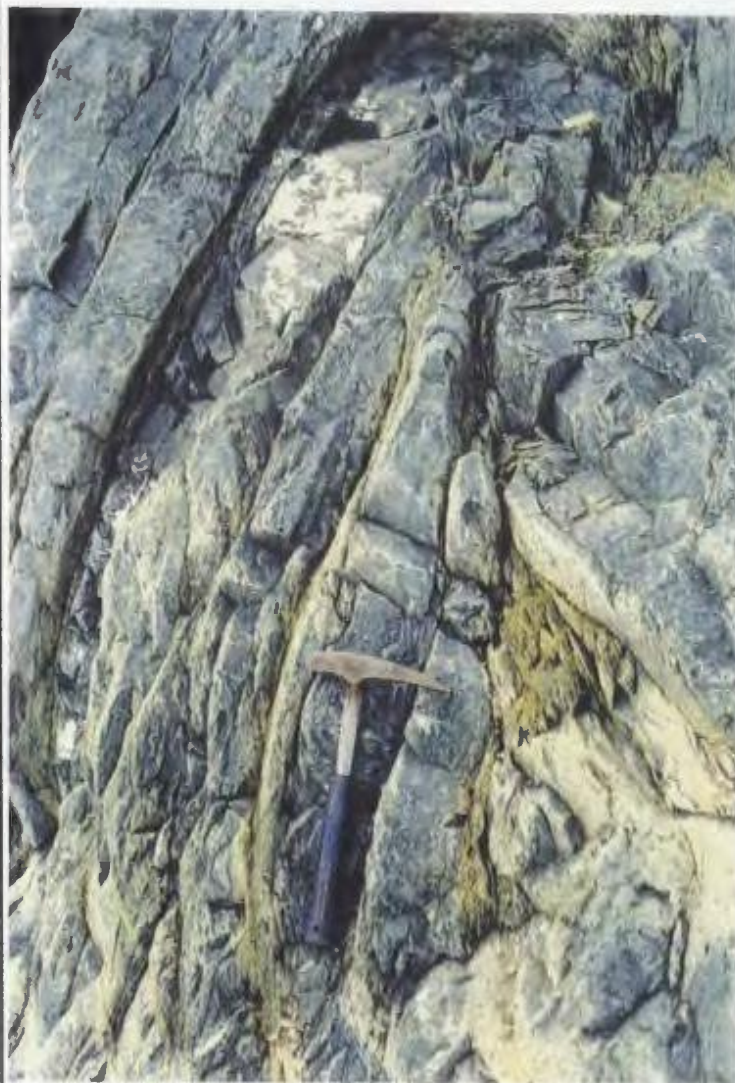
The sub-Cambrian angular unconformity is exposed along the shoreline, just north of the Bacon Cove, in the Bacon Cove area (Figs. 2.8, 2.9). Conception Group strata beneath the generally flat-lying unconformable surface range from moderately southwest-dipping to vertical and north-trending (Fig. 2.9BB', CC'). Mesoscopic, open, box-style, west-verging and south plunging  $F_1$  folds form in the steeply southwest-dipping Conception Group units underlying the unconformity (Fig. 2.22). Outcrop exposures show that  $S_2$  clearly cross-cuts the main east-west-trending axial surface of these folds, which suggests that the folds are  $F_1$ . Extensive en echelon, quartz and carbonate filled extension veins occur in the Conception Group underlying the sub-Cambrian unconformity (e.g., Fig. 2.16). The veins are  $F_2$  meso-folded with axial planar  $S_2$ . The veins may represent hydrothermal activity associated with  $D_1$  faulting.

Zone 1 (Fig. 2.8) is bounded by the West Limb fault, Cowboy fault and Cambrian strata in the Bacon Cove area. In Zone 1, the sub-Cambrian unconformity truncates northwest-trending, east-verging folds in the Conception Group (Figs. 2.8, 2.23B). The truncation of these folds by the sub-Cambrian unconformity necessitates them to be  $F_1$ . Outcrop exposures show that the axial surface of these steeply southeast-plunging  $F_1$  folds are clockwise cross-cut by  $S_2$  by more than  $50^\circ$  in map view (Fig. 2.23B).

### ***D<sub>1</sub> Junction and Pigeon Faults, Marysvale Area***

The steep, northeast-trending Junction and northwest-trending Pigeon faults terminate against the sub-Cambrian unconformity in the Marysvale area (Figs. 2.6, 2.7BB'). The Pigeon fault formed in massive dacitic and basaltic tuffs. The Junction fault marks the nonconformable boundary between steeply northwest-dipping and younging Conception Group sediments and massive Harbour Main Group volcanic tuffs and flows. A strong fault-parallel foliation is present in the Conception Group along the Junction fault, while  $S_2$





HARBOUR MAIN GROUP  
Sandstone and minor chlorite schist



Mica-rich band ( $S_1$ )



Bedding



$S_1$  cleavage



$S_2$  cleavage



$F_1$  anticline (overturned)

Fig. 2.21 Sketch of the photograph shows the hinge zone of an overturned  $F_1$  anticline in the upper sedimentary units of the Harbour Main Group at Seal Head, Brigus area. Axial plane  $S_1$  is locally developed in chlorite schist.  $S_2$  cross-cuts  $S_1$  by more than 20 degrees.

East

West

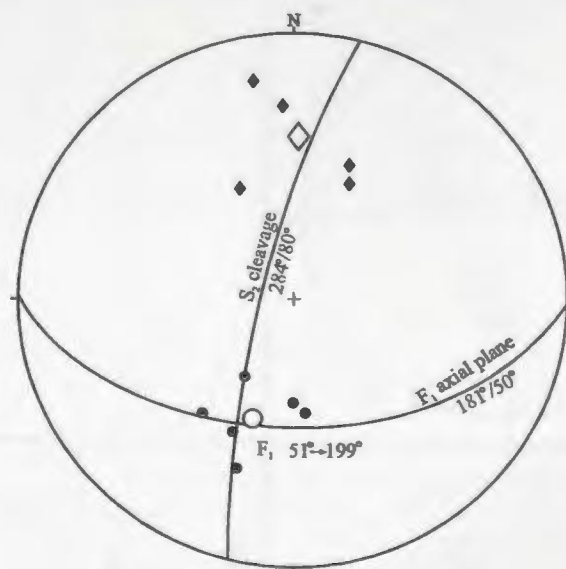


Fig. 2.22 Photograph shows a down-plunge view of z-symmetry, west-verging  $F_1$  parasitic folds in lower Conception Group units, underlying the sub-Cambrian unconformity in the Bacon Cove area. A summary stereo plot shows that measured  $F_1$  fold axial surfaces are cross-cut at high angles by  $S_2$ .  
 at a high angle by  $S_2$  cleavage. ○ mean of measured fold axes, ●, ◆ mean of measured axial planes, ◆.

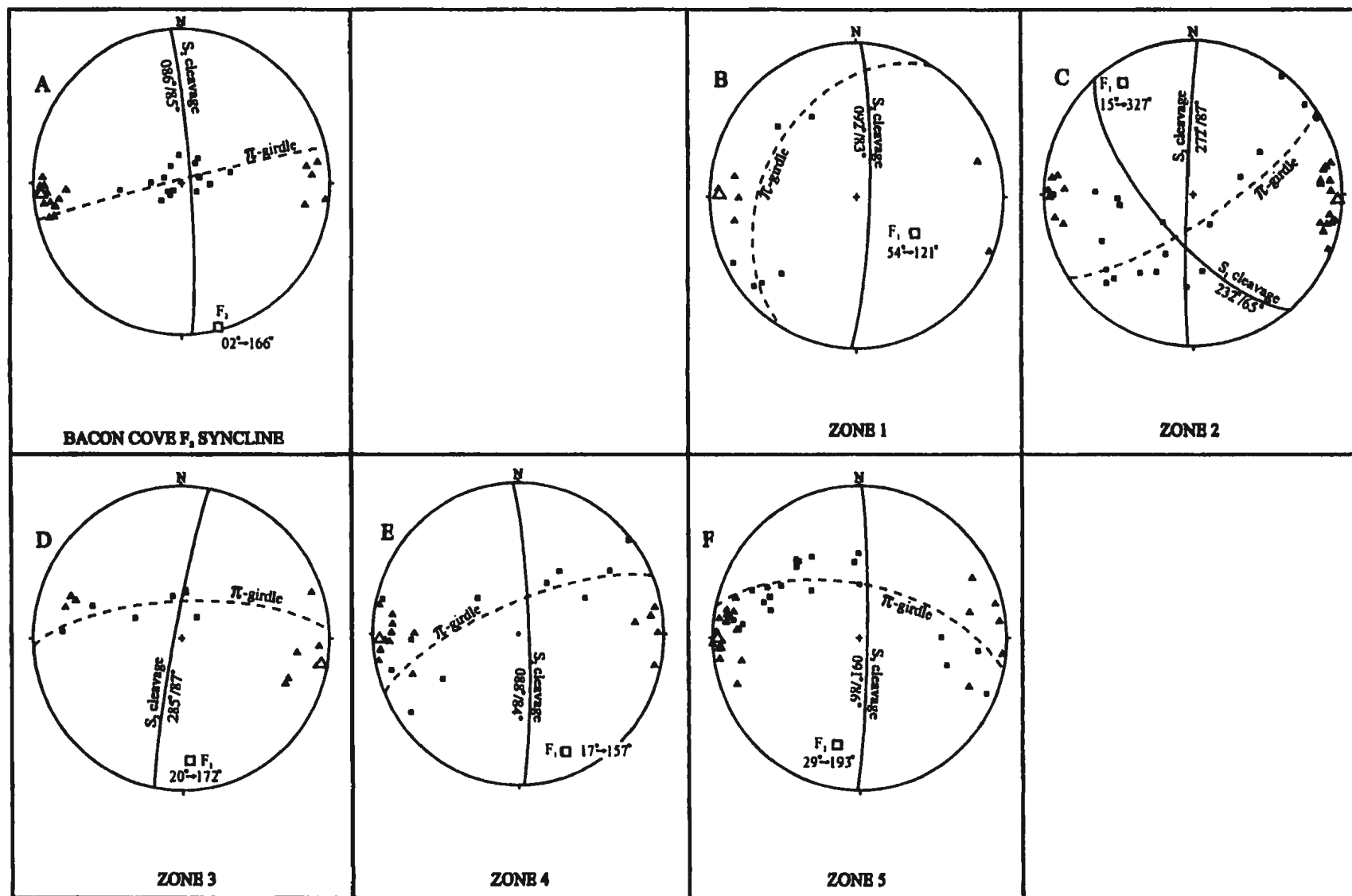


Fig. 2.23 Summary stereo plots of the Bacon Cove F<sub>1</sub> syncline (A) and the five zones in the Conception Group surrounding the syncline (B-F). See Fig. 2.8 for zone locations). □ = pole to π-girdle (poles to S<sub>0</sub>, π), △ = mean of poles to S<sub>1</sub> cleavage, ▲.

orientation remains relatively constant across the fault. These relationships indicate that the Proterozoic rocks were affected by tilting and the northeast-trending Junction and northwest-trending Pigeon faults during  $D_1$ .

### **2.3.1.2 $D_1$ Normal Faults**

#### ***$D_1$ Brigus Fault Zone***

The steeply west-dipping Brigus fault zone separates rocks of the Conception Group to the west from older rocks of the Harbour Main Group to the east of the fault zone in the Brigus area (Fig. 2.24). The fault zone is up to 100 metres wide and contains horses both of the Harbour Main and Conception group rocks (Fig. 2.25). East of the fault zone, Cambrian rocks unconformably overlie massive volcanic rocks and layered sedimentary rocks of the Harbour Main Group, best exposed at North Head and Seal Head (Fig. 2.4). To rationalize these stratigraphic associations, the Brigus fault must have down-thrown rocks of the Conception Group relative to rocks of the Harbour Main Group prior to the onlap of Cambrian rocks, indicating normal separation on the Brigus fault zone in  $D_1$ . This is a significant  $D_1$  relationship which depicts the Brigus fault zone as a pre-Cambrian structure and assumes that at least the lower Conception Group blanketed the Harbour Main Group in the study site.

#### ***Chapels Cove Area***

Analogous to the Brigus area, east of the steeply west-dipping Little Brook fault in the Chapels Cove area, the sub-Cambrian unconformity terminates against the fault and overlies a steeply-dipping panel of Harbour Main Group basaltic and dacitic tuffs and granitic dykes of the Holyrood Intrusive Suite (Fig. 2.13). A steeply east-dipping homocline of the Conception Group occurs west of the South Brook fault. The north-northwest-trending Little Brook fault is interpreted to be a splay of the major north-trending South Brook fault. These stratigraphic associations suggest that uplift and erosion of the Conception Group occurred in Proterozoic



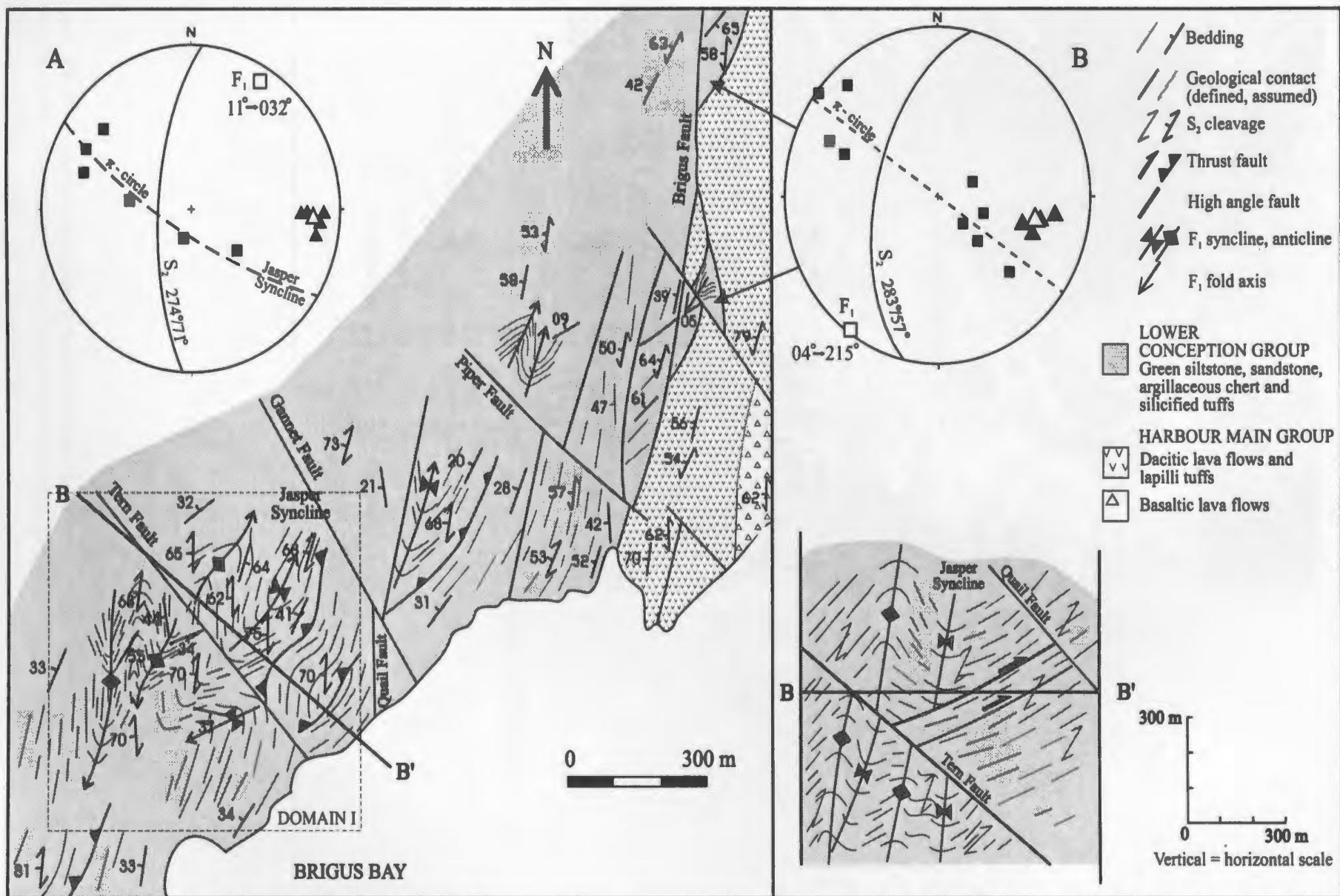
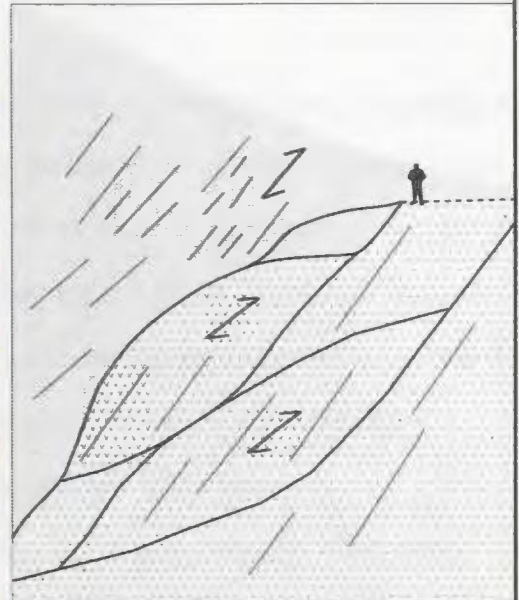
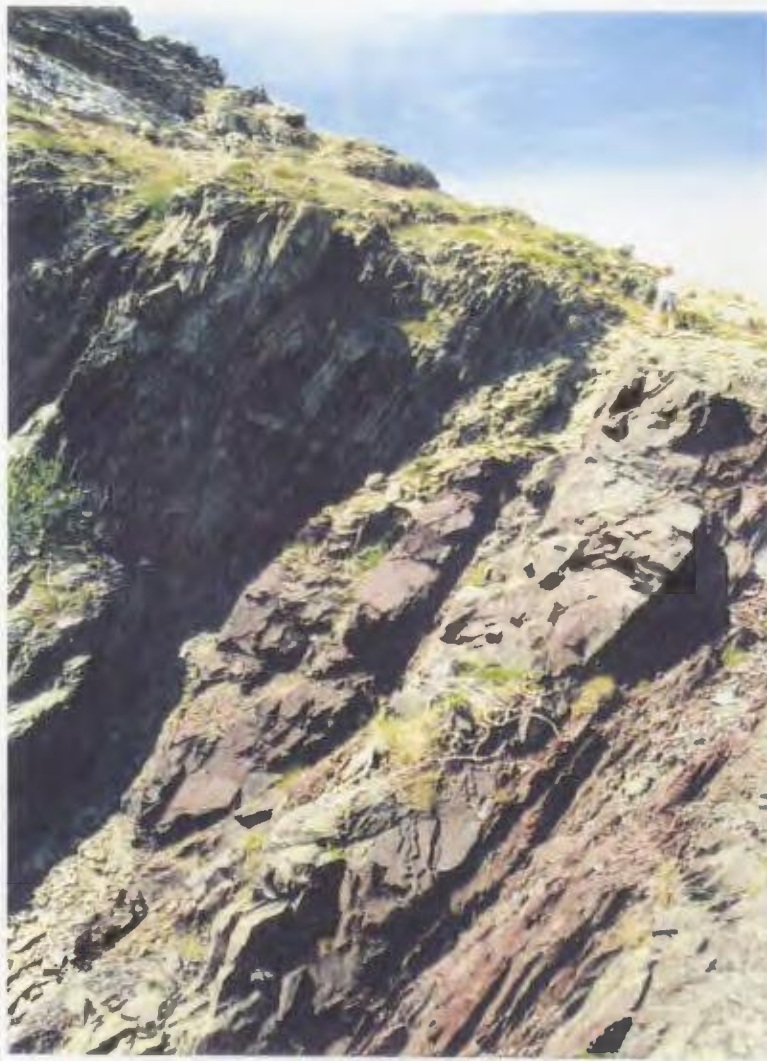


Fig. 2.24 Cross-section BB' across Domain I in the Brigus area, shows open to closed northeast- to north-trending  $F_1$  folds (projected along the plunge of the Jasper Syncline). These sub-cylindrical folds occur along east-verging,  $S_0$ -parallel thrusts in layered Conception Group rocks shown by stereo plot A, and in horses in the Conception Group along the Brigus fault (shown by stereo plot B).  $S_2$  cross-cuts their axial surfaces by more than 20 degrees in plan view.  $\square$   $\pi$ -pole to  $\pi$ -circle (poles to  $S_0$ ),  $\Delta$  mean of poles to  $S_2$ ,  $\blacktriangle$



- LOWER CONCEPTION GROUP**  
 Green siltstones and sandstones, argillaceous cherts, silicified tuffs
- HARBOUR MAIN GROUP**  
 Dacitic and basaltic lapilli tuffs
- Bedding
- S<sub>2</sub> cleavage
- High angle fault

Fig. 2.25 The sketch of the photograph shows the Brigus fault zone, defined by mesoscopic horses, which separate fault sub-parallel Conception Group rocks from Harbour Main Group tuffaceous layers to the east. Looking northwest, Gull Cove, Brigus map area.

time, east of the Little Brook fault and probably in the horse bounded by the Little Brook and South Brook faults. Thus, the Little Brook and South Brook faults underwent apparent normal separation during  $D_1$ .

#### ***D<sub>1</sub> West Limb-Cowboy Horst, Bacon Cove Area***

The steeply dipping red tillite beds interpreted to belong to the Gaskiers Formation of the Conception Group are separated from adjacent green turbiditic Conception Group rocks by the west-dipping West Limb fault and east-dipping Cowboy fault in the Bacon Cove area (Fig. 2.8, 2.9BB'). The red tillite is unconformably overlain by the lower Cambrian sequence, and is assumed to represent beds that are stratigraphically below the green turbiditic rocks. To rationalize these stratigraphic relationship, the West Limb and Cowboy faults must have undergone normal separation during  $D_1$ , if we assume that the red tillite unit is stratigraphically older than the green turbiditic units of the Conception Group. This fault-bounded block is referred to as the West Limb-Cowboy Horst.

#### ***D<sub>1</sub> Beach-Salmon Cove Horst***

The steep, north-northeast-trending Beach and Salmon Cove faults in the Salmon Cove area, bound a zone about 400 m wide, of Harbour Main dacitic and basaltic lava flows and tuffs, and separate it from adjacent Conception Group rocks (Figs. 2.10, 2.11). This zone is referred to as the Beach-Salmon Cove Horst. Cambrian beds disconformably overlie the horst which suggests that the horst formed during  $D_1$ .

Exposures of the steeply west-dipping Salmon Cove fault surface show dip-slip slickensides. The Beach fault is extrapolated from an aerial photograph lineament and from the termination of Conception and Harbour Main group sequences on either side of the fault. The Beach fault is assumed to be a vertical fault based on its rectilinear morphology.

## **2.3.2 D<sub>2</sub> Post-Cambrian Structures**

### **2.3.2.1 F<sub>2</sub> Folds and Associated Faults**

#### ***North Head, Brigus Area***

At North Head (Fig. 2.4), moderately east-dipping basal Cambrian units nonconformably overlie massive volcanic tuffs of the Harbour Main Group (Fig. 2.26). In basal Cambrian mudstones, siltstones and shales and nodular limestone beds, a mesoscopic open, s-symmetry syncline formed with slightly convergent axial plane S<sub>2</sub>, which cross-cuts the nonconformity with negligible refraction. S<sub>2</sub> is weakly formed in the underlying massive tuffs and flows of the Harbour Main Group. This syncline is necessarily a post-Cambrian structure because it deforms Cambrian strata. Its axial planar relationship with S<sub>2</sub> suggests the syncline is an F<sub>2</sub> fold. In Cambrian shales, slickensides rake 65° to the south on S<sub>0</sub>-parallel (moderately east-dipping) shear surfaces, compatible with F<sub>2</sub> flexural slip. In general, S<sub>2</sub> forms at high angles to Cambrian bedding in the Brigus area, making an angle of about 85° (Fig. 3.26B). The s-symmetry of the syncline suggests west-vergence, consistent with the s-symmetry of open, macroscopic folds throughout the generally east-dipping panel of Cambrian rocks, farther south in the Brigus area (e.g., Fig. 2.1B).

#### ***F<sub>2</sub> Marysvale Syncline-Anticline Pair***

The Marysvale syncline and associated subordinate anticline (Figs. 2.6, 2.7) in Cambrian strata are open, shallowly south-southwest-plunging folds extrapolated from mapping and air photo interpretations. These structures are necessarily post-Cambrian F<sub>2</sub> structures because they affect Cambrian rocks and show axial planar S<sub>2</sub> in sectional view.

The F<sub>2</sub> syncline-anticline pair is parallel to and terminates against and east of the steeply west-northwest-dipping Marysvale fault. The Conception Group occurs west of the fault. These relationships, combined with the consistent north-trend of S<sub>2</sub> across the fault,



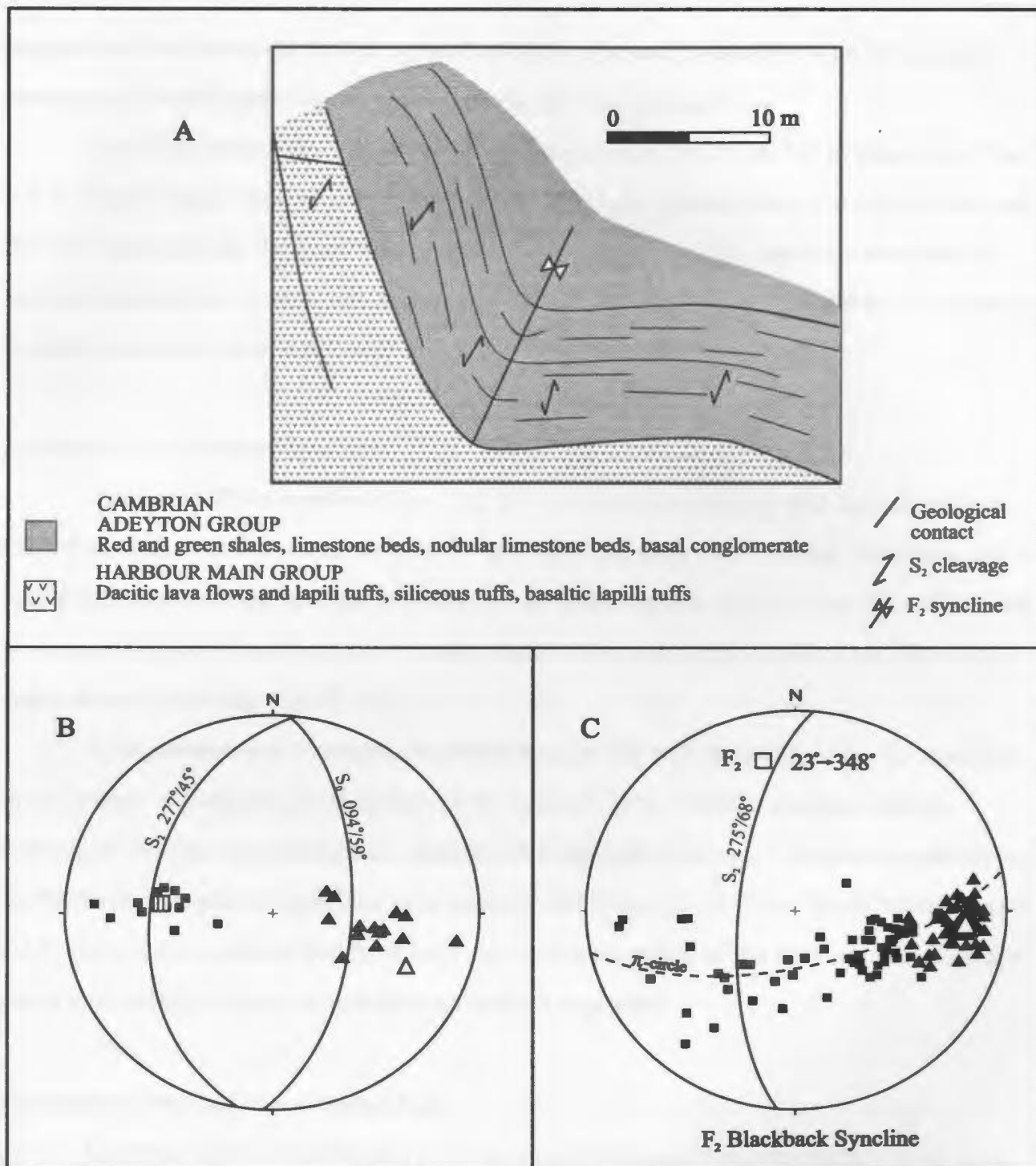


Fig. 2.26 A) shows a sketch of a profile section projected along the plunge of a mesoscopic F<sub>2</sub> syncline (oriented 17°-030°) in basal Cambrian units that nonconformably overlie Harbour Main Group tuffs (looking north at North Head, Brigus area). B) is a summary stereo plot that shows S<sub>2</sub> make a large angle with Cambrian S<sub>0</sub> in the Brigus area. C) is a summary stereo plot of the sub-cylindrical F<sub>2</sub> Blackback Syncline in the Conception Group, with axial plane S<sub>2</sub>.  
□ π-pole to π-circle (poles to S<sub>0</sub>), ▣, Δ mean of poles to S<sub>2</sub>, ▲, ▢ mean of poles to S<sub>0</sub>.

suggest that the Marysvale fault is a post-Cambrian structure, compatible with an apparent reverse and dextral strike-slip component along the fault during  $F_2$ .

The  $F_2$  syncline-anticline pair axial trace is transected by  $S_2$  by  $12^\circ$  in plan view (Figs. 2.6, 2.7-stereo plot). This transection is interpreted to have resulted from the local control on the fold orientation by the Marysvale fault, and does not reflect the regional stress field. A regional, approximately east-west shortening associated with  $D_2$  is represented by the pervasive  $S_2$  in this area, as it does in the other areas.

### ***$F_2$ Bacon Cove Periclinal Syncline***

The Bacon Cove syncline (Figs. 2.8, 2.9) is an open, periclinal fold formed in lower Cambrian rocks, and thus necessarily an  $F_2$  structure. The periclinal syncline terminates into a horizontal homocline and a series of thrusts to the south towards Bacon Cove. Cambrian beds are bounded by the West Limb and Cowboy steep faults, and by the Upper Cove, Wharf and Aspen thrust faults (Fig. 2.9BB', CC').

$S_2$  is penetrative in Cambrian strata throughout this fold. In profile view,  $S_2$  is parallel to the steeply east-dipping axial surface of the syncline (Fig. 2.9BB'), showing slightly convergent cleavage morphology, as observed at hinge zone outcrops. However, in plan view,  $S_2$  clockwise transects the synclinal axial trace by  $10^\circ$  (Figs. 2.8, 2.23A). The  $S_2$  transection of the  $F_2$  periclinal syncline probably reflects the very open nature of the syncline, which would result in a variably oriented synclinal axial trace in map view.

### ***$F_2$ Chapels Cove Syncline-Anticline Pair***

Cambrian beds in the Chapels Cove area were deformed into the Chapels Cove open, north-northeast trending and west-verging syncline-anticline pair (Figs. 2.13, 2.14), which is necessarily ascribed to an  $F_2$  structure. Small, variably oriented thrust faults affect both Cambrian and Harbour Main groups in the area of the Chapels Cove fold pair and are consistent with  $D_2$ . The orientation of the Chapels Cove fold pair appears to be strongly

controlled by the orientation of the north-northeast-trending Pelee, Pebble, and Rose faults, rather than by the regional east-west shortening direction indicated by  $S_2$ .

The regional, north-northeast-trending  $S_2$  is penetrative in both Proterozoic and Cambrian rocks across the area. In sectional view,  $S_2$  is axial planar to the open Chapels Cove syncline-anticline pair (Fig. 2.14AA', BB'). However, in plan view,  $S_2$  clockwise transects the axial traces of the folds by about  $14^\circ$  (Fig. 2.13-stereo plot).  $S_2$  transection may reflect the influence the orientation that the Pelee, Pebble and Rose faults have on the orientations of the axial trace of the Chapels Cove syncline-anticline pair and does not reflect the regional stress field during  $D_2$ .

### ***Salmon Cove Syncline***

The open, north-trending Salmon Cove syncline formed in Cambrian strata with axial plane  $S_2$  in map and sectional view (Figs. 2.10, 2.11BB') and is thus an  $F_2$  structure. The syncline is bounded by the Beach fault to the west and the Salmon Cove fault to the east.

In the eastern limb of the open syncline, in a zone extending to 6 metres from the Salmon Cove fault, Cambrian strata are steep to overturned with shallowly east-dipping  $S_2$ . The angle between  $S_0$  and  $S_2$  is about  $50^\circ$  (Fig. 2.27A). Subordinate  $S_0$ -parallel thrust faults and associated steeper, mesoscopic, west-directed thrusts show minor offsets of Cambrian strata. The orientation of extension veins with respect to fault surfaces further indicates thrust movement on the faults, compatible with  $D_2$ . Further up-section, towards the core of the Salmon Cove syncline, west from the Salmon Cove fault, Cambrian strata shallow in dip from overturned to moderately west-dipping, while  $S_2$  steepens (Fig. 2.27B). These geometric relationships between Cambrian strata and  $S_2$  suggest that (anomalously) shallow  $S_2$  and steep Cambrian  $S_0$  adjacent to the Salmon Cove fault may represent the core of a slightly overturned, mesoscopic  $F_2$  anticline (Fig. 2.27B). This structure is subsequently truncated by normal movement on the Salmon Cove fault.

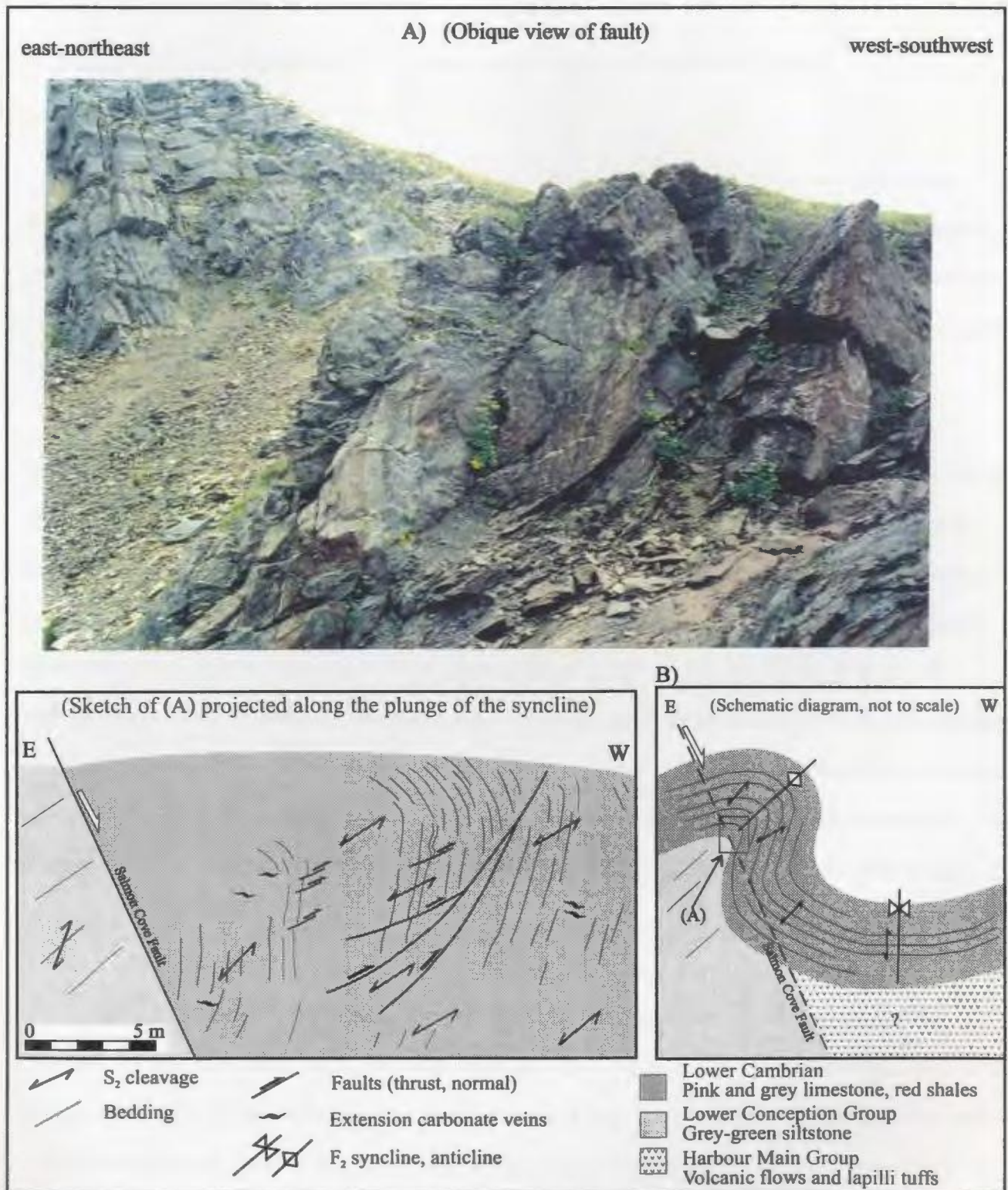


Fig. 2.27 A) Photograph and sketch show the Salmon Cove normal fault. In the hangingwall, both Cambrian strata and  $S_2$  are rotated possibly representing convergent cleavage morphology in the eastern limb of an  $F_2$  mesoscopic anticline (B). Subordinate west-directed thrusts are related to this folding. Rotated Cambrian  $S_0$  and  $S_2$  terminate against the Salmon Cove fault. Alternatively, rotation of  $S_2$  and Cambrian  $S_0$  may represent commensurate rotation in post- $S_2$  time along the Salmon Cove fault. Looking south-southeast in the photograph, eastern shore of Salmon Cove. Sketches are projected along the plunge of the Salmon Cove  $F_2$  syncline.

### **2.3.2.2 D<sub>2</sub> Reverse, Oblique-slip and Thrust Faults**

#### ***D<sub>2</sub> Bacon Cove Fault Zone***

A steeply east and west dipping cleavage is very strong in zones up to 500 metres wide, adjacent to the Bacon Cove fault in Conception and Harbour Main group argillaceous units. This cleavage is consistent in orientation with regional S<sub>2</sub>. This is further supported by Conception Group conglomerate cobbles that are flattened in strongly developed and sinuous S<sub>2</sub>, by the Fishing Cove, adjacent to the Bacon Cove fault (Fig. 2.8).

A sectional view photomicrograph of one such conglomerate shows lithic clasts aligned parallel to strongly developed S<sub>2</sub> (Fig. 2.28A). The degree of flattening or stretching of the clasts in the cleavage plane is uncertain, since the original shapes of the clasts are not known. A plan view photomicrograph of the conglomerates shows c-s shear fabrics where S<sub>2</sub> ('s' planes) is progressively rotated and flattened towards S<sub>0</sub>-parallel shear planes ('c' planes). This indicates a minor component of apparent sinistral strike-slip during D<sub>2</sub> (Fig. 2.28B). A c-s shear fabric is not obvious at the mesoscopic scale. S<sub>2</sub> orientation remains relatively constant adjacent to the fault in both plan and sectional views (Figs. 2.8, 2.9AA'). Thus based on these observations, it is interpreted that the Bacon Cove fault is a D<sub>2</sub> structure which underwent predominantly east-west shortening, accompanied by minor, apparent sinistral strike-slip.

#### ***D<sub>2</sub> West Limb-Cowboy Inverted Horst and Associated Faults, Bacon Cove Area***

The Bacon Cove periclinal syncline in Cambrian rocks forms in a horse partly bounded by the west-dipping West Limb fault and east-dipping Cowboy fault (Fig. 2.8). This stratigraphic association indicates that the faults were active during post-Cambrian time and underwent apparent reverse slip (Fig. 2.9). Thus, the D<sub>1</sub> West Limb-Cowboy Horst, described above, was reactivated during D<sub>2</sub> contraction, suggesting that the fault-bounded block represents an inverted D<sub>1</sub> horst.



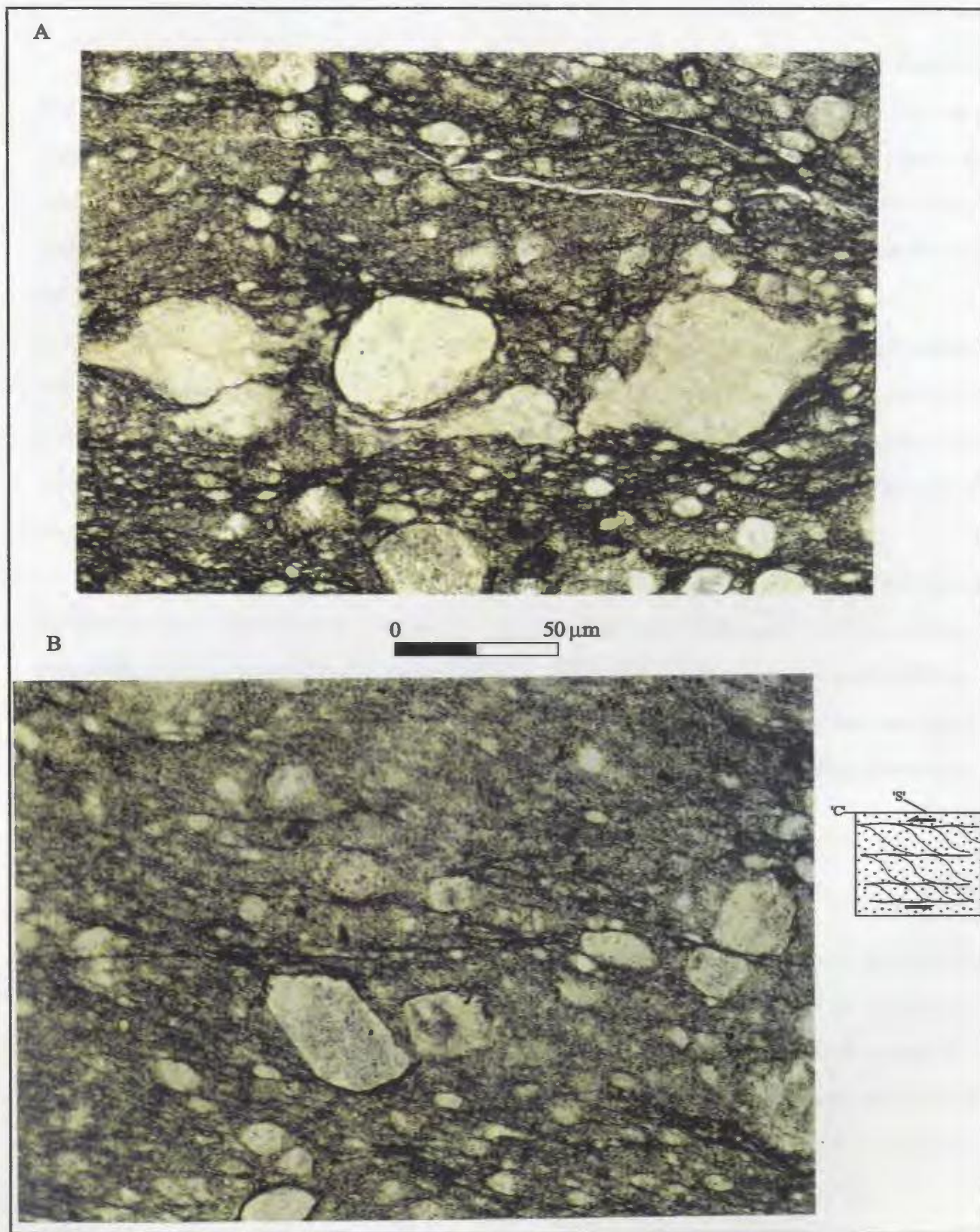


Fig. 2.28 Photomicrographs (plane-polarized light) of Conception Group conglomerate adjacent to the Bacon Cove fault, Bacon Cove area. A) Sectional view of photomicrograph shows strongly developed  $S_2$ -parallel  $S_2$ . Lithic clasts show minor rotation, however, not significant enough to provide kinematic indications. B) Plan view of photomicrograph and sketch show a c-s shear fabric. Sigmoidal  $S_2$  cleavage ('s') is rotated and flattened towards  $S_0$ -parallel, shear planes ('c') indicating apparent  $D_2$  sinistral strike-slip.

The sub-Cambrian unconformity terminates at the Upper Cove and Aspen thrusts. The unconformity is rotated to overturned dips into the faults while  $S_2$  orientation and dip remain constant (Figs. 2.8, 2.9BB'). This rotation of Cambrian beds is best interpreted to have resulted from thrusting along the west-directed Upper Cove and east-directed Aspen thrust faults, compatible with  $D_2$ . Exposures of these thrusts along the unconformable contact near the wharf reflect the complex structural relationships in this area.

The Bacon Cove syncline terminates southward as Cambrian strata form a horizontal homocline and are segmented by a complex array of thrusts ranging in trend from northwest to northeast (Figs. 2.8, 2.9BB', CC'). The east-directed Wharf thrust carries Conception Group strata onto basal Cambrian rocks. Slickensides on the thrust surface indicate east-directed dip-slip. The Wharf thrust is consistent with contraction associated with  $F_2$  folding.

In the footwall of the Wharf thrust, a minor southwest-directed shallow thrust truncates the sub-Cambrian unconformity surface and shows slickensides raking  $80^\circ$  to the southeast, on a shallowly, northeast-dipping surface (Fig. 2.9CC'). This thrust terminates at the Wharf thrust and may represent a minor component of detachment proximal to the unconformity during  $D_2$ . The shallow thrust is consistent with deformation during contraction, associated with  $S_2$  development.

#### ***D<sub>2</sub> Red and Park Faults, Marysvale Area***

To the south of the Marysvale syncline-anticline pair, the Red and Park faults truncate and displace the syncline-anticline pair, indicating post-Cambrian movement on the faults (Figs. 2.6, 2.7). The Park fault may be a splay of the Red fault which terminates against the Marysvale fault. The Park fault was extrapolated from stratigraphic associations and a linear feature on air photographs. However, exposed surfaces of the Red fault indicate a variation in its orientation from shallowly southwest-dipping to steeply northwest-dipping, with slickensides that rake  $40^\circ$  to the southwest on northwest-dipping surfaces. Based on slickensides and stratigraphic associations, the fault underwent at least post-Cambrian, apparent oblique-slip displacement.

The lower Cambrian stratigraphic section bounded by the Red and Park faults, is over 200 metres thick, which is about 80 metres thicker than the lower Cambrian stratigraphic section contained in the Marysvale syncline (e.g., Hutchinson 1962) (Fig. 2.7CC'). This increase in stratigraphic thickness may represent structural thickening by thrust stacking or stratigraphic variations. The former interpretation is most likely because these Cambrian sequences are more deformed than Cambrian sequences in the Marysvale syncline-anticline pair.

### **2.3.2.3 D<sub>2</sub> Normal Faults**

#### ***D<sub>2</sub> Ray and Long Pond faults, Brigus Area***

The north-northeast-trending Ray fault cuts tuffs and sedimentary interlayers of the Harbour Main Group and unconformably overlying Cambrian strata (Fig. 2.4). Based on cross sectional interpretations, the fault displaces the unconformity about 40 metres in a predominantly dip-slip sense (Fig. 2.5). The parallel Long Pond fault occurs in Harbour Main Group rocks and truncates Cambrian sequences (Fig. 2.29). The control on the magnitude of apparent dip-slip on the Long Pond fault is not as well constrained as that for the Ray fault. However, based on offsets in the Harbour Main Group, the Long Pond fault must have undergone at least 60 metres of vertical displacement. Based on the relative normal offsets of the Ray and Long Pond faults and rotation of adjacent Cambrian rocks and S<sub>2</sub>, the faults underwent post-Cambrian normal separation.

#### ***D<sub>2</sub> North Head Shallow Fault, Brigus Area***

The minor, shallow North Head fault crops out at North Head in the Brigus area (Fig. 2.4) and varies from sub-horizontal to east-dipping across and along the sub-Cambrian nonconformable surface between basal Cambrian units and Harbour Main Group tuffs (Fig. 2.30). The centimetre-scale displacement accommodated by the imbrication of both rock types, combined with the commensurate rotation of S<sub>2</sub> and the nonconformable contact into



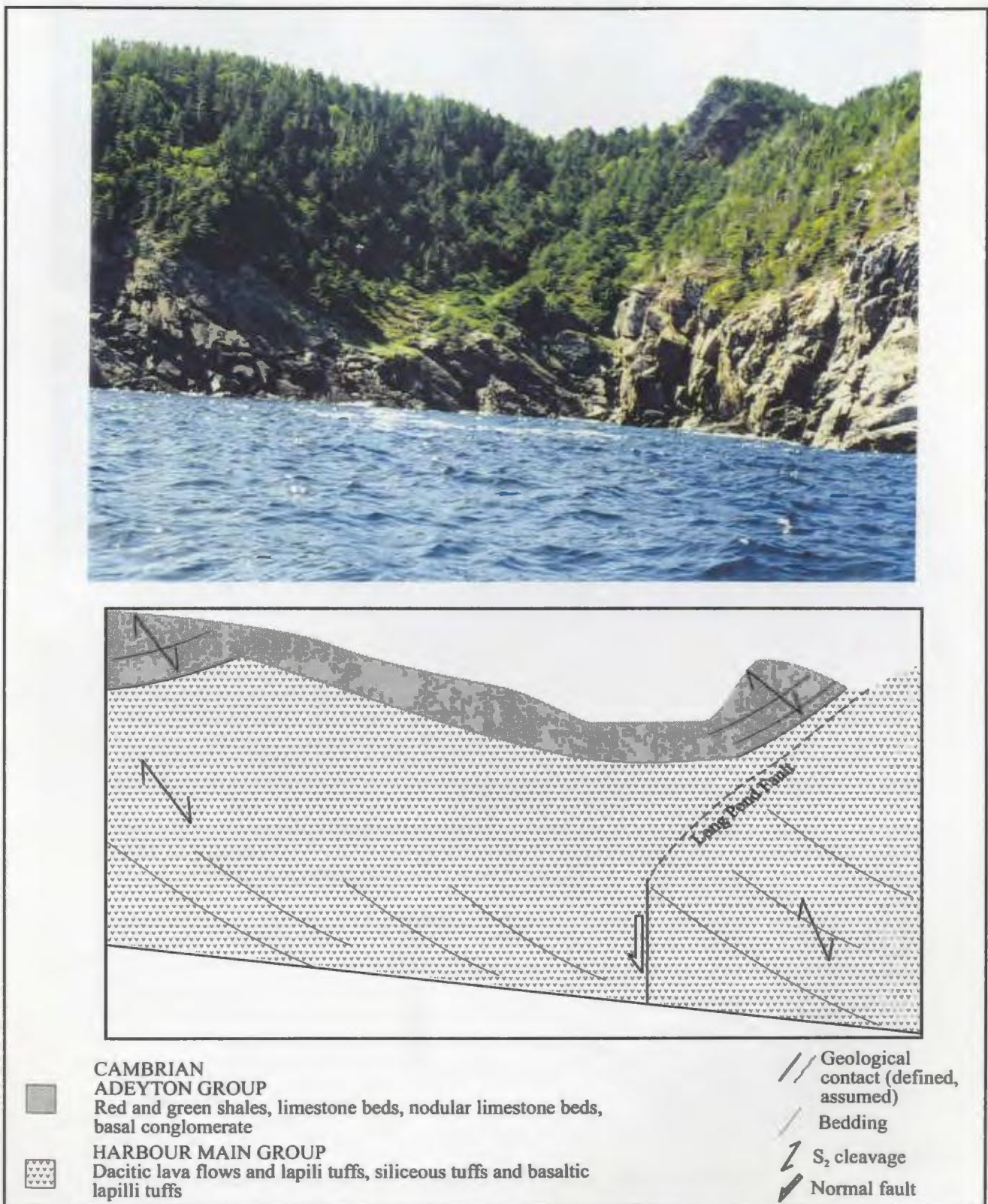


Fig. 2.29 The sketch of the photograph shows the steeply east-dipping Long Pond fault separating Cambrian rocks nonconformably overlying Harbour Main Group tuffs in the hangingwall from Harbour Main Group tuffs in the footwall. The rotation of Cambrian and Harbour Main Group  $S_0$ , and  $S_2$  towards the fault, as well as the absence of Cambrian rocks in the footwall, suggest that the fault underwent a component of post- $S_2$  normal displacement. Note that the photograph shows both map and sectional apparent views. Looking south-southeast, about 400 m southeast of Tur Point, Brigus area.



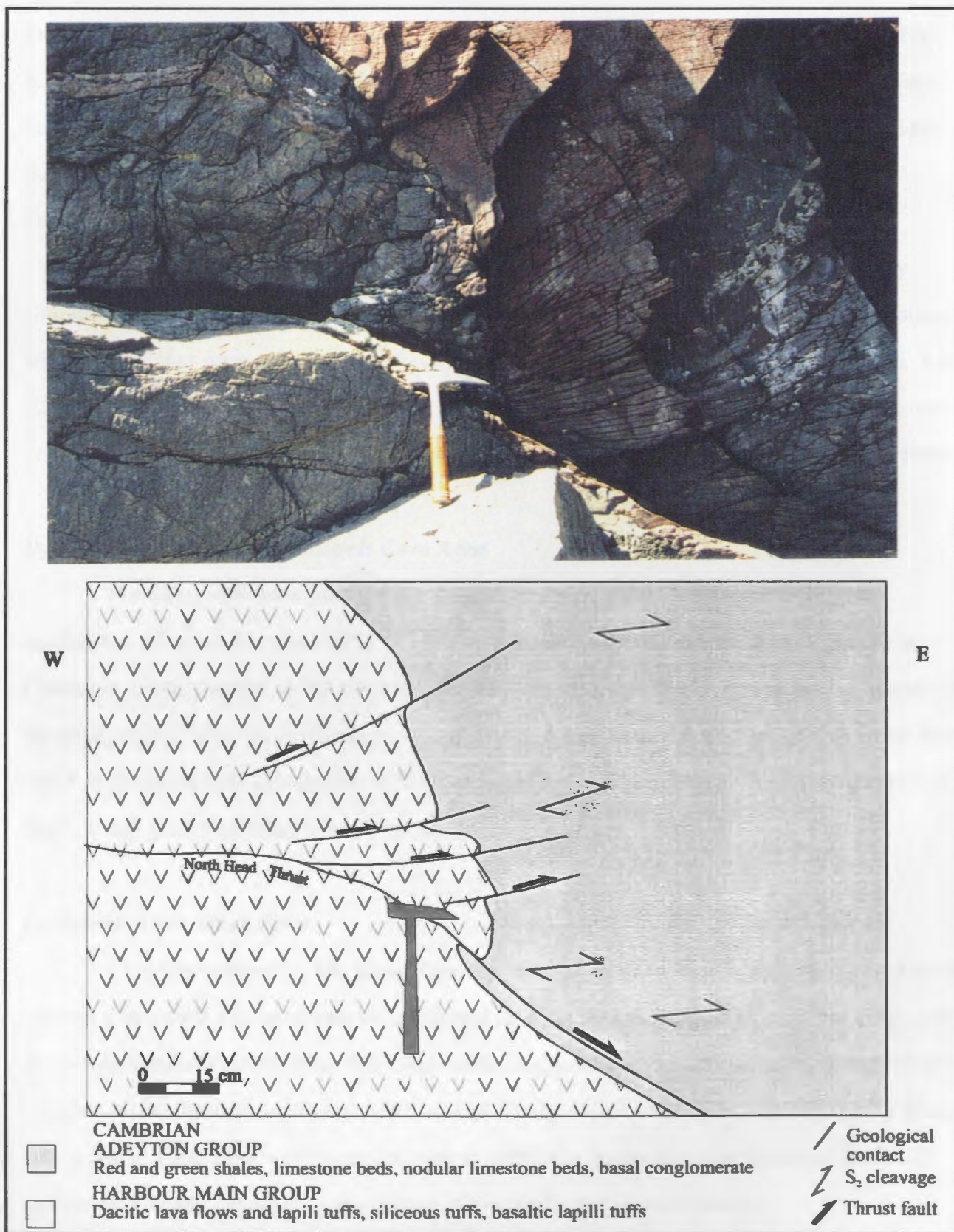


Fig. 2.30 The sketch of the photograph shows the east-directed North Head minor shallow fault across the nonconformable contact between basal Cambrian shale and underlying Harbour Main Group tuffs. The fault is accommodated by the imbrication of both rock types. The contact and S<sub>2</sub> are rotated which suggests that the fault underwent post-S<sub>2</sub> movement.

the fault, in a zone of up to 50 centimetres wide, suggest that the fault is east-directed (Fig. 2.30). A c-s shear-type fabric, defined by the alignment of chlorite and sericite in the fault zone further indicates that the fault underwent east-directed shear (Fig. 3.31). Slickensides rake 40° to the south, on the moderately east-dipping, bed-parallel portion of the fault, indicating dip-slip on the fault.

S<sub>2</sub> displays sub-horizontal dips adjacent to the fault that cannot be construed by simple S<sub>2</sub> refraction. Furthermore, east-directed movement on the fault would be inconsistent with F<sub>2</sub> folds that were interpreted to have been west-verging in the Brigus area (*cf.* Figs. 2.1B, 2.26A). Thus, commensurate rotation of S<sub>2</sub> and S<sub>0</sub> along the fault is interpreted to represent drag folding associated with post-S<sub>2</sub> apparent normal displacement on the North Head fault.

#### ***D<sub>2</sub> Pelee and Rose Faults, Chapels Cove Area***

The Pelee and Rose faults in the Chapels map area show normal stratigraphic separations of up to 70 metres (Fig. 2.14AA'). Similarly, the steep Pebble fault occurs in Cambrian strata, parallel to the trend of the Chapels Cove syncline-anticline pair. Adjacent to the fault, in a zone of up to 50 metres wide, post-S<sub>2</sub> commensurate rotation of Cambrian strata and S<sub>2</sub> into the fault is compatible with an apparent west-side down (normal) movement on the fault during post-Cambrian time (Fig. 3.32).

#### ***D<sub>2</sub> Salmon Cove Fault Zone***

An interpretation for the significant dip rotation in Cambrian S<sub>0</sub> and S<sub>2</sub> adjacent to the Salmon Cove fault was given above, attributed to a slightly overturned F<sub>2</sub> anticline (Fig. 2.27). An alternative interpretation for this observation suggests that the deformation is attributed to commensurate rotation associated with normal displacement on the Salmon Cove fault during post-S<sub>2</sub> time. Field observations are consistent with both interpretations, whereby the whole system was rotated adjacent to the Salmon Cove fault, during and post-S<sub>2</sub>.

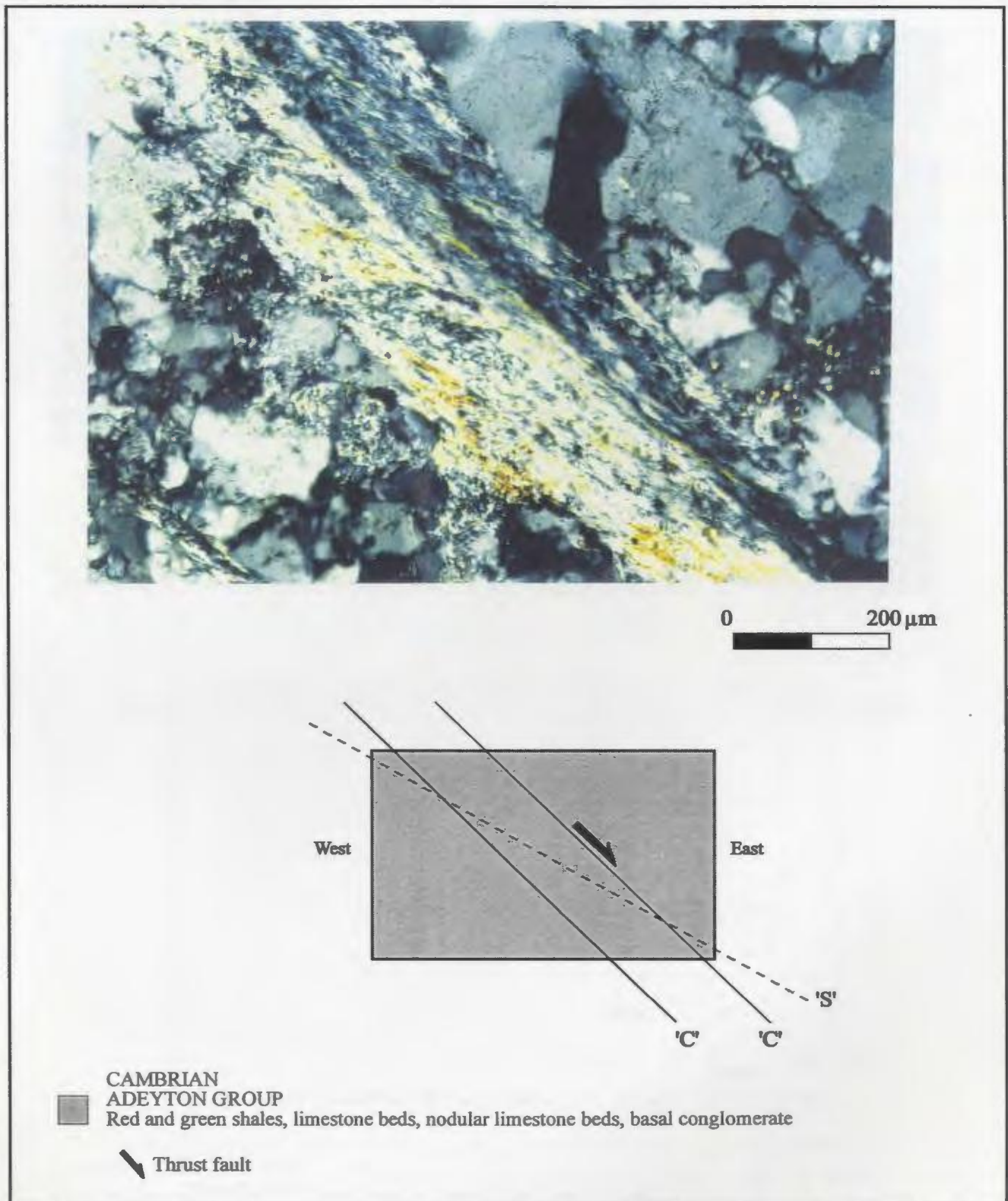


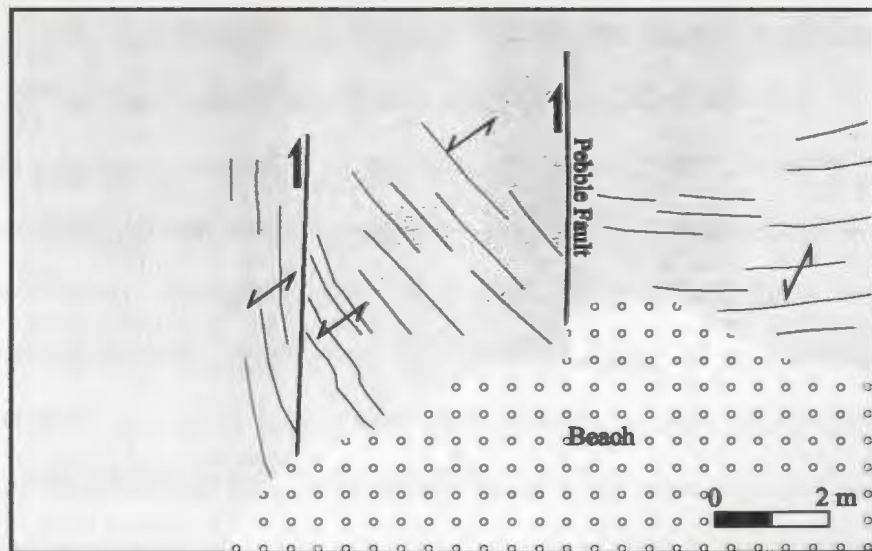
Fig. 2.31 A schematic representation of the photomicrograph shows the east-directed Cambrian  $S_0$ -parallel North Head fault (quartz-filled zone) shown by the c-s shear-fabric defined by the alignment of chlorite and sericite. Looking north, North Head, Brigus area. Cross-polarized light. Section cut perpendicular to  $S_1$  and  $S_2$  and parallel to slickenside striae.





ESE

WNW



CAMBRIAN  
Adeyton Group  
Red and green shales and limestones, nodular limestones



Bedding  
S<sub>2</sub> cleavage  
Reverse fault

Fig. 2.32 Photograph and sketch of the normal post-S<sub>2</sub> Pebble fault and minor parallel fault in lower Cambrian strata. Looking south-southwest, Pebble cove, Chapels Cove area.

### 2.3.3 Criteria Established to Distinguish D<sub>1</sub> from D<sub>2</sub> Structures

In multiply deformed areas such as the study site, the account of geometric features and the cross-cutting of structures provide field relationships which can be used to distinguish between structures of different relative ages. Based on field relationships presented above with respect to the sub-Cambrian unconformity as a control of the relative age of structures, certain criteria were established to distinguish between pre- and post-Cambrian structures. The criteria include the following:

- 1) The truncation of tilted, folded and faulted Proterozoic rocks against the sub-Cambrian unconformity with an angular discordance, are necessarily pre-Cambrian or D<sub>1</sub> in age relative to the truncated structures. Similarly, structures that developed in Cambrian rocks were necessarily post-Cambrian or D<sub>2</sub> in age.
- 2) The sub-Cambrian unconformity overlying fault-bounded blocks of the Harbour Main Group, Holyrood Intrusive Suite or basal Conception Group (possibly Gaskiers Formation) indicated horst development in the affected Proterozoic blocks which occurred during post-Conception Group and pre-Cambrian time.
- 3) Mesoscopic, open and box-style to isoclinal and overturned F<sub>1</sub> folds in layered Proterozoic rocks, which were truncated by the sub-Cambrian unconformity, are pre-Cambrian in age. F<sub>1</sub> folds are slightly to strongly reclined, with three main orientations: a) north-northeast-trending, moderately southwest-plunging, b) north-northwest-trending, steeply southeast-plunging, and c) east-west-trending, steeply south-southwest-plunging. Axial plane S<sub>1</sub> developed only in a) and b) where folds were tight to isoclinal.
- 4) Mesoscopic to macroscopic, sub-cylindrical, upright, open F<sub>2</sub> folds and associated S<sub>2</sub> in Cambrian beds are post-Cambrian structures. F<sub>2</sub> formed north- to north-northeast-trending, periclinal open synclines or syncline-anticline pairs, locally preserved in D<sub>2</sub> inverted D<sub>1</sub> horsts.
- 5) The generally north-trending, steep, post-Cambrian S<sub>2</sub> cleavage is the regionally penetrative cleavage across the study site. In contrast, S<sub>1</sub> occurs in discrete hinge zones of

tight  $F_1$  folds.  $S_1$  is axial planar to  $F_1$  in plan and sectional view.  $S_2$  cross-cuts  $F_1$  and  $S_1$  in plan view at high angles, commonly  $40^\circ$ , and obliquely in sectional view.  $S_2$  is axial planar to  $F_2$  folds in sectional view, however, generally transects  $F_2$  axial traces by  $10^\circ$  to  $15^\circ$  in plan view. Based on this consistent relationship and the pervasive occurrence of  $S_2$  across the study site, the cross-cutting relationship (of more than  $15^\circ$ ) of  $F_1$  by  $S_2$  was used to distinguish between  $F_2$  and  $F_1$  folds in both plan and sectional view.

- 6) The rigid body rotation of Cambrian rocks and  $S_2$  proximal to north-trending, steep faults indicates apparent post- $S_2$  normal fault displacement. Moreover, the commensurate rotation of  $S_2$  and Cambrian beds along minor northwest-trending faults, indicate a minor component of post- $S_2$  strike-slip along northwest-trending faults.

## **2.4 Zones Without the Sub-Cambrian Unconformity as an Age Control for Deformation**

The criteria established above were tested in zones in the study site where the sub-Cambrian unconformity was not preserved and therefore could not be used as a temporal control for deformation. Based on these criteria, structures in Proterozoic rocks were assigned to pre-Cambrian ( $D_1$ ) or post-Cambrian ( $D_2$ ) structures.

### **2.4.1 $D_1$ Pre-Cambrian Structures**

#### **2.4.1.1 $F_1$ Folds and Associated Faults**

##### ***Domain I, Brigus Area***

Layered sequences of the Conception Group in Domain I (Fig. 2.24) are folded into a series of macroscopic, north-northeast-trending anticline-syncline pairs. The folds are shallowly plunging to the north-northeast and south-southwest. They are open, upright, east-verging folds associated with minor northeast-trending thrust faults (Fig. 2.24BB'-projected along the plunge of the Jasper syncline). Slickensides rake  $45^\circ$  to the southwest on the thrust

surfaces. Both thrusts and folds terminate against the steeply northeast-dipping Tern and Gannet faults (Fig. 2.24BB').

Outcrops of fold closures show that  $S_2$  clockwise cross-cuts the fold axial surfaces by more than  $20^\circ$  in plan view and is approximately parallel to their axial surfaces in profile view (Fig. 2.24BB'). The large cross-cutting angle (i.e.  $> 15^\circ$ ) between the folds and  $S_2$ , as well as the north-northeast fold orientation suggest that the folds are  $F_1$  structures. However, unlike the north-northeast-trending  $F_1$  folds that terminate at the sub-Cambrian unconformity at Seal Head, these  $F_1$  folds are shallowly plunging and not reclined.

### ***Domain II, Brigus Area***

Domain II, in the Brigus area (Fig. 2.4) comprises a series of macroscopic, north-northeast- to northeast-trending open folds, segmented by a northwest-trending fault, similar to the folds and faults formed in Domain I above. Fold closures are not observed in this domain but are extrapolated from mapping and air photograph interpretations. A stereo plot of Conception Group beds form a loose  $\pi$ -girdle in Domain II and a shallowly north-northeast-plunging fold axis (pole to  $\pi$ -girdle) which are not well constrained (Fig. 2.33A). Thus, based on the stereo plot, the cross-cutting angle of  $14^\circ$  of the fold axial trace by  $S_2$  is unsubstantiated.

However, fold axial traces extrapolated from mapping and air photograph interpretations are cross-cut by  $S_2$  by more than  $20^\circ$  in map view (Fig. 2.4). Thus, based on these overprinting relationships, and their similarity in style and orientation with  $F_1$  folds formed in Domain I, it is inferred that the structures in Domain II have the same  $D_1$  temporal relationships as their counterparts in Domain I.



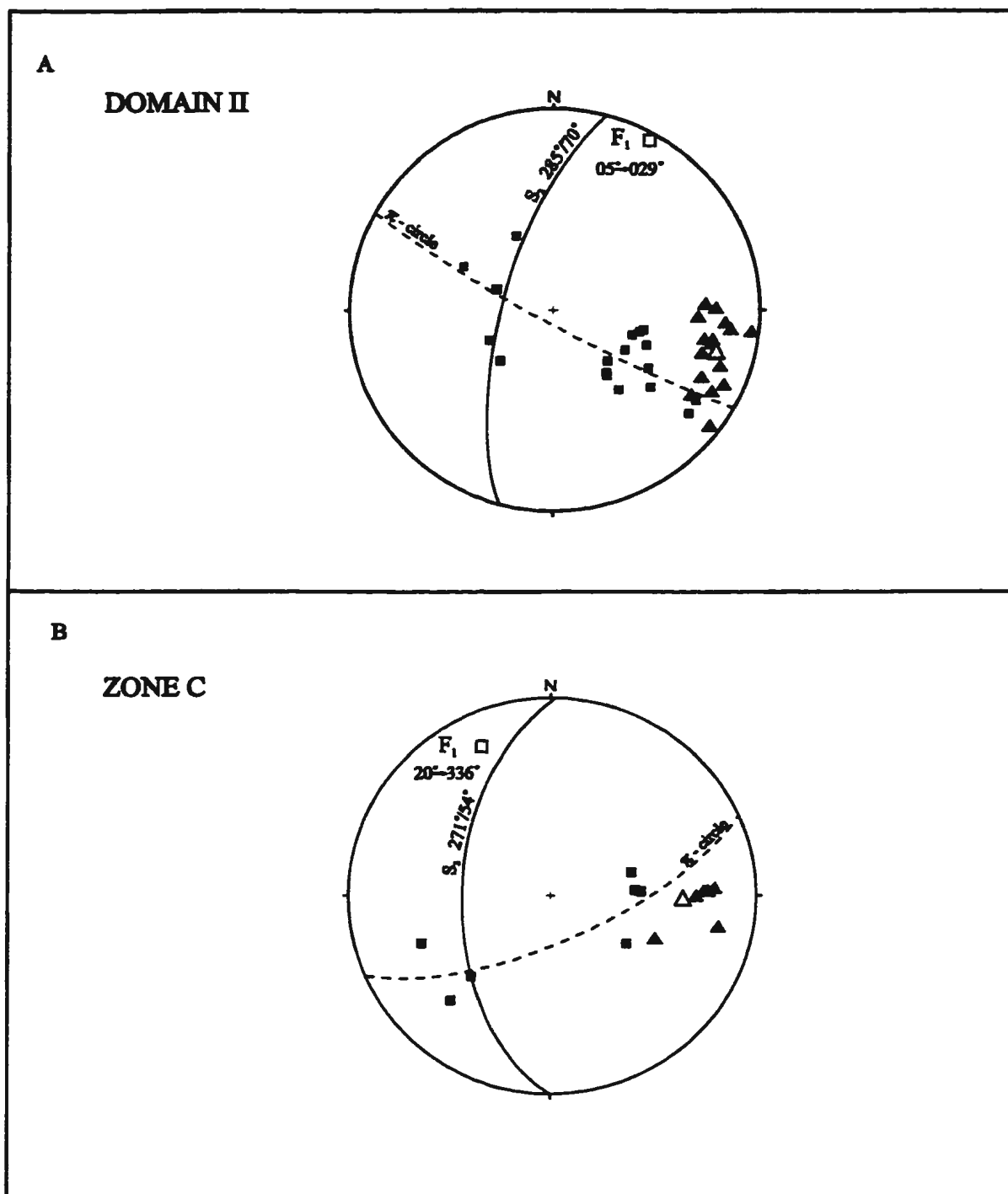


Fig. 2.33 Summary stereo plots of Domain II and Zone C of the Brigus area. A) Domain II shows a sub-cylindrical  $F_1$  fold cross-cut by  $S_2$  by about 15 degrees . B) Zone C shows a north-northwest plunging  $F_1$  fold cross-cut by  $S_2$  by more than 20 degrees.  
 □  $\pi$ -pole to  $\pi$ -circle (poles to  $S_2$ ),  $\Delta$  mean of poles to  $S_2$ ,  $\blacktriangle$ .

### ***Bacon Cove***

Zone 2 in the Bacon Cove area is bounded by the northwest-trending high angle Redpole, Humber and Cowboy faults (Fig. 2.23C). Outcrop exposures show mesoscopic, northwest-trending, west-verging folds with a local and weak axial plane cleavage (Fig. 2.34B). Outcrop exposures show that these folds and associated cleavage are clockwise cross-cut by regional  $S_2$  by more than  $40^\circ$  in plan view. Thus, based on these cross-cutting relationships, these structures are  $F_1$  and  $S_1$  structures.

A cleavage parallel to the northwest-trending  $S_1$  in Zone 2 is preserved in the Conception Group in the limbs of mesoscopic, shallowly south-plunging  $F_2$  folds adjacent to the Bacon Cove fault (Fig. 2.34A) and in open northwest-trending folds near Colliers Point (Fig. 2.34C).  $S_1$  is locally weak in discrete zones across the Bacon Cove map area. The axial planar relationship between  $S_1$  and northwest-trending folds suggest that the folds are  $F_1$ . The cross-cutting relationship of  $F_1$  and  $S_1$  by  $S_2$  by more than  $40^\circ$  in plan and sectional view (Figs. 2.34A, C) further suggest that the structures are  $D_1$  in age.

Some open, northwest-trending, mesoscopic folds in the Conception Group near Colliers Point do not show a developed axial plane cleavage. The axial trace of these folds is clockwise cross-cut by more than  $40^\circ$  by  $S_2$  (Fig. 2.8). Their similar orientation to northwest-trending  $F_1$  folds discussed above, in addition to the cross-cutting relationship with  $S_2$ , indicate that the folds are  $F_1$ .

These open, northwest-trending  $F_1$  folds show brittle deformation in the peripheral units in the form of extensional and shear fractures that are perpendicular to bedding and parallel to the fold axis (Fig. 2.35). These extension fractures may result from tangential strain in the thicker peripheral sandstone beds and may represent reactivated northwest-trending embryonic cleavage ( $S_1$ ). Layer-parallel compression in the inner arc of the folds formed  $S_0$ -parallel extension veins and imbrication of layers along meso-conjugate thrusts (Fig. 2.35). The lack of any obvious solution cleavage development in the inner arc zone suggests the rock deformed under brittle conditions (relatively low pressure and temperature).

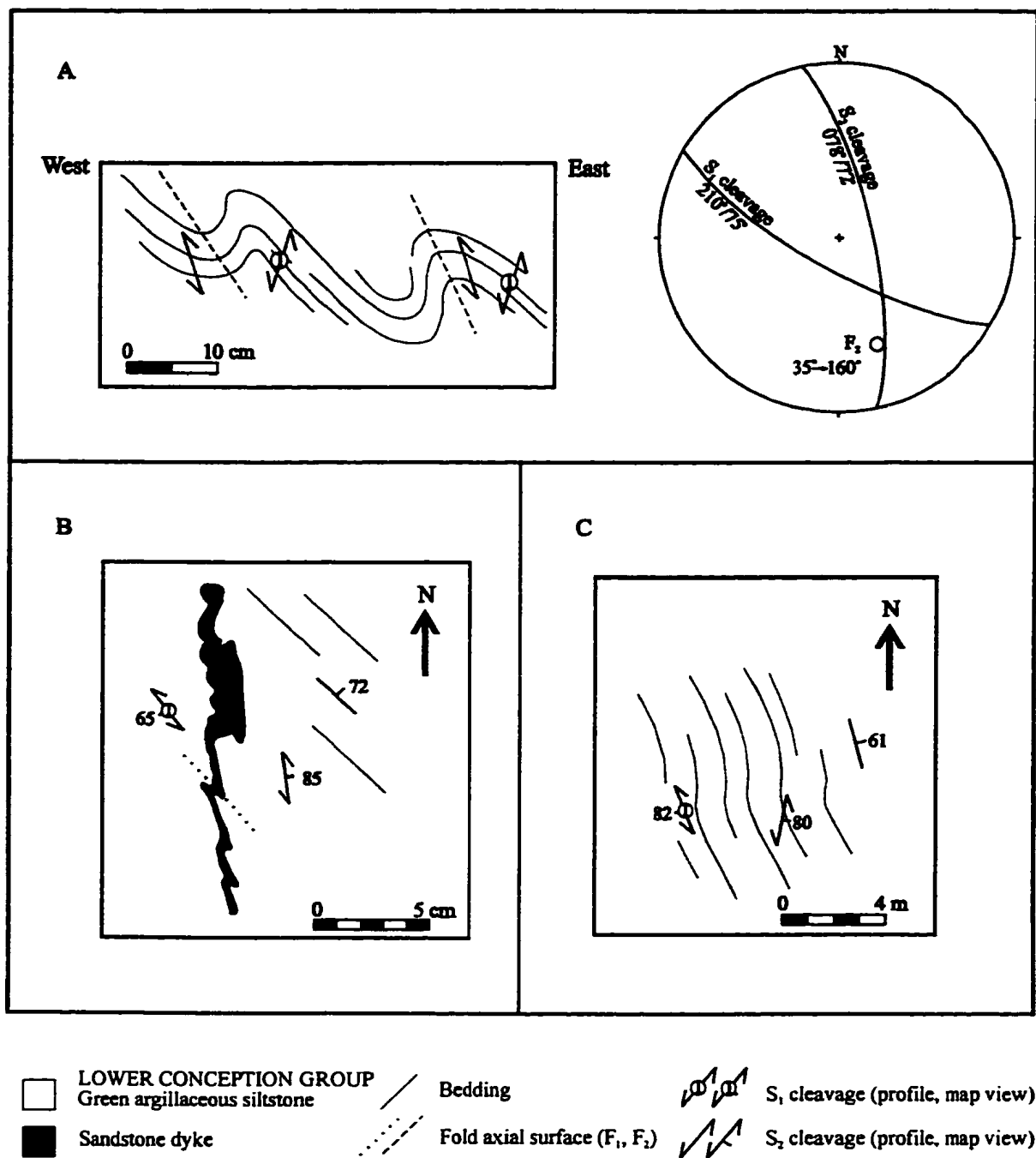


Fig. 2.34 A) The sketch illustrates a sectional view of west-verging, cm-scale  $F_1$  folds and axial planes  $S_2$  in Conception Group siltstones. Weak  $S_1$  is folded and cross-cut by  $S_2$  and is demonstrated in the stereo plot. Looking north, adjacent to the Bacon Cove fault. B) Sketch shows an east-verging  $F_1$  fold in a sandstone dyke in the Conception Group with strong  $S_1$ , and cross-cut by  $S_2$  (from Zone 1 in the Bacon Cove area). C) Sketch shows a flexure in the Conception Group with locally developed  $S_1$  which is cross-cut by  $S_2$ . Near Colliers Point, Bacon Cove area.  
 O Mean of measured  $F_1$  fold axes.

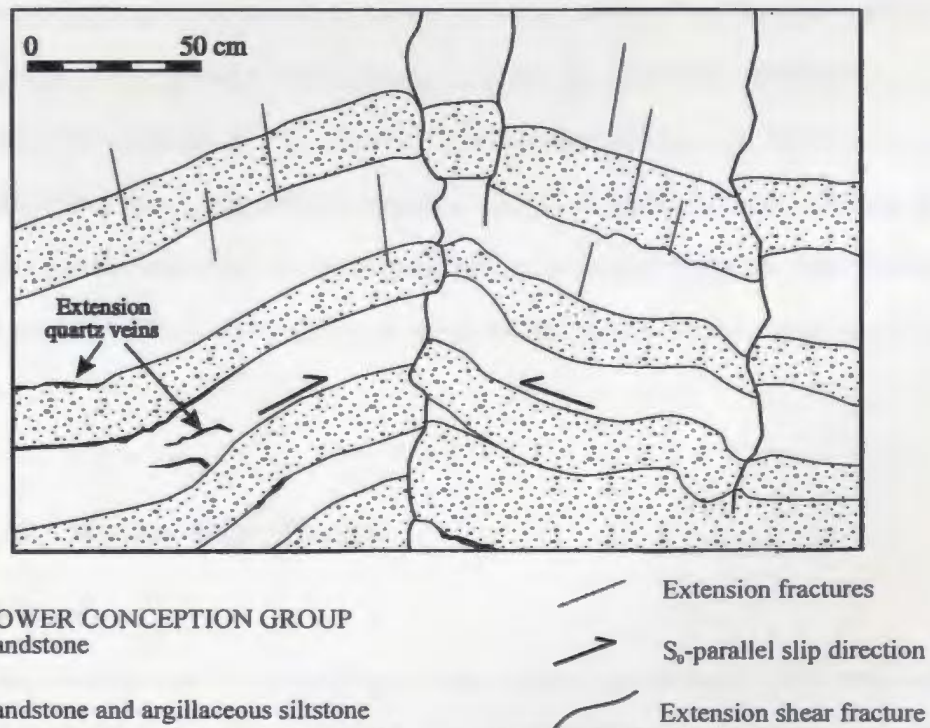


Fig. 2.35 The photograph and sketch show a flexural slip, northwest-trending  $F_1$  fold in Conception Group sandstone and argillaceous siltstone interlayers. Increased shearing on the sandstone-argillaceous bed interfaces produced the present extensional vein geometry. Extension fractures occur in the outer arc region of the fold, shear fractures occur mainly peripheral to the fold, and contractional structures such as imbrication of layers and  $S_0$ -parallel shearing occurs in the core of the fold. Looking down-plunge, east-southeast, near Colliers Point, Bacon Cove area.

Thus far,  $F_1$  folds and associated  $S_1$  exposed in the Bacon Cove map area have been northwest-trending. This suggests that these contractional structures formed under northeast-southwest shortening during  $D_1$  in the Bacon Cove area.

In zones 3 and 4, Conception Group strata were folded into open mesoscopic folds plunging gently to the north and south (Fig. 2.23D, E). Fold closures were not exposed in these zones and therefore fold trace interpretations were based on mapping of spotty outcrops. Based on the cross-cutting relationship of the fold axial traces and  $S_2$ , by  $17^\circ$  and  $23^\circ$ , the folds are interpreted to be  $F_1$ .

### ***Chapels Cove***

West of the South Brook fault, east-verging, reclined, northwest-trending mesoscopic folds occur in steeply east-dipping to overturned Conception Group, thickly bedded sandstone and siltstone units. Cleavage axial planar to the folds were not observed. North-northeast-trending  $S_2$  cross-cuts the axial traces of these folds at high angles both in plan and sectional view (Figs. 2.13, 2.14AA') indicating they are  $D_1$  structures. Furthermore, east of the South Brook fault, the contrast in the angular discordance between the sub-Cambrian unconformity and the underlying steeply dipping panel of Harbour Main Group basaltic and dacitic tuffs and granitic dykes of the Holyrood Intrusive Suite, suggests that the steeply east-dipping homocline in the Conception Group, west of the South Brook fault, also developed during  $D_1$ .

## **2.4.1.2 $D_1$ Strike-slip Faults**

### ***$D_1$ Brigus Fault Zone***

Along the steeply east-dipping Brigus fault zone, mesoscopic north-northeast-trending folds form in horses of Conception Group rocks (Fig. 2.24B). These folds are cross-cut by  $S_2$  by more than  $20^\circ$ , and are similar in orientation to the  $F_1$  folds in domains I and II in the Brigus area (Figs. 2.4, 2.24A). Based on these relationships, the folds are inferred to be  $F_1$ . The possibility that the cleavage is actually a transecting  $S_1$  cleavage on  $F_1$  folds is unlikely

since  $S_1$  is not developed in the adjacent contractional structures in domains I and II, and the cross-cutting angle by  $S_2$  is greater than  $15^\circ$ .

The north-northeast trend of the  $F_1$  folds along the fault zone, in addition to similarly oriented  $F_1$  folds in domains I and II, suggest that shortening during  $D_1$  folding was north-northwest—south-southeast in the Brigus area. This implies that the Brigus fault zone underwent an apparent sinistral strike-slip separation during  $D_1$  folding. It was reported above that the Brigus fault zone also underwent an apparent  $D_1$  normal separation, associated with the Brigus horst. Furthermore, north-northwest—south-southeast oriented  $D_1$  shortening in the Brigus area is opposite to the northeast-southwest oriented  $D_1$  shortening interpreted from northwest-trending  $F_1$  folds in the Bacon Cove area. These contrasting relationships are further discussed below.

Northwest-trending faults segment the Brigus fault zone and the mesoscopic  $F_1$  folds, similar to northwest-trending faults (e.g., Tern fault, Gannet fault) in domains I and II. The apparent displacement along these faults is unclear, however, some show apparent dextral strike-slip displacements of about 50 metres across the Brigus fault zone (Fig. 2.24). This apparent sense of displacement is opposite to that of the north-northwest-trending Lobster fault demonstrated by the apparent sinistral offset of about 100 metres across the Brigus fault (south of Brigus Bay; Fig. 2.4). Both senses of movement along the northwest-trending faults are consistent with northeast-trending  $F_1$  folds and a north-northwest—south-southeast shortening direction. Furthermore,  $S_2$  cross-cuts the faults with a constant orientation which further suggest that the northwest-trending faults may be associated with the northeast-trending  $F_1$  folds.

#### ***D<sub>1</sub> Bacon Cove Fault Zone***

Northwest-trending  $F_1$  and  $S_1$  in the Conception Group east of the Bacon Cove fault, and in the Harbour Main Group adjacent to the Bacon Cove fault, imply northeast-southwest shortening in the Bacon Cove area during  $D_1$  (Fig. 2.8). These relationships suggest that the Bacon Cove fault underwent a component of apparent dextral strike-slip displacement in  $D_1$ .

It was noted above that the Bacon Cove fault also underwent an apparent  $D_1$  normal separation, associated with the Brigus horst. These relationships are analogous to those along the Brigus fault zone, in which the fault underwent two episodes of  $D_1$  displacements. Unlike the apparent  $D_1$  sinistral strike-slip Brigus fault zone, the Bacon Cove fault underwent apparent dextral strike-slip movement during  $F_1$  folding.

***$D_1$  Pigeon Fault and Parallel Faults, Marysvale Area***

The  $D_1$  northwest-trending Pigeon fault, described above, is parallel to the Turks and Downy faults that occur in Proterozoic rocks in the Marysvale area (Fig. 2.6). These northwest-trending  $D_1$  faults are delineated by zones of up to 3 metres wide of tectonic breccia in basaltic flows of the Harbour Main and Conception group. The fault zones show extensive quartz veining, chloritization and minor sulphide mineralization. Slickensides rake from  $45^\circ$  to  $65^\circ$  to the northwest, on steep, northwest-trending fault surfaces, indicating oblique slip.

The Turks and Downy faults show an apparent sinistral strike separation of up to 25 metres, indicated by the displacement of the Conception-Harbour Main group contact (Fig. 2.6). The Turks, Downy and three parallel faults to the northeast all terminate against the Marysvale fault and show a weak, fault-parallel foliation in the Harbour Main Group adjacent to the fault. Outcrop and map interpretations show that  $S_2$  obliquely overprinted the fault and fault fabric. These relationships, combined with the oblique slip indicated by the slickensides on the faults and the parallelism between the  $D_1$  Pigeon fault and Turks fault, Downy fault and three parallel faults to the northeast, further suggest these northwest-trending faults underwent at least a component of apparent sinistral oblique slip during  $D_1$ . Furthermore, the Turks, Downy and parallel faults in the Marysvale area are parallel to and show the same sense of apparent displacement as the Lobster fault in the Brigus area, interpreted to be  $D_1$  in age (*cf.* Fig. 2.4).



#### ***D<sub>1</sub> Roger's Fault and Parallel Faults, Bacon Cove Area***

The steep, northeast-trending Roger's fault crops out on the southwestern shore of the Bacon Cove, and is parallel to a series of faults across the Bacon Cove area, bounded by the Bacon Cove and West Limb faults (Fig. 2.8). The Roger's fault was formed in an open flexure in the Conception Group rocks, where beds changed in orientation from moderately southwest-dipping to moderately southeast-dipping. The  $S_2$  orientation is constant across the fault which suggests that the fault is pre- or syn- $S_2$ . The Roger's fault does not provide any kinematic indicators.

#### ***D<sub>1</sub> Pepper Fault and Parallel Faults, Bacon Cove Area***

The northwest-trending Pepper fault in the Conception Group crops out on the southeastern shore of Bacon Cove, about 200 metres east of the Roger's fault (Fig. 2.8). Slickensides rake  $25^\circ$  to the southeast on a steeply northeast-dipping surface, indicating apparent strike-slip on the Pepper fault. A fault-parallel mesoscopic drag fold occurs adjacent to the fault, with a symmetry suggestive of an apparent dextral strike-slip on the fault.  $S_2$  remains constant in orientation across the fold and fault, which suggests that the fold, and by association the Pepper fault, are  $D_1$  structures.

The orientation, timing and kinematic characteristics of the Pepper fault are similar to northwest-trending faults in the Brigus area that were interpreted to have formed during  $D_1$  (cf. Fig. 2.4). Whether the steep northwest-trending faults across the Bacon Cove area show the same  $D_1$  sense of apparent dextral strike-slip as does the parallel Pepper fault is inconclusive. The northwest-trending faults terminate against the north-northwest-trending West Limb and Cowboy faults.

#### **2.4.1.3 $D_1$ Kink Bands**

Kink bands form in anisotropic, multilayer rocks with characteristic, very straight limbs and axial planes, usually oblique (about  $45^\circ$ ) to layers or fabric ( $S_{0(ext)}$ ) (Biot 1965). The

orientation of the maximum compression axis,  $\sigma_1$ , is assumed to be parallel to the layers for conjugate kink band structures (or box-style folds) and inclined to the layers for single kink band sets (Cobbold 1976) (Fig. 2.36A).

Along the Brigus and Marysvale faults, mesoscopic kink bands developed in Conception Group thinly bedded, argillaceous units, in zones designated A, B and C. Macroscopic kink bands developed in Conception Group medium to thickly bedded sandstone and siltstone units in the Brigus and Bacon Cove areas, in zones designated D and E.

### ***Zone A***

Zone A, exposed on the shore of Woody Island Cove, adjacent to the Brigus fault (Fig. 2.4), shows thinly bedded siltstones and shales of the Conception Group deformed into an open, mesoscopic syncline that plunges moderately to the north-northwest (Fig. 2.36B) and terminates against the Brigus fault. Adjacent to the fault, the eastern, long limb of the open fold comprises steeply northwest-dipping strata that were deformed into centimetre-scale, steeply southwest-dipping kink bands (Fig. 2.37) with axes plunging parallel to the mesoscopic synclinal axis (Fig. 2.36C). These kink bands have an apparent dextral shear.

Regionally,  $S_2$  is highly oblique to the axial trace of the mesoscale syncline in plan view (Fig. 2.36B), indicating that this syncline is a  $F_1$  structure.  $S_2$  is weak or absent in these strongly banded and kinked argillites and was not directly observed in outcrop. Thus, the relative age of the kink bands is inconclusive, although their similar orientation with the mesoscopic  $F_1$  syncline suggests they are  $D_1$ .

### ***Zone B***

Zone B, along the Brigus Bay (Fig. 2.4), exposes moderately northwest-dipping sandstone and siltstone and shale interlayers of the Conception Group that were deformed into millimetre- to centimetre-scale lens-shaped, westerly-trending, kink bands along the

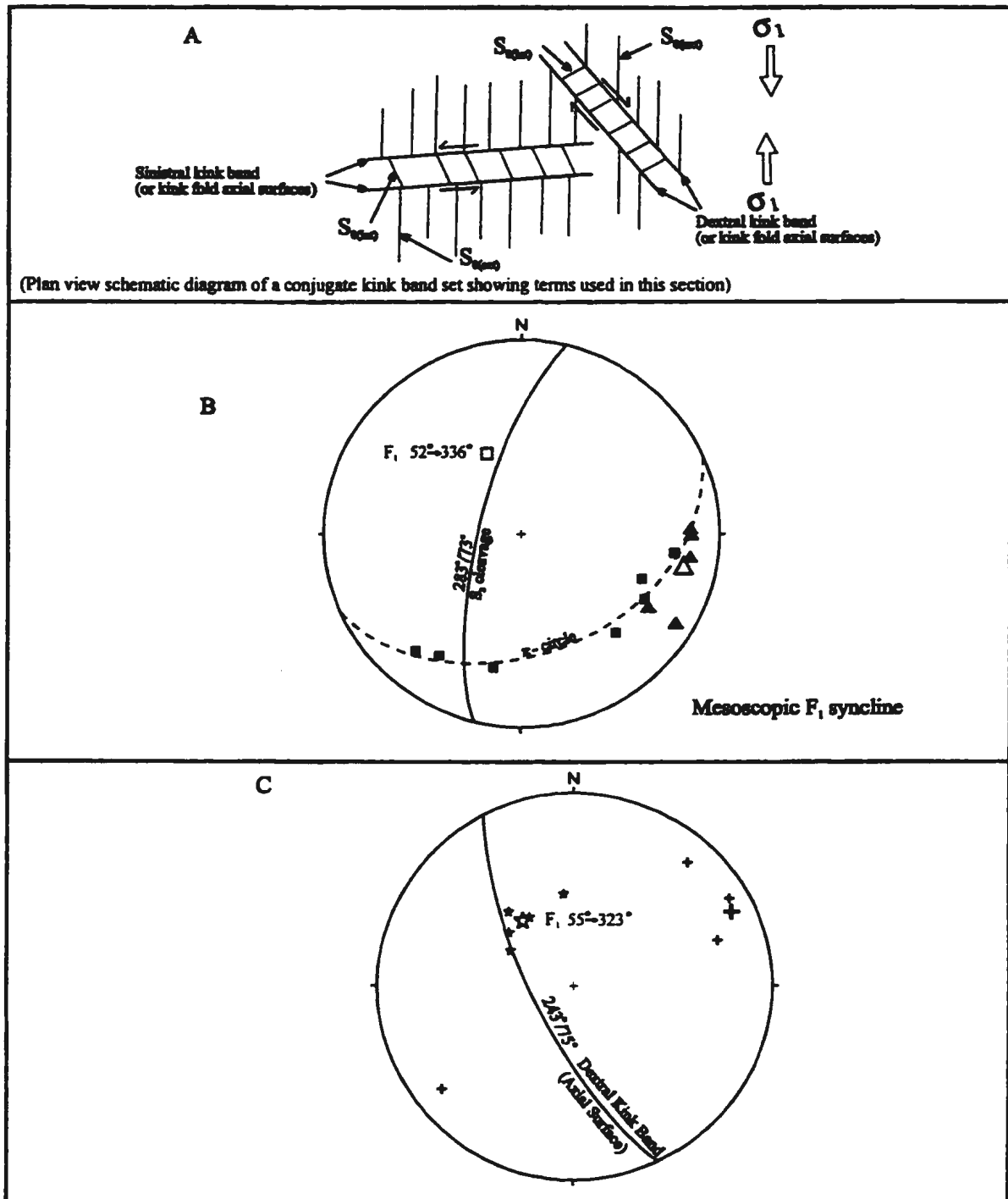
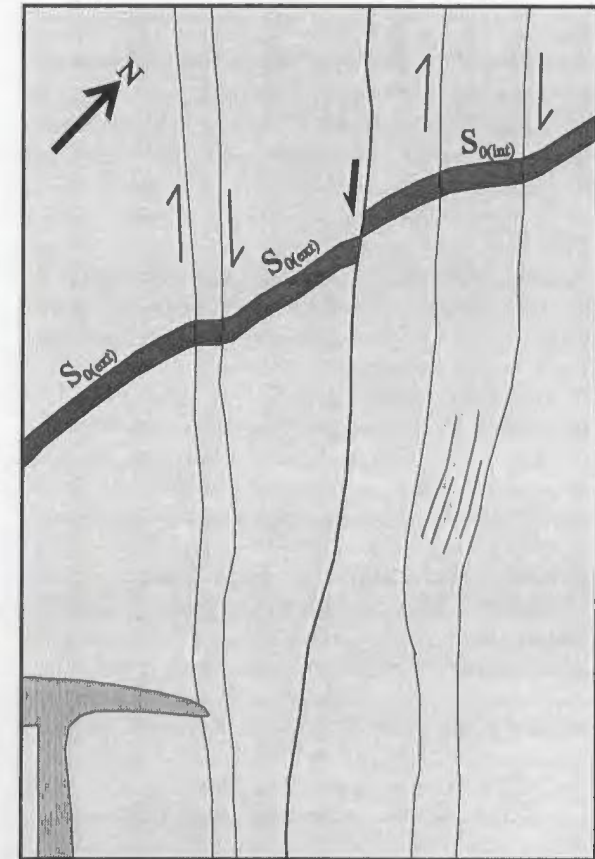
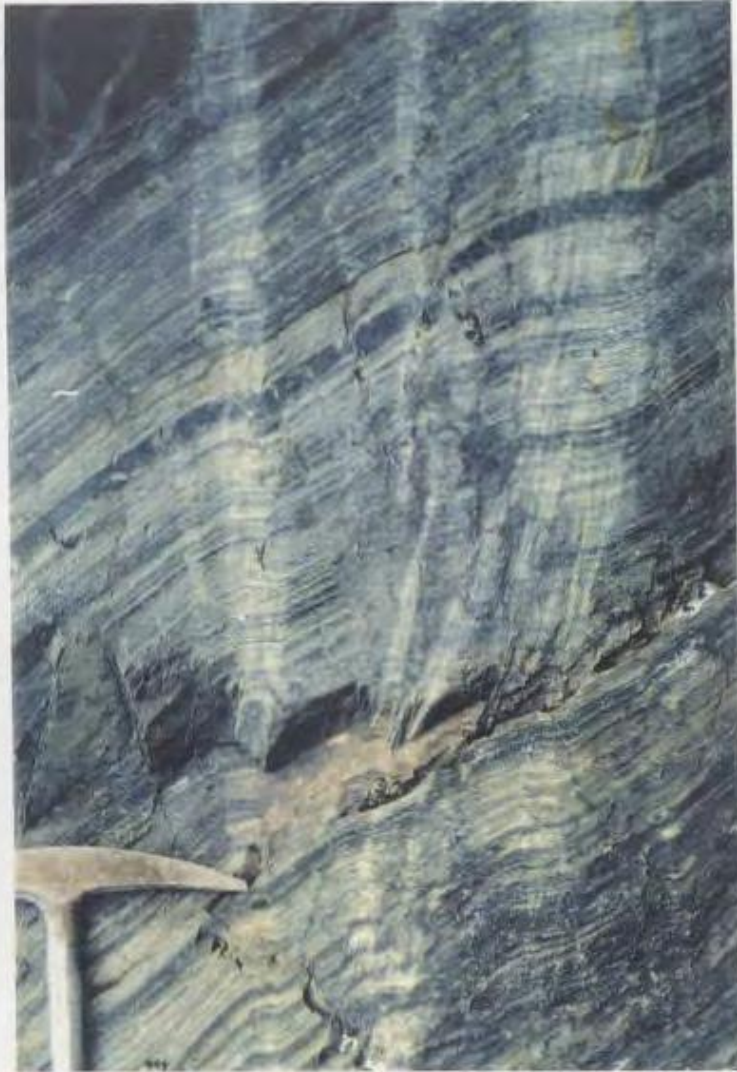


Fig. 2.36 Zone A: A) Sketch shows terms used in the kink band geometry descriptions. B) Summary stereo plot shows the mesoscopic F<sub>1</sub> syncline formed in Conception Group argillaceous siltstones. C) Summary stereo plot shows measured cm-scale dextral kink bands and F<sub>1</sub> folds that form parallel to the mesoscopic F<sub>1</sub> fold in (B). Abbreviations include S<sub>0</sub> (layering orientation outside kink bands) and S<sub>1</sub> (layering orientation inside kink bands). Brugis area.  
 □ π-pole to π-circle (poles to S<sub>0</sub>, ■), Δ mean of poles (Δ) to S<sub>1</sub>, + mean of poles (+) to kink bands, ☆ mean to measured F<sub>1</sub> fold axes (\*)



- |  |                               |
|--|-------------------------------|
| Lower Conception Group   |                               |
| <span style="display: inline-block; width: 10px; height: 10px; background-color: lightgrey; border: 1px solid black;"></span> Green shale        | Shear direction on kink bands |
| <span style="display: inline-block; width: 10px; height: 10px; background-color: black; border: 1px solid black;"></span> Green-grey shale layer | Strike-slip fault             |

Fig. 2.37 Zone A: Steeply northwest-dipping Conception Group shales are buckled and form a steeply southwest -dipping dextral kink band set. The intersection lineation of  $S_{0(ext)}$  and the kink bands is parallel to the kink fold axis. A mesoscale fault that is parallel to the kink bands shows an apparent sinistral strike-slip. Brigus area.

Brigus fault zone (Fig. 2.38). In a south-facing cross-section, the kink bands have dextral shear patterns. They are superimposed by  $S_2$  by more than  $30^\circ$  in plan view (Fig. 2.38), indicating they are  $D_1$  structures.

### ***Zone C***

Zone C comprises a series of northwest-trending faults (e.g., the Flicker, Sparrow and Tickleace faults) that segmented and are associated with a macroscopic z-symmetry flexure of west-northwest-dipping Conception Group thickly bedded sandstone and siltstone units in the Brigus area (Figs. 2.4, 2.5). Rotation of both Conception Group units adjacent to the northwest-trending faults formed fault-parallel drag folds, suggesting associated, apparent dextral strike-slip on the faults. These geometric associations resemble dextral kink bands, similar to those observed in zones A and B in the Brigus area. Unlike zones A and B, however, the kink bands in Zone C developed at a larger scale and distal to the Brigus fault zone.

$S_2$  is consistently north-trending across the faults, cross-cutting the axial trace of the drag folds by more than  $20^\circ$  in plan view (Figs. 2.4, 2.33B), which suggests the kink bands are  $D_1$ . Fold closures were not exposed and  $S_1$  was not observed in this zone. Furthermore, a series of east-directed thrust faults (e.g., Pine thrust) were also affected by the dextral kink bands, suggesting they are  $D_1$  structures, consistent with kink band development.

The occurrence of single, dextral kink band sets in zones A, B and C thus far, suggests that  $\sigma_1$  was slightly inclined to the layering, oriented approximately north-south to north-northeast—south-southwest during  $D_1$  kink band development.

### ***Zone D***

In Zone D, kink bands generally occurred locally in deformed horses ranging up to 200 metres wide along the Marysvale fault, in steeply west-dipping, anisotropic, thinly bedded siltstone units of the Conception Group (Fig. 2.6). The fact that kink bands are absent from Cambrian shales adjacent to the fault suggests either that i) the kink bands formed in  $D_1$ , or ii)



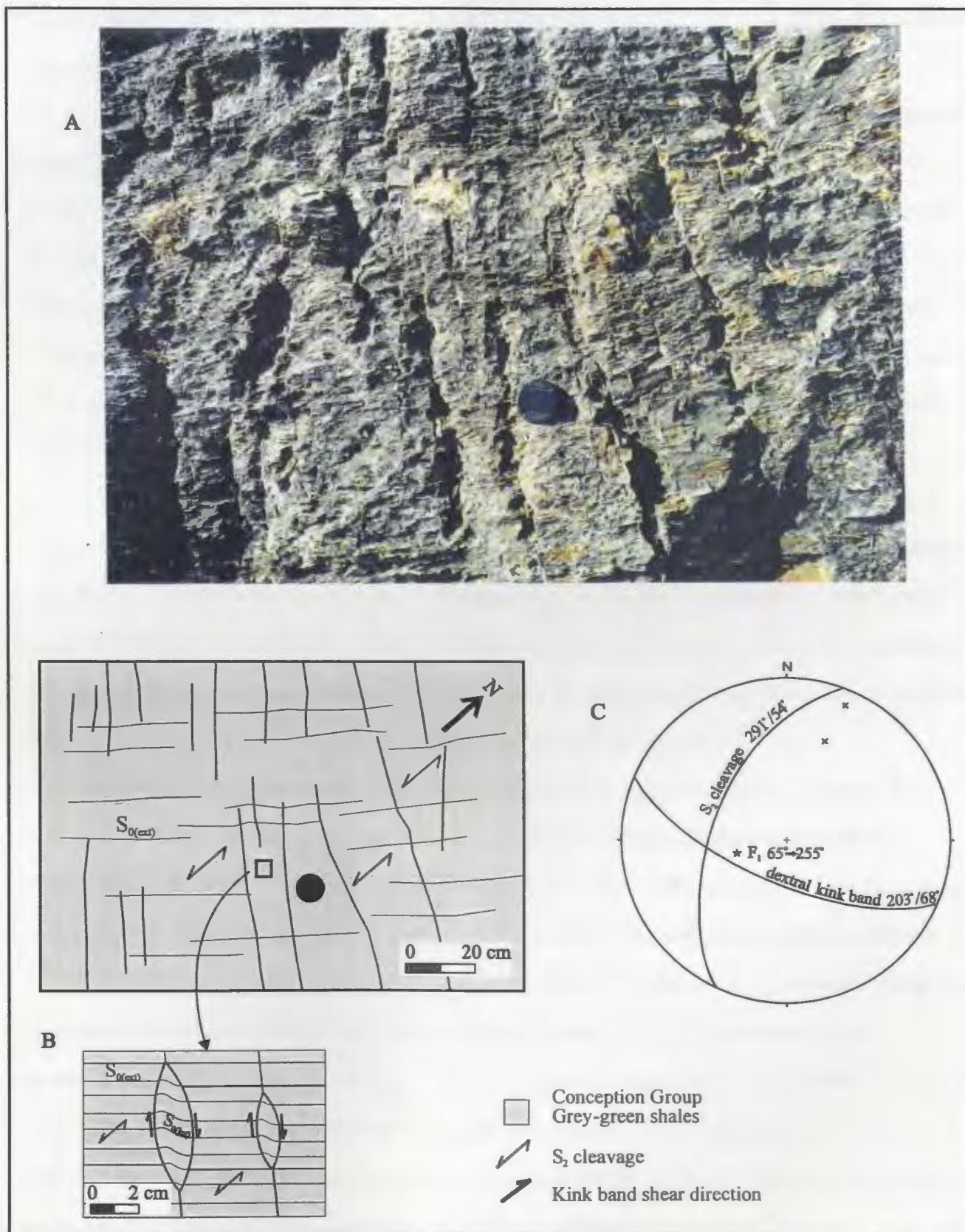


Fig. 2.38 Zone B: A) Sketch of the photograph shows a map view of cm-scale, dextral kink band sets cross-cut by  $S_2$ . B) A detailed sketch of lens-shaped dextral kink bands. C) Summary stereo plot shows the relationship between kink bands and kink fold axes.  $S_1$  cross-cuts the kink bands by more than 90 degrees.  $\star$  Kink fold axis,  $\times$  pole to dextral kink band. Brigus area.

Cambrian units do not provide the mechanical properties suitable for kink band development. This study suggests the former as outlined below.

Kink band geometry in Zone D varies from i) single kink band sets with an apparent sinistral sense of shear (Fig. 2.39), to ii) conjugate kink band sets (Fig. 2.40A). The kink bands range in width from a few centimetres to a few decimetres and commonly developed en-echelon, lens-shaped morphologies. Sinistral kink band sets dip steeply to the north. Conjugate kink band sets comprise steeply north-dipping, sinistral kink bands and steeply southwest-dipping dextral kink bands (Fig. 2.40B). The orientation of the dextral kink band set is approximately parallel to the dextral kink bands in the Brigus area (*cf.* Figs. 2.4, 2.36C, 2.38C). In general, kink band orientations in Zone D vary only slightly (Fig. 2.6).

In argillaceous layers,  $S_2$  is locally developed.  $S_2$  is slightly inclined to the fabric outside the kink bands ( $S_{0(ext)}$ ) (Fig. 2.39B) and obliquely cross-cuts both dextral and sinistral kink bands. Based on the correlation in orientation between the dextral kink bands formed in Zone D with those interpreted to have developed during  $D_1$  in zones A, B and C, in addition to the superposition of these structures by  $S_2$  and their absence in adjacent Cambrian sequences, the kink bands in Zone D are interpreted to have formed during  $D_1$ .

The relationship between the conjugate kink band geometry and  $S_{0(ext)}$  imply that  $\sigma_1$  was locally parallel to  $S_{0(ext)}$ , or approximately oriented north-south during kink band development in  $D_1$ . This interpretation is relatively consistent with the dextral kink band sets in zones A, B and C, which suggest that  $\sigma_1$  was oriented north-northeast—south-southwest.

A mesoscopic fold interference pattern developed locally on  $S_{0(ext)}$  surfaces comprising centimetre-scale, s-symmetry, northwest-trending  $F_1$  kink folds and centimetre-scale symmetrical north-trending folds (Fig. 2.40B).  $S_2$  is axial planar to the latter folds, indicating they are  $F_2$  folds. Thus, the observed mesoscopic dome and basin-type pattern on  $S_{0(ext)}$  surfaces represents  $F_1/F_2$  composite folds. This superposition by  $F_2$  may explain the slightly scattered distribution of kink band data (e.g., Fig. 2.40B).



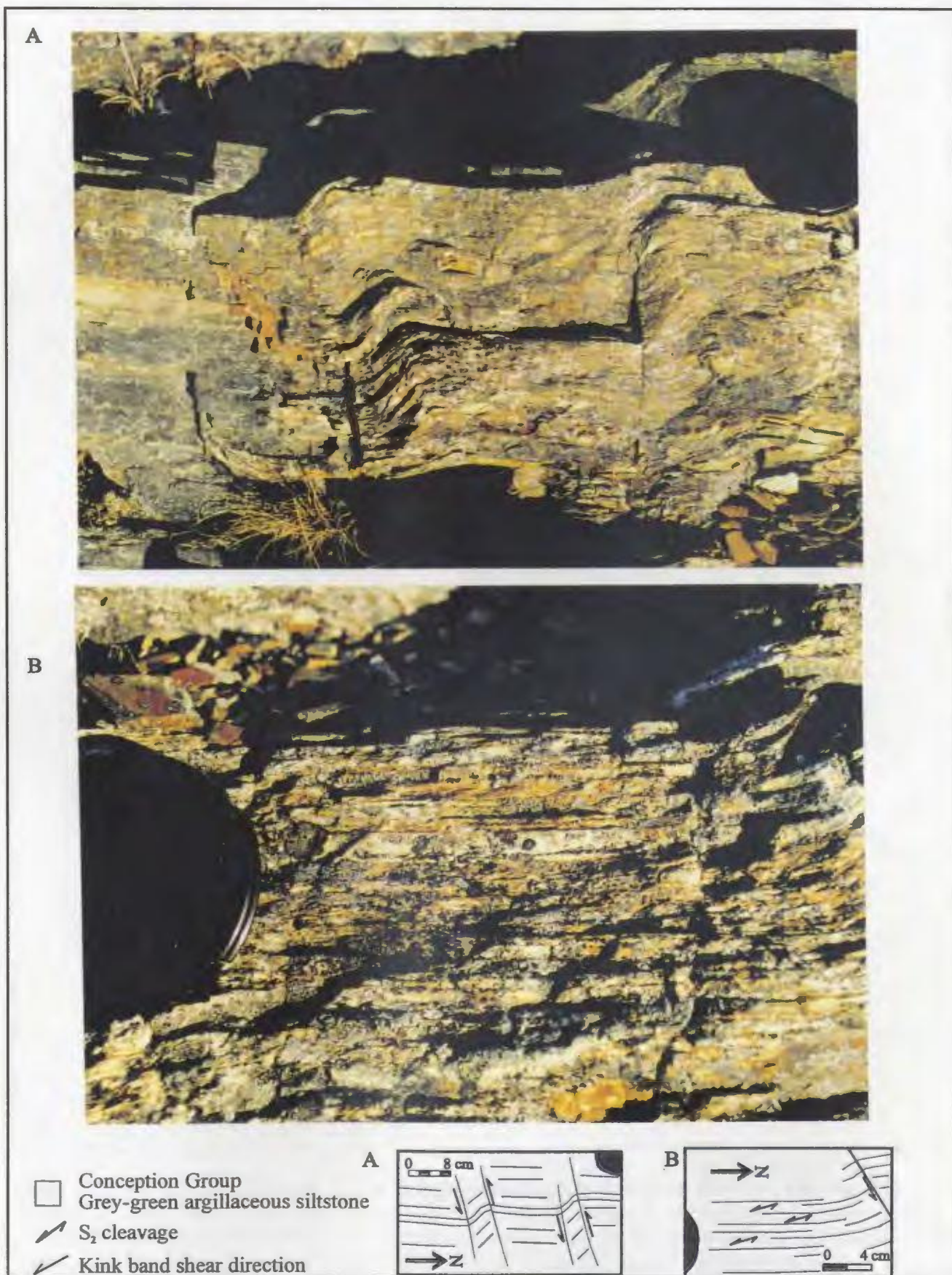


Fig. 2.39 Zone D: Sketches of photographs in the Conception Group, Marysvale area. A)  $D_1$  sinistral kink bands in strongly anisotropic argillaceous siltstones. B)  $S_2$  preserved in the Conception Group and cross-cuts the kink bands at high angles.



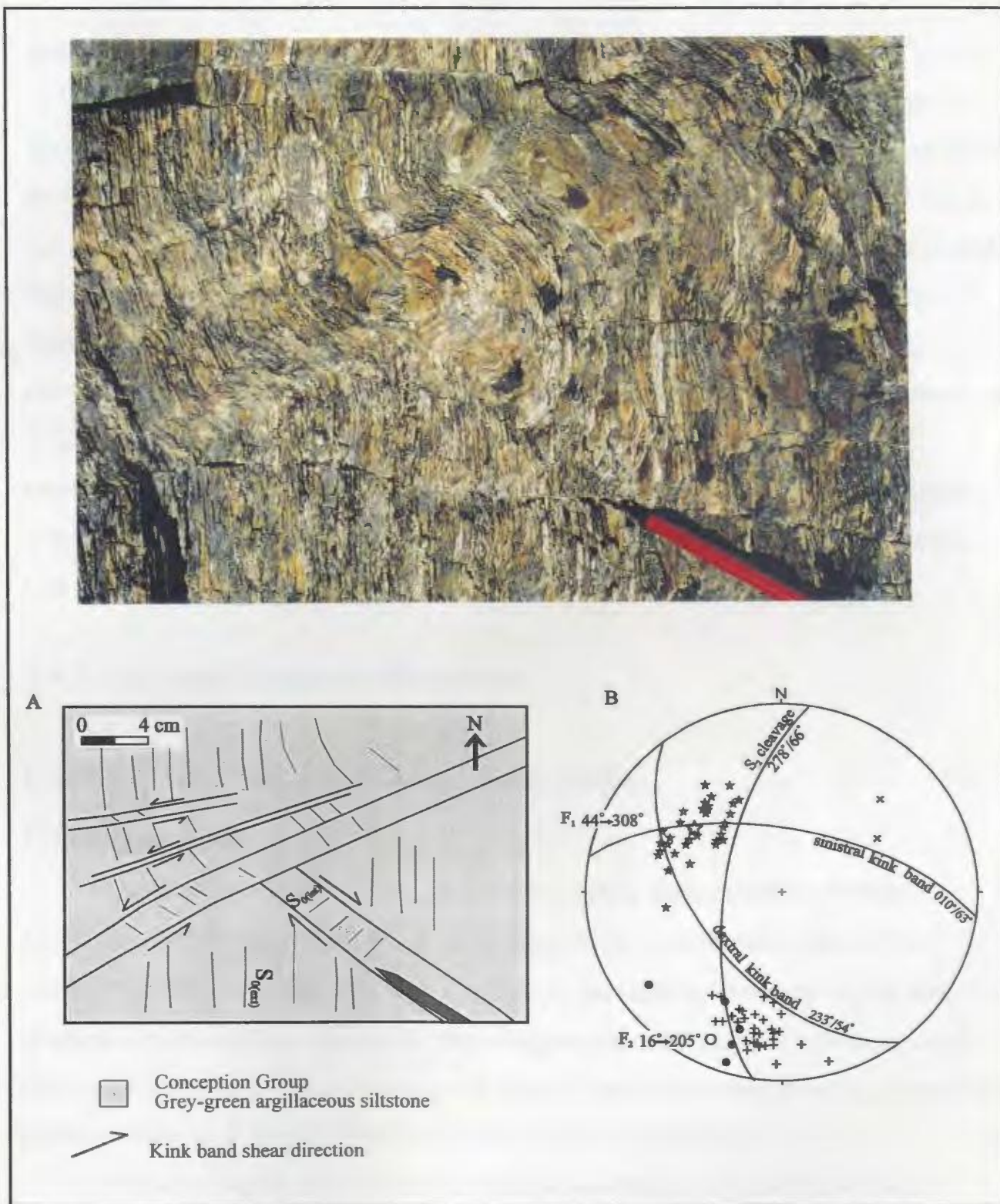


Fig. 2.40 Zone D, Marysvale area: A) The sketch and photograph show a  $D_1$  conjugate kink band set in moderately west-dipping Conception Group argillaceous units. Shear on the kink bands indicate apparent sinistral and dextral displacements. B) A summary stereo plot shows the mean of measured kink fold axes plunging to the northwest. Symmetrical north-trending  $F_2$  folds and coplanar  $S_2$  (observed outside the photograph) cross-cut the kink band fabric.  
 \* poles to dextral kink bands, + poles to sinistral kink bands, ☆ mean to measured  $F_1$  kink fold axes (☆),  
 O mean to measured  $F_2$  fold axes (●).

## ***Zone E***

Zone E, south of the Bacon Cove, in the Bacon Cove area (Fig. 2.8), comprises a macroscopic, open, box-style anticlinal fold in the Conception Group, in which the northwest-trending Pepper fault and northeast-trending Roger's fault may represent conjugate shears associated with the box fold (Fig. 2.8). Since the Pepper fault and associated parallel  $F_1$  fold described above, have been interpreted to be  $D_1$  structures, then by association, it may be inferred that the box-style, anticlinal fold and associated conjugate shears are also  $D_1$  structures. Note that an open box-fold of uncertain age was also observed in the northern part of Zone 2 in Conception Group rocks in the Bacon Cove area (Fig. 2.8). Geometric associations between the box fold and conjugate shears suggest that  $\sigma_1$  was approximately north-south during  $F_1$  box-fold development, consistent with  $\sigma_1$  orientations deduced from kink band zones A to D.

## **2.4.2 $D_2$ Post-Cambrian Structures**

### **2.4.2.1 $F_2$ Folds and Associated Faults**

#### ***$F_2$ Blackback Syncline***

The Blackback syncline is an open, north-trending, sub-cylindrical structure (Fig. 2.26C), up to 400 metres in half-wavelength, which forms in argillaceous units of the Conception Group (Figs 2.4, 2.5).  $S_2$  is axial planar and slightly convergent in plan and sectional view, as observed in outcrop, which suggests that the Blackback syncline is an  $F_2$  structure. At sandstone-siltstone interfaces of folded Conception Group units,  $S_0$ -parallel shear surfaces locally show dip-slip striae, compatible with  $F_2$  flexural slip.

The axial trace of the  $F_2$  Blackback syncline terminates at the moderately west-northwest-dipping Spruce thrust, based on aerial photo and mapping interpretations (Fig. 2.4). The fault surface shows slickensides raking  $60^\circ$  to the southwest suggesting dip slip on the fault. These relationships are compatible with an east-directed movement on the Spruce thrust, associated with the  $F_2$  Blackback syncline.

The eastern limb of the syncline is considerably shallower than the western limb, and is cut by two sub-parallel, northwest-trending faults that are parallel to and align with the Flicker and Sparrow faults (Figs 2.4, 2.5). The eastern limb of the syncline resembles the macroscopic dextral kink band in Zone C (Fig. 2.4), interpreted above as a  $D_1$  structure.

A possible scenario that may explain these relationships suggests that the Conception Group in the southwestern region of the Brigus area may have been deformed into macroscopic dextral kink band sets during  $D_1$ , accommodated along north-northeast-trending thrust faults (e.g., Pine and Spruce thrusts). Subsequent east-west shortening during  $D_2$  resulted in movement along the Spruce thrust and the development of the  $F_2$  Blackback syncline. The Spruce thrust acted as a detachment between the preserved  $D_1$  dextral kink band in the foot wall and the  $F_2$  Blackback syncline in the hanging wall of the thrust (Fig. 2.5).

### ***Domain III***

In Domain III (Fig. 2.4), open, north-trending anticlines separated by east-directed thrusts occur in the Conception Group. Fold closures were observed in outcrop for both anticlines.  $S_2$  formed parallel to the axial surfaces of the anticlines both in plan and sectional view, indicating that the structures are  $F_2$  folds. The thrusts in Domain III resemble the Spruce thrust and are east-verging and compatible with  $F_2$  folding. Both folds and thrusts terminate against the northwest-trending Quidi fault (Fig. 2.4) suggesting that the Quidi fault was active during  $D_2$  or later.

### ***Bacon Cove***

In Zone 5 in the Bacon Cove area (Fig. 2.8), steeply southeast-dipping Conception Group strata were folded into mesoscopic open folds plunging gently to the south (Fig. 2.23F). Folds developed axial planar to the regional  $S_2$  which suggests that the folds are  $F_2$ . The cross-cutting angle of  $17^\circ$  of the axial trace by  $S_2$  (Fig. 2.23F) may be a result of the scattered  $S_2$  cluster stereo plot, which in turn may be a result of a non-uniform or ( $F_1$ ) folded Conception Group sequence prior to  $F_2$  folding.

### ***Chapels Cove***

In the Chapels Cove area, the commensurate rotation of the steeply east-dipping panel of the Conception Group to overturned dips, adjacent to the South Brook fault, while  $S_2$  dips remained relatively constant, suggests apparent reverse separation along the fault, consistent with  $F_2$  (Fig. 2.14BB'). Reverse separation may also be extended to the second-order Little Brook fault interpreted above to be a splay of the South Brook fault. This sense of displacement along the faults may explain how Cambrian beds were preserved east of the faults.

## **2.4.2.2 $D_2$ Strike-Slip Faults**

### ***Salmon Cove***

Steep, northwest-trending strike-slip faults show apparent sinistral and dextral strike-slip in the Salmon Cove area (e.g., Figs. 2.10, 2.11BB'). The faults segment Proterozoic rocks across the area and are characterized by zones of tectonic breccia ranging from a few centimetres to several metres in width. Drag folds associated with apparent dextral slip along the faults form in Conception Group strata, rotating both  $S_0$  and  $S_2$ . Based on these relationships, the faults are necessarily post- $S_2$  structures.

Some of these faults show slickensides that indicate both strike-slip and dip-slip movement. On the northern margin of the mapped area, sinistral strike-slip separation is indicated on the Point fault in the Conception Group by the apparent offset of a minor northeast-trending fault (Fig. 2.10). On the western margin of the mapped area, some northwest-trending faults bring rocks of the Conception Group against Harbour Main Group strata, indicating both apparent sinistral and dextral strike-slip of up to 100 metres.

These northwest-trending faults closely resemble the northwest-trending strike-slip faults that segment Proterozoic rocks in the Bacon Cove, Marysvale and Brigus areas, all of which were interpreted to have undergone apparent sinistral and dextral strike-slip during  $D_1$ .

Evidence in the Salmon Cove area suggests that these northwest-trending  $D_1$  faults were reactivated during post- $S_2$  time with apparent dextral and sinistral strike-slip.

### ***Chapels Cove***

East and west of, and adjacent to the South Brook fault, in the Chapels Cove area,  $S_2$  appears to have been rotated clockwise, suggesting a component of apparent dextral strike-slip on the South Brook fault during post- $S_2$  time (Fig. 2.13). Apparent, post- $S_2$  dextral strike-slip is also demonstrated by the commensurate rotation of Cambrian strata and  $S_2$  along a mesoscopic, east-west-trending fault, east of the Pelee fault.

### **3. STRUCTURAL EVOLUTION OF THE STUDY SITE — A MODEL**

#### **3.1 Introduction**

Based on the criteria established above, this chapter identifies four deformational events;  $D_{1a}$ ,  $D_{1b}$ ,  $D_{2a}$  and  $D_{2b}$ .  $D_{1a}$  and  $D_{1b}$  represent two phases of a  $D_1$  pre-Cambrian deformational event which affected Proterozoic rocks.  $D_{2a}$  and  $D_{2b}$  represent two distinctive  $D_2$  post-Cambrian deformational events which affected both Proterozoic and Paleozoic rocks in the study site. These events are incorporated into a model for the structural evolution of the study site and Avalon Peninsula (Fig. 3.1). The validity of the model is tested in areas outside the study site, in the Avalon Peninsula.

A pre- $D_{1a}$  tectonic event is interpreted to have been associated with the emplacement of the Holyrood Intrusive Suite along the Topsail fault zone, into the Harbour Main Group and interdigitating basal Conception Group rocks (Fig. 3.2). Pre- $D_{1a}$  deformation comprises block faulting and rigid body rotation of the 635–590 Ma rock package along major north-trending faults, interpreted to be related to the 630–600 Ma tectonostratigraphic event proposed by O'Brien and others (1990, 1992, 1996) for the western Avalon Zone. Pre- $D_{1a}$  is best expressed by the sub-Conception Group unconformity exposed outside the study site (Fig. 3.1A).

Certain assumptions are made and incorporated into the model. They include: i) All structures indicate brittle to semi-brittle, low metamorphic-grade deformation, ii) the bulk of the Conception Group (part of the 590–545 Ma rock package) is stratigraphically younger than the bulk of the Harbour Main Group rocks (part of the 635–590 Ma rock package), and iii) the Conception, St. John's and Signal Hill groups of the 590–545 Ma rock package blanketed the Avalon Peninsula, covering the Harbour Main Group and the Holyrood Intrusive Suite.



Assumption iii) implies that over 7 km of clastic rocks were uplifted and eroded, during the development of the Harbour Main Massif and the deposition of the Signal Hill and Musgravetown groups. This implies that the source for the volcanic and granitic detritus found in the Conception Group was not the Harbour Main Group and Holyrood Intrusive Suite that crop out in the Harbour Main Massif. Rather, the sources were from the north, south and west of the massif, as demonstrated by paleocurrent data by King (1990).

**Figure 3.1** Structural evolution model of the study site and Avalon Peninsula showing the A) D<sub>1a</sub>, B) D<sub>1b</sub>, and C) D<sub>2a</sub> and D<sub>2b</sub> deformational events.

## LEGEND

### EARLY TO MIDDLE CAMBRIAN



### LATE PROTEROZOIC

#### SIGNAL HILL GROUP (including Bull Arm Formation)



#### Heart's Desire Formation, Flat Rock Cove Formation (Piccos Brook Member)



#### ST. JOHN'S GROUP



#### CONCEPTION GROUP



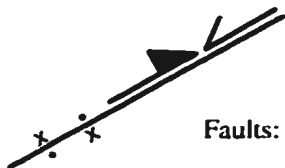
#### HOLYROOD INTRUSIVE SUITE



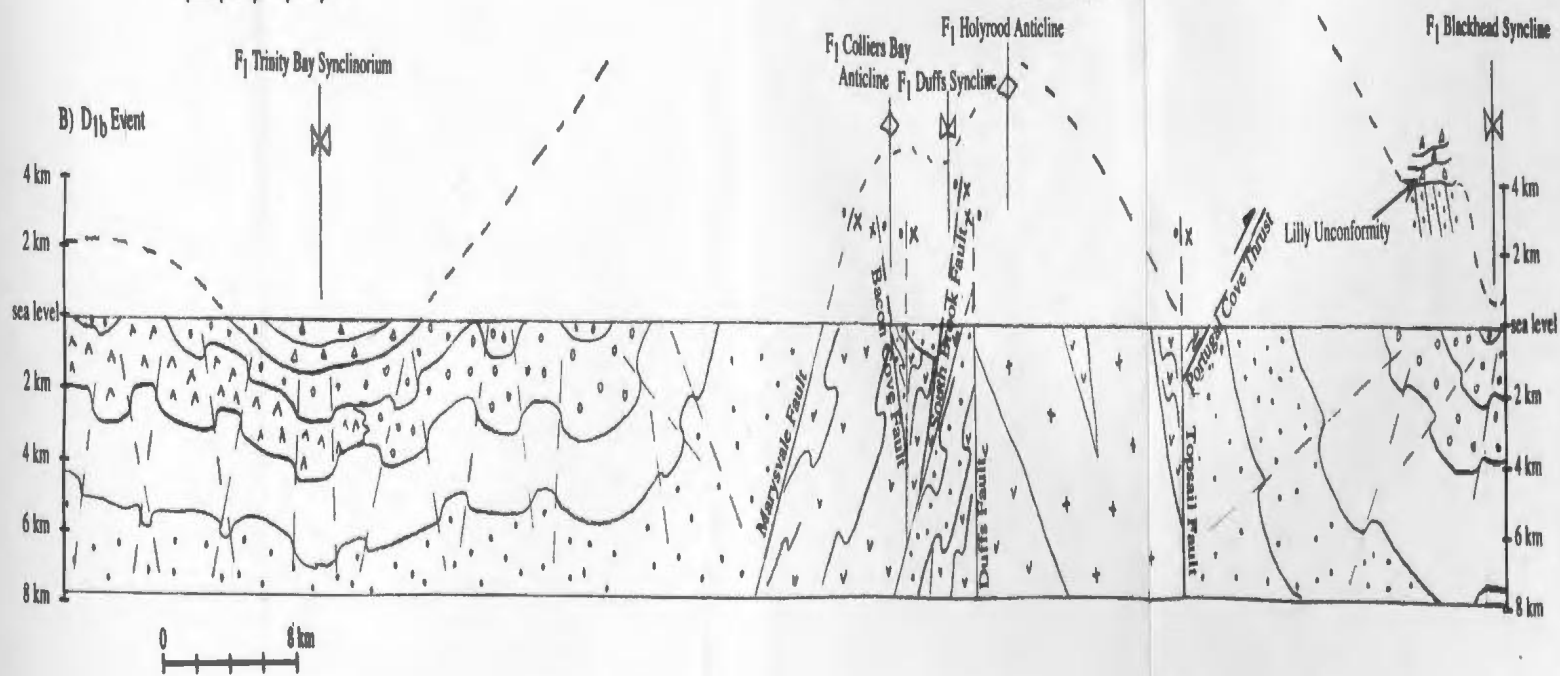
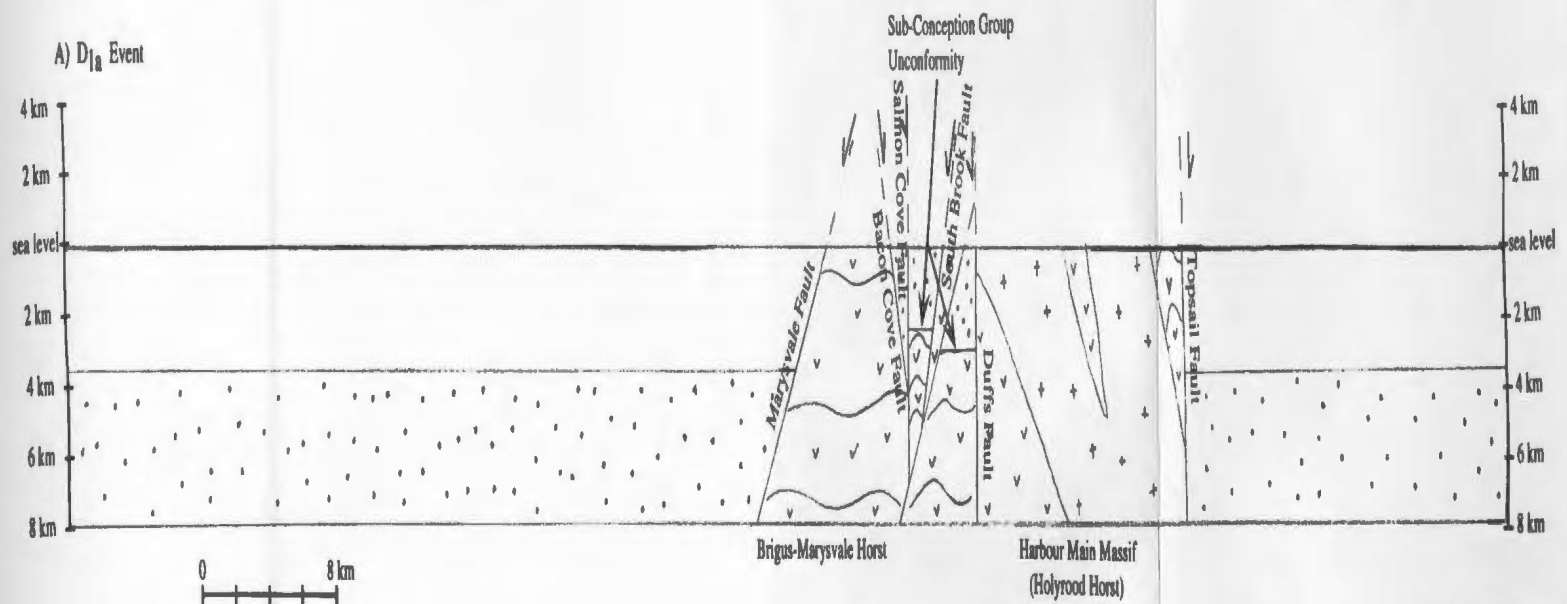
#### HARBOUR MAIN GROUP

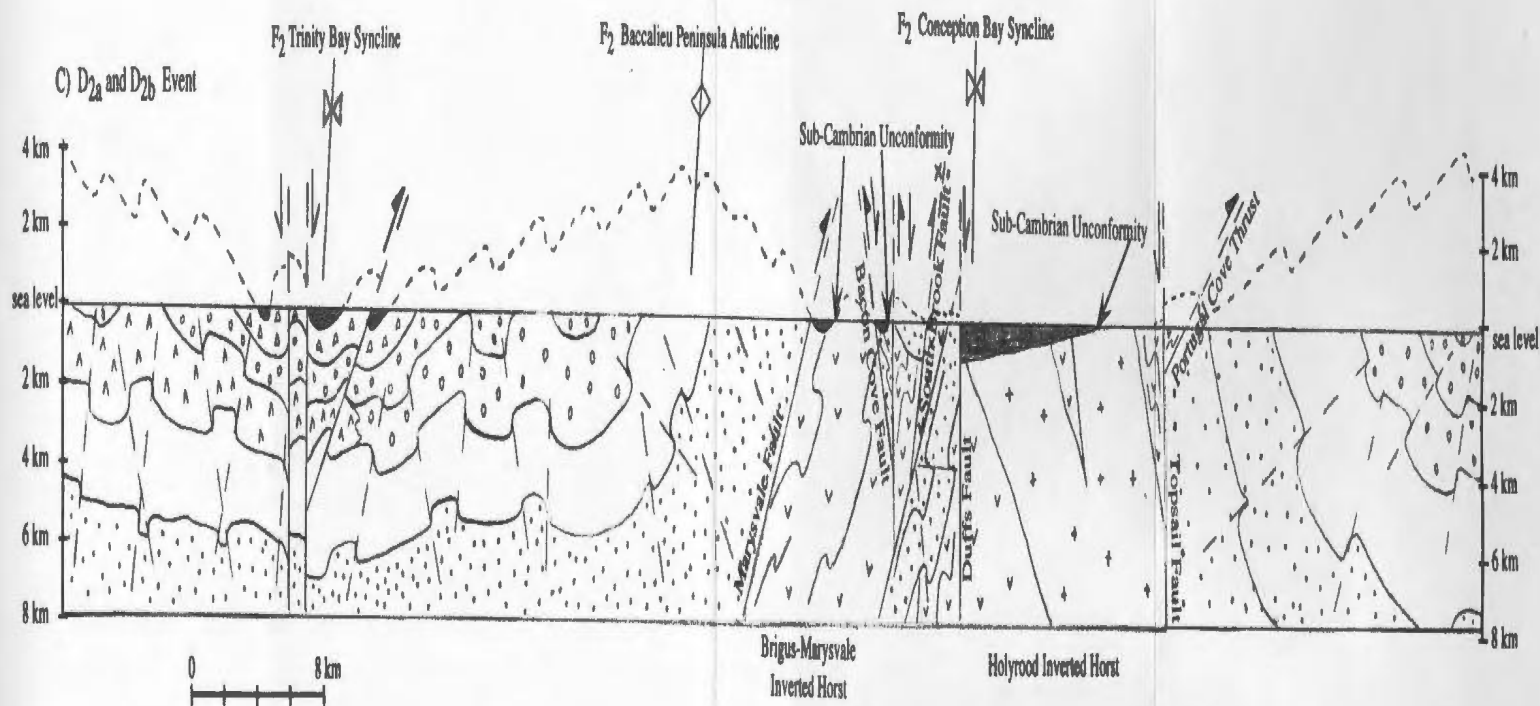


## SYMBOLS



Faults: dextral strike-slip; sinistral strike-slip, reverse or thrust, normal





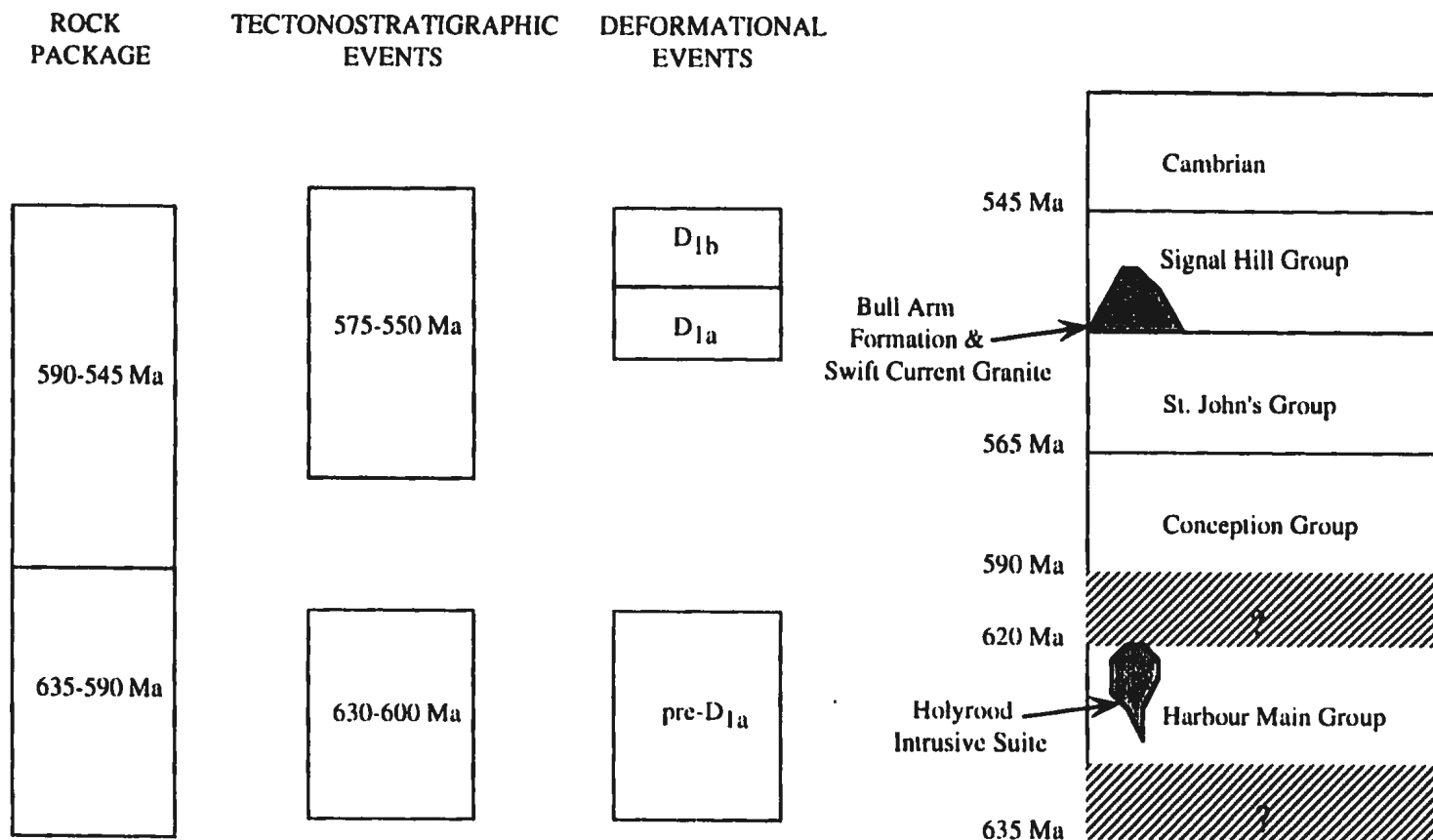


Figure 3.2 Schematic diagram showing the relative stratigraphic, tectonic and time relationships between the late Proterozoic pre-D<sub>1a</sub>, D<sub>1a</sub> and D<sub>1b</sub> deformational events.



## **3.2 Model**

### **3.2.1 $D_{1a}$ Block Faulting Extensional Event**

Following the emplacement of the Holyrood Intrusive Suite, and a period of relatively quiescent deposition of the bulk of the Conception and St. John's groups in a deep marine basin, tectonic uplift commenced to the north of the Avalon Peninsula (e.g., King 1990). This tectonic uplift is interpreted to have initiated in response to igneous activity of the Bull Arm Formation and Swift Current granite, as well as have provided a source for the Signal Hill and Musgravetown groups (Fig. 3.2).

$D_{1a}$  is an extensional, non-folding event, characterized by block faulting and the development of north-trending horsts and grabens in Proterozoic rocks (Fig. 3.1A). The maximum extension axis,  $\sigma_3$ , is interpreted to have been approximately east-west and the maximum compression axis,  $\sigma_1$ , approximately vertical during  $D_{1a}$ .

In the study site, the Harbour Main Group is juxtaposed against lower Conception Group rocks along the steep, north-northwest- to north-northeast-trending Brigus, Marysvale, Bacon Cove, Salmon Cove and South Brook faults. The Harbour Main Group, locally granitic dykes of the Holyrood Intrusive Suite, and the lower Conception Group are unconformably overlain by Cambrian sequences in the study site. These stratigraphic associations are the most significant evidence for  $D_{1a}$ , in which the faults were interpreted to have down-thrown rocks of the lower Conception Group relative to rocks of the Harbour Main Group and granitic dykes of the Holyrood Intrusive Suite, prior to the onlap of Cambrian sequences (Fig. 3.1A).

The lack of contractional structures adjacent to these faults and associated with displacement along the faults, refute reverse displacement on the faults. Thus, the north-northwest- to north-northeast-trending faults in the study site are interpreted to be Proterozoic post-Conception Group normal faults along which horst and grabens developed; they include the Brigus-Marysvale, Beach-Salmon Cove and West Limb-Cowboy horsts.  $D_{1a}$  normal displacement along the Topsail, Peter's River, Peak-Pond, Duffs and parallel Holyrood faults

is consistent with the unroofing of the Holyrood Intrusive Suite and formation of the Harbour Main Massif or Holyrood Horst (Fig. 3.1A).  $D_{1a}$  is best expressed by the unconformable contact between Cambrian rocks and underlying horsts of the Harbour Main Group and Holyrood granite.

### **3.2.2 $D_{1b}$ Conjugate Kink Band Contractional Event**

Subsequent to  $D_{1a}$  block faulting, the bulk of the Signal Hill Group was deposited with continued tectonic uplift to the north of the Avalon Peninsula (e.g., King 1990).  $D_{1b}$  contraction is interpreted to be associated with this tectonic uplift which occurred during the deposition of the bulk of the Signal Hill and Musgravetown groups (Fig. 3.2).  $D_{1b}$  developed generally non-cleavage-forming, northwest-trending dextral kink band sets and northeast-trending sinistral kink band sets, best observed in anisotropic, layered, late Proterozoic sedimentary rocks (Fig. 3.1B).  $D_{1b}$  is compatible with the regional dome and basin structures in Proterozoic rocks across the Avalon Peninsula, and the development of the  $F_1$  Trinity Bay synclinorium and  $F_1$  Blackhead syncline (Fig. 3.1B).

The factor that determines whether kink bands develop in anisotropic layered sequences or not is the orientation of the principal compression axis,  $\sigma_1$ , with respect to the layering or fabric. If  $\sigma_1$  is parallel or sub-parallel to the layering, then conjugate kink bands will develop, and if  $\sigma_1$  is oblique to layering, then single kink band sets will develop. Geometric relationships across the study site suggest that the maximum compression axis,  $\sigma_1$ , was approximately north-south during  $D_{1b}$ .

$D_{1b}$  macroscopic and mesoscopic conjugate kink band sets developed in argillaceous Conception Group rocks along the Marysvale fault (e.g., Zone D; Fig. 2.40) and in the Bacon Cove area (e.g., Zone E, Fig. 2.8). Box-style folds formed in Proterozoic rocks underlying the sub-Cambrian unconformity at Seal Head (e.g., Fig. 2.19) and the Bacon Cove area (e.g., Fig. 2.22). Kink band shearing and flexural slip accommodated  $F_1$  kink band development (e.g., Zone C, Figs. 2.4; 2.35).

Macroscopic and mesoscopic northwest-trending dextral kink bands and parallel open  $F_1$  folds developed in layered Conception Group units in the Brigus (e.g., Figs. 2.4, 2.37, 2.38) and Bacon Cove (e.g., Fig. 2.8) areas. In some areas (e.g., zones 1 and 2 in the Bacon Cove area, Fig. 2.8), open to tight northwest-trending  $F_1$  folds and axial plane  $S_1$  cleavage developed in argillaceous, thinly bedded units of the Conception Group without any associated parallel kink bands.

Macroscopic northeast-trending sinistral kink bands and parallel open  $F_1$  folds developed in the Conception Group in the Marysvale (e.g., Zone D, Fig. 2.39) and Chapels Cove (e.g., Fig. 2.13) areas. In some regions in the Brigus area, macroscopic to mesoscopic northeast-trending open to isoclinal  $F_1$  folds and axial plane  $S_1$  developed in argillaceous and thinly bedded sedimentary units of the Conception and Harbour Main groups: For example at Seal Head (Fig. 2.19), Domain I (Fig. 2.24), Domain II (Fig. 2.4), and along the Brigus fault zone (Fig. 2.24).

An  $F_1$  northeast-trending macroscopic anticlinal axis is inferred to have formed along Colliers Bay, based on east-verging  $F_1$  folds in Harbour Main Group rocks at Seal Head, Brigus area (e.g., Fig. 2.18), and west-verging  $F_1$  folds in the Conception Group in the Bacon Cove area (e.g., Fig. 2.22). Nixon (1975) also inferred an anticlinal axis along Colliers Bay. This anticline is referred to as the  $F_1$  Colliers Bay anticline (Fig. 3.1B). Based on the generally west-dipping panel of Conception Group rocks adjacent to and west of Duffs fault outside the study site, the  $F_1$  Duffs syncline is inferred to have formed along Holyrood Bay (Fig. 3.1B). Based on verging directions, a regional  $F_1$  anticline is also inferred along the Harbour Main Massif, referred to as the  $F_1$  Holyrood Anticline (Fig. 3.1B).

Most of the folding and tilting of Proterozoic strata in the study site and across the Avalon Peninsula are interpreted to have been accommodated by  $D_{1b}$  prior to the deposition of Cambrian sequences.  $D_{1b}$  kink band development is consistent with the reactivation of some  $D_{1a}$  faults.  $D_{1b}$  produced apparent sinistral strike-slip along reactivated  $D_{1a}$  north- to north-northeast-trending faults; they include the Brigus, Marysvale, South Brook and Topsail faults

(Fig. 3.1B).  $D_{1b}$  also produced apparent dextral strike-slip along reactivated  $D_{1a}$  north- to north-northwest-trending faults; they include the Bacon Cove, Duffs and Holyrood faults (Fig. 3.1B).

$D_{1b}$  is best expressed by the unconformable onlap of Cambrian beds on layered Harbour Main and Conception group rocks in the study site. Outside the study site, the sub-Musgravetown Group and the sub-Signal Hill Group unconformity (e.g., Lilly Unconformity) may provide the best temporal constraints on  $D_{1b}$  (Fig. 3.1B).

### **3.2.3 $D_{2a}$ $S_2$ Cleavage Contractional Event**

The end of the  $D_{1a}$  and  $D_{1b}$  late Proterozoic deformational phases is marked by the onlap of the Cambrian-Ordovician platformal sequence during a period of quiescence and transgression, followed by the deposition of Silurian to Mesozoic rocks.  $D_{2a}$  is a contractional event which affected Cambrian and Proterozoic rocks in the study site (Fig. 3.1C). The angular discordance between the sub-Cambrian unconformity and the underlying Proterozoic rocks represents the most distinctive and clear relationship between Proterozoic  $D_{1a}$  and  $D_{1b}$  and post-Cambrian  $D_2$  deformation (Fig. 3.1C).

The regionally pervasive and consistently north- to north-northeast-trending  $S_2$  cleavage in Cambrian and Proterozoic rocks across the study site, indicates that the principal mechanism for deformation during  $D_{2a}$  was east-west oriented layer-parallel shortening. Detachment was minimal along and proximal to the sub-Cambrian unconformity during  $D_{2a}$ , demonstrated by shallow thrusts (e.g., Fig. 2.9CC').

Open, sub-cylindrical  $F_2$  folds vary in orientation from north-northwest to north-northeast.  $F_2$  folds developed axial plane  $S_2$  in sectional view, but were commonly transected by  $S_2$  by up to  $15^\circ$  in plan view. The transection of  $F_2$  folds by  $S_2$  in the study site was interpreted to reflect the local differential dependency of fold orientations on the orientations of  $D_{2b}$  reactivated Proterozoic faults, as well as a natural relationship in the synchronous

development of fold and cleavage in low-grade metamorphic terranes. Thus, transected  $F_2$  folds are consistent with  $D_{2a}$  east-west shortening, however, they do not directly represent the regional  $D_{2a}$  stress field.

Cambrian strata in the study site were preserved in open synclines or syncline-anticline pairs in inverted  $D_{1a}$  horst bounded by  $D_2$  reverse faults (e.g., Marysvale, West Limb, Cowboy, Little Brook, Duffs and Topsail faults) (Fig. 3.1C). The north-northeast-trending Marysvale fault underwent apparent dextral strike-slip and reverse-slip. The steep, north-trending faults underwent a major component of  $D_2$  shortening, as demonstrated by flattened cobbles in  $S_1$  in the Bacon Cove area (e.g., Fig. 2.28). A major component of shortening along the Topsail fault zone is also consistent with  $D_{2a}$ .

West-vergence of mesoscopic and macroscopic  $F_2$  folds is demonstrated by Cambrian bed and  $S_2$  angular relationships in i) the eastern limb of the Salmon Cove  $F_2$  syncline (e.g., Fig. 2.27), ii) the  $F_2$  Chapels Cove anticline-syncline pair (e.g., Fig. 2.13), and iii) the moderately east-dipping panel of Cambrian rocks in the Brigus area (e.g., Fig. 2.1B). The consistent west-vergence of  $F_2$  folds in Cambrian strata across the study site suggests that a macroscopic north-northeast-trending  $F_2$  antichlinal axial trace occurred to the west of the study site, along the Baccalieu Peninsula and adjacent to the ( $F_2$ ) Trinity Bay Syncline (Fig. 3.1C). This anticline is referred to here as the  $F_2$  Baccalieu Peninsula anticline (Fig. 3.1C).

West-verging  $F_2$  folds in Cambrian strata across the study site further suggest that a macroscopic, north-northeast-trending  $F_2$  synclinal axial trace occurred to the east of the study site, possibly along the Conception Bay and Proterozoic Harbour Main Massif, where Cambrian-Ordovician sequences crop out in a northwest-facing homocline on Bell Island and along the southeastern shore of Conception Bay. This syncline is referred to as the Conception Bay  $F_2$  syncline (Fig. 3.1C). The low amplitude and large wavelength of the  $F_2$  Conception Bay syncline may reflect the buttressing effect of the underlying Holyrood Intrusive Suite. The more brittle, underlying Proterozoic rocks may have accommodated much of the shortening in  $D_2$  along faults, such as the Topsail fault zone. These relationships

further imply that Paleozoic rocks across the Avalon Peninsula were preserved in  $F_2$  macroscopic synclines, bounded by  $D_{2a}$  reverse and thrust faults and inverted horsts (e.g.,  $D_{1a}$  Brigus-Marysville  $D_{2b}$  inverted horst (Fig. 3.1C).

### 3.2.4 $D_{2b}$ Block Faulting Extensional Event

$D_{2b}$  is characterized by normal faulting along north-trending faults, affecting all rock types in the study site (Fig. 3.1C). Most of these faults were reactivated  $D_{1a}$  (e.g., Salmon Cove fault) and/or  $D_{2a}$  (e.g., Nautiyal 1967) faults.  $D_{2b}$  structures terminate against the north-trending Long Pond, Ray and Salmon Cove faults and the north-northeast-trending Pebble fault. These structures locally underwent commensurate rotation and normal separation of up to several 10's of metres along the faults (e.g., Figs. 2.5, 2.11, 2.14, 2.29). These relationships suggest that north-northeast-trending faults underwent predominantly apparent normal slip during  $D_{2b}$  (Fig. 3.1C).

Apparent dextral  $D_{2b}$  strike-slip was locally observed along the north-trending South Brook fault (Figs. 2.13, 3.1C). Furthermore, apparent sinistral and dextral  $D_{2b}$  strike-slip was locally demonstrated (e.g., Figs. 2.10, 2.13) along northwest-trending faults by the commensurate rotation of  $S_2$  and Conception Group strata adjacent to the faults. Thus,  $D_{2b}$  structures are consistent with a maximum extension axis,  $\sigma_3$ , oriented approximately northwest-southeast and the maximum compression axis,  $\sigma_1$ , oriented approximately vertical. Vertical tectonics is not consistent with  $D_{2a}$ .

Across the study site, Cambrian beds are preserved in down-faulted blocks (Fig. 3.1C) along the  $D_{2b}$  Beach and Salmon Cove faults in the Salmon Cove area (Figs. 2.10, 2.11) and the  $D_{2b}$  Long Pond fault in the Brigus area (Figs. 2.4, 2.5). At North Head in the Brigus area, the shallowly east-dipping North Head fault that is sub-parallel to the sub-Cambrian unconformity, may represent a splay of the adjacent, steep  $D_{2b}$  Long Pond fault. The North Head fault underwent apparent normal separation, demonstrated by the east-directed imbrication of the unconformable contact and the commensurate rotation of  $S_2$  to sub-



horizontal dips (e.g., Fig. 2.30). These relationships are consistent with  $D_{2b}$  extensional tectonics. The  $D_{2b}$  North Head fault may represent a minor detachment surface formed through reactivation of a  $D_{2a}$  thrust.

The relative age of  $D_{2b}$  is unknown because of the lack of Devonian and younger rocks in the Avalon Peninsula. Across the study site, the uplift and crustal thickening of Cambrian rocks, associated with  $D_{2a}$  is interpreted to have been relatively insignificant to have resulted in a relaxing or extensional phase following  $D_{2b}$ . Thus  $D_{2b}$  is interpreted to be associated with an extensional event independent of  $D_{2a}$ .

### 3.3 Validity of Model — A Discussion

The structural evolution model presented above suggests that the study site and Avalon Peninsula were affected by four distinctive deformational events: They include a  $D_{1a}$  late Proterozoic block faulting phase and  $D_{1b}$  late Proterozoic conjugate kink band contractional phase; a  $D_{2a}$  post-Cambrian  $S_2$  contractional event; and a  $D_{2b}$  post- $S_2$  block faulting extensional event. The following tests the validity and limits of the model based on its application to areas outside the study site.

$D_{1a}$  is interpreted to be related to the emplacement of the (548 Ma to 580 Ma) Swift Current granite and volcanism of the Bull Arm Formation (Fig. 3.2). Based on the age dates of the granite,  $D_{1a}$  is consistent with the 575-550 Ma tectonism proposed by O'Brien and others (1990, 1992, 1996). The relative age of  $D_{1a}$  may be tested outside the study site by evaluating areas where the Bull Arm Formation and the Swift Current granite crop out, as well as in the Musgravetown Group that is unconformably overlain by Cambrian rocks (e.g., Cape St. Mary's, or southern shore of Trinity Bay; Fig. 1.2).

$D_{1a}$  implies a penecontemporaneous development of the Harbour Main Massif and the deposition of the Signal Hill Group in an alluvial-flood plain. Abundant Conception Group detritus in the lower Signal Hill Group (e.g., King 1990) support this interpretation. Paleocurrent data suggest that most of the Signal Hill Group came from an uplifted source to

the north of the Avalon Peninsula (King 1990). However, they do not refute the possibility that at this time, tectonic uplift was in addition, developing the Harbour Main Massif and shedding Conception Group debris from an uplifted source marginal into the depositional basin.

The  $D_{1b}$  conjugate kink band contractional event affected all Proterozoic rocks in the study site. The geometric relationships between northwest-trending dextral kink band sets and northeast-trending sinistral kink band sets, with respect to generally north-trending anisotropic multilayers external to the kink bands suggest that  $\sigma_1$  was oriented approximately north-south in a convergent tectonic environment during  $D_{1b}$ . The absence of normal kink bands or pinch-and-swell structures within the kink bands refutes the possibility that  $\sigma_1$  may have been oriented perpendicular or at high-angles to the anisotropic multilayers (Kidan and Cosgrove 1996).

Goscombe and others (1994) suggest that kinking, at any scale, may result from a temporally distinctive event and in a strain field nearly orthogonal to that during the main orogenic episode. Stubley (1989, 1990) interprets kinking by the local reorientation of  $\sigma_1$  to lower angles to the orogenic belt, an important mechanism accompanying late-stage strike-slip faulting that develops under regional compression normal to the orogen.

$D_{1b}$  is interpreted to represent a late contractional phase during 575-550 Ma tectonism. North-south  $D_{1b}$  shortening is indeed orthogonal to the regional Avalonian orogenic belt and  $D_{1a}$  structures, whereby  $\sigma_1$  was rotated from approximately vertical during  $D_{1a}$  to sub-horizontal and north-south oriented during  $D_{1b}$ . The fact that kink band sets were developed in zones along and adjacent to the major Brigus, Marysvale and Bacon Cove faults across the study site, and generally north-trending faults are common across the Avalon Peninsula (e.g., King 1988), suggest that kink bands and consequently dome and basin structures were formed in relation to strike-slip along major faults, as suggested by Stubley (1989, 1990). Under these conditions, north-trending faults may have undergone sinistral or dextral strike-slip, depending on the local angle made between the faults and  $\sigma_1$ .

Regional dome and basin and periclinal structures in late Proterozoic rocks across the Avalon Peninsula (e.g., King 1988) generally comprise northeast- and northwest-trending

axial traces and non-penetrative fabrics (e.g., Western Island Pond Basin; King 1990). These structures are transected by a regional cleavage, interpreted here as  $S_2$ , at high angles (of more than  $15^\circ$ ) (e.g., King 1988) and are therefore interpreted to be Proterozoic in age. The  $D_{1b}$  conjugate kink band contractional event can best explain the nature of these structures as demonstrated in the study site.

The distribution of kink bands in multiply deformed areas may reflect i) the heterogeneity of the curved and kinked fault morphologies (Freund 1974) which may have resulted from the intersection of the north- to north-northwest-trending Brigus and Bacon Cove faults and the north-northeast-trending Marysvale fault; and ii) the bulk mechanical anisotropy of the multilayers and faults (Honea and Johnson 1976) distinctive to the area. This latter point is demonstrated in layered sedimentary Harbour Main Group units at Seal Head, Brigus area, in the up-stratigraphic-section transition from a high strain enclave of overturned isoclinal  $F_1$  folds and  $S_1$  in thinly bedded shale and siltstone, into a lower strain zone of open box-like  $F_1$  folds in thickly bedded sandstones and siltstones (e.g., Fig. 2.19). It is in these discrete high strain zones where  $S_1$  is locally developed.

An important mechanism for the initiation and amplification of kink bands is layer-parallel shear along strongly anisotropic foliation, external to the kink band(s). Experimental card deck models suggest that the amount of strain required to initiate a kink band is small (Gay and Weiss 1974). Increasing the confining pressure increases the yield strength of the layers, reducing the finite fold amplitude (Gay and Weiss 1974). Therefore, the initiation of kink bands is easier at lower confining pressures, in strata buried at shallower depths. This further implies that  $S_1$  is not a penetrative fabric across and outside the study site because  $D_{1b}$  occurred in a semi-brittle deformational regime under low temperature and mean stress conditions.

The apparent sinistral strike-slip along the Brigus fault inferred by the oblique vergence of northeast-trending  $D_{1b}$  contractional structures with respect to north- to north-northeast-trending faults, combined with the locally observed reclined nature of  $F_1$  folds, may suggest sinistral transpression in  $D_{1b}$ . Similarly, east of the Topsail fault zone, an apparent

restraining bend is demonstrated by the oblique vergence of northeast-trending contractional structures at Portugal Cove (King 1988) with respect to the Topsail fault zone (Fig. 3.1B). Here, east-directed, reverse fault-parallel overturned folds in layered Harbour Main and Conception group rocks, with a strong axial plane cleavage are interpreted to be Proterozoic structures (Smith 1987). Sinistral transpression, however, fails to explain the simultaneous development of northeast- and northwest-trending  $D_{1b}$  contractional structures and parallel kink band sets, and regional dome and basin structures.

It may also be argued that  $D_{1b}$  may represent a fold and thrust regime (e.g., Brun and Bale 1990), also demonstrated by the Portugal Cove thrust system (Smith 1987). Thrust tectonics would require significant thickening of units due to fault imbrication which is not observed in the map area. Furthermore, a fold and thrust system does not explain the apparent strike-slip component along mainly contractional structures as observed in the map area. In addition, a fold and thrust system does not explain the obliquity between north-northeast- to north-northwest-trending strike-slip faults and northeast- and northwest-trending contractional structures across the study site, which is adequately explained by a conjugate kink band contractional setting.

In the eastern Avalon Zone, the Avalonian Orogeny has traditionally been associated with the emplacement of the Holyrood Intrusive Suite into the Harbour Main Group, structural doming and folding, and nonextensive penetrative fabric development, in a prehnite-pumpellyite to chlorite facies regional metamorphic regime. The model shows that after the emplacement of the Holyrood Intrusive Suite, the 590-545 Ma rock package was affected by the  $D_{1a}$  and  $D_{1b}$  early and late phases of the 575-550 Ma tectonostratigraphic event (Fig. 3.2). If the 575-550 Ma tectonostratigraphic event is associated with the Avalonian Orogeny, then  $D_{1a}$  and  $D_{1b}$  are part of a late episode of the progressive and diachronous late Proterozoic Avalonian event.

Acadian deformation has traditionally been regarded as the dominant mid-Paleozoic event that affected the Avalon Zone (e.g., Younce 1970, Williams 1993), while the mid-Ordovician Taconic event is absent (Rodgers and Neale 1963, Greenough et al. 1993). Recent

data (O'Brien et al. 1996) indicate that the Silurian Salinic event was more predominant in the western Avalon Zone than previously thought. In the offshore Avalon Zone, Ordovician and Silurian sequences are disconformably overlain by Devonian units (Durling et al. 1987).

In the southwestern Avalon Peninsula, Silurian (ca. 440 Ma) mafic sills intrude Cambrian sequences, and are both deformed into open, north-trending macroscopic folds which resemble the typical Acadian deformation documented in the eastern Avalon Zone (Greenough et al. 1993). Arguably, "typical Acadian deformation" on the Avalon Peninsula may represent Acadian (Devonian) or Silurian (Salinic) deformation because there is no age control to differentiate between the two (S. O'Brien, personal comm.). Furthermore, Salinic deformation affected rocks as young as 420 Ma, therefore the mafic sills could have been affected by the Salinic as well as Acadian events. Thus, due to the lack of age control in the Avalon Peninsula, it is impossible to assign  $D_{2a}$  to either the Salinic or Acadian orogenic events, and therefore  $D_{2a}$  is referred to represent mid-Paleozoic tectonism in this study.

The  $D_{2a}$  contractional event affected all rocks in the study site and reactivated many  $D_{1a}$  and/or  $D_{1b}$  faults to thrust or reverse faults (e.g., Marysvale, Bacon Cove and Portugal Cove thrust faults; Fig. 3.1B).  $F_2$  folds are characterized by open, shallowly plunging, north-northeast- to north-northwest-trending periclinal folds in Cambrian rocks in the study site. Similarly, farther west, folds in Cambrian rocks are moderately tight, north-trending and periclinal. The periclinal nature of the folds may reflect the shallow plunge of the folds and the irregularity of the depositional surface upon which Cambrian rocks were overlain.  $F_2$  folds developed either axial plane regional  $S_2$  cleavage or were transected in plan view by up to  $15^\circ$ . The relative age of periclinal, north-trending folds which occur in Proterozoic rocks in and outside the study site were interpreted to represent either  $F_1$  or  $F_2$  based on their cross-cutting relationships with respect to  $S_2$  by more or less than  $15^\circ$  in plan view.

The  $D_{2b}$  extensional event affected all rocks in the study site. East of the study site, the gently northwest-dipping Cambrian-Ordovician homocline unconformably overlies the Holyrood Intrusive Suite and Harbour Main Group in the Holyrood Horst, and possibly the Conception Group beneath the Conception Bay (Miller 1983). These relationships indicate

that Cambrian-Ordovician sequences were preserved in a down-faulted block along the Topsail fault zone and Duffs fault at least after early Ordovician Arenig time (e.g., Miller 1983). These relationships are consistent with the  $D_{2b}$  extensional event, which may imply that the  $D_{1a}$  Holyrood Horst represents a  $D_{2b}$  inverted  $D_{1a}$  horst (Fig. 3.1C). Thus, Cambrian-Ordovician rocks across the Avalon Peninsula are preserved in  $D_{2a}$  synclines, commonly in  $D_{1a}$  horsts that were inverted during  $D_{2b}$ .

The relative age of the post- $S_2$   $D_{2b}$  extensional event is inconclusive. As mentioned in chapter 1, block faulting may represent part of a strike-slip tectonic system of the mid-Devonian to early Permian Alleghenian-Hercynian Orogeny and/or Mesozoic vertical tectonism. The northwest-southeast maximum extension direction inferred by the orientation of Triassic dykes in the southern Avalon Peninsula is consistent with fault-bounded, Alleghenian-Hercynian and Mesozoic sedimentary basins in the offshore Avalon Zone, as well as with structural and stratigraphic relationships in  $D_{2b}$ . Furthermore, due to the erosion of most Devonian and younger rocks in the onland Avalon Zone, there is no age control to differentiate between Alleghenian-Hercynian and younger deformational events. Thus,  $D_{2b}$  is regarded in this study as a distinctive, post- $S_2$  extensional event, associated with the Paleozoic Alleghenian-Hercynian Orogeny and/or the Mesozoic vertical tectonic system.

The limit in the application of the model outside the study site lies in the contrast in deformational styles which is observed across the Avalon Zone (e.g., Williams 1993). This contrast may result from regional strain partitioning between shortening, strike-slip and extension, which can produce a variety of structures in a complex and diachronous pattern (e.g., Burchfield and Royden 1995). Strain partitioning, combined with the buttressing effect of the Harbour Main Massif and major, north-trending Proterozoic faults in the Avalon Peninsula may have further contributed to the distinctive styles of the  $D_{1a}$ ,  $D_{1b}$ ,  $D_{2a}$  and  $D_{2b}$  deformational events in the Avalon Peninsula.



## **4. DISCUSSION AND CONCLUSIONS**

### **4.1 Discussion**

Regional zones of strong non-coaxial movement related to contractional and extensional structures are widespread in orogens, and therefore it is often difficult to distinguish between contractional and extensional phases in the evolution of an orogen (Krabbendam and Leslie 1996). Major north-trending faults across the study site and Avalon Peninsula represent long-lived and reactivated faults.  $D_{1a}$  block faulting occurred along these major faults, which were reactivated to sinistral and dextral strike-slip faults during  $D_{1b}$  north-south oriented shortening; and to reverse and strike-slip faults in  $D_{2a}$  east-west oriented shortening; and to normal faults in  $D_{2b}$ . Structures associated with movement along these faults, as well as the stratigraphic offsets projected in cross sections have provided a relative sense of displacement on the faults, in which the orientation of the stress regime was induced for each deformational event.

It is generally accepted that axial plane cleavage indicates that both cleavage and folding formed at the same time. Non-axial plane cleavage is commonly attributed to either, cleavage overprinting earlier formed folds or to represent transpressional folding (Williams 1976). The non-axial plane cleavage of transected folds (assuming folds are synchronous with cleavage development) may be explained by the difference of the three-dimensional, heterogeneous stress and strain behaviour between adjacent layers (Duncan 1985) which has been used as strong evidence for regional transpression (Sanderson et al. 1980; Soper and Hutton 1984; Woodcock et al. 1988). In the study site, the lack of evidence for  $D_{2a}$  transpression, but rather regional east-west contraction, solicits for an alternative explanation for  $S_2$  transected  $F_2$  folds.

A modest obliquity between cleavage and the axial plane of same generation folds is common in low-grade metamorphic terranes (Borradaile 1978, Stringer and Treagus 1980, Treagus and Treagus 1981). This suggests that the modest (up to  $15^\circ$ ) discrepancy between  $F_2$  axial planes and  $S_2$  orientations in Cambrian rocks in the study site may not represent true  $S_2$

transected  $F_2$  folds as defined by Ghosh (1966), Powell (1974) and Borradaile (1978), but rather reflects the irregular Proterozoic depositional surface of Cambrian rocks, and a natural relationship in fold and cleavage development in low-grade metamorphic terranes.

Furthermore, the Proterozoic Marysvale fault, Bacon Cove fault and Red Rock and parallel faults occur in and adjacent to parallel  $F_2$  folds in Cambrian rocks in the study site. The parallelism between  $F_2$  folds and reactivated Proterozoic faults raises the possibility that the orientations of the  $F_2$  fold axial traces were controlled by these faults and do not reflect the regional east-west principal compressive stress in  $D_{2a}$ . In contrast,  $S_2$  reposes regional east-west  $D_{2a}$  contraction, and remains relatively constant in orientation across the study site.

Therefore, in addition to the very open nature and therefore variable orientation of  $F_2$  fold axial traces across the study site and Avalon Peninsula, the noted transection of  $F_2$  folds by  $S_2$  is interpreted to reflect the differential dependency of fold orientations on fault orientations, as well as a natural relationship in the synchronous development of fold and cleavage in low-grade metamorphic terranes. Therefore, transected  $F_2$  folds are consistent with  $D_{2a}$  east-west shortening, however, they do not directly represent the regional  $D_{2a}$  stress field.

Detailed, field-based structural and stratigraphic future work in areas outside the study site can test the model presented in this study. These areas do not necessarily require the sub-Cambrian unconformity as a control for deformation. The sub-Signal Hill Group, sub-Musgravetown Group and sub-Conception Group unconformities can provide relative age controls on  $D_{1a}$ ,  $D_{1b}$  and pre- $D_{1a}$  within the late Proterozoic suite of rocks. Future work in these areas may cast more insight into the complex and prolonged nature of the late Proterozoic Avalonian Orogeny.

Similarly, the problem of the relative timing of  $D_{2a}$ , of whether it represents Salinic and/or Acadian tectonism could be addressed in the 440 Ma mafic sills preserved in the southwestern Avalon Peninsula. Detailed structural and stratigraphic future work may delineate cross-cutting relationships with the use of the regional  $S_2$  cleavage. An upper limit could be placed on  $D_{2b}$  by testing whether  $D_{2b}$  block faulting affected the northeast-trending Triassic dykes across the Avalon Peninsula.

## 4.2 Conclusions

The primary objective of this study was to determine whether field-based structural and stratigraphic criteria could be used to distinguish between pre- and post-Cambrian deformation. The angular discordance between folded Proterozoic rocks and the sub-Cambrian unconformity, and the cross-cutting relationship between  $F_1$  and  $S_2$  were used successfully as a control to differentiate between  $D_1$  and  $D_2$  structures.

$S_2$  developed either axial planar to  $F_2$  folds or mildly non-axial planar with transection angles of up to  $15^\circ$  in plan view.  $S_2$  commonly cross-cut  $F_1$  folds by  $40^\circ$  in plan view, and cut  $F_1$  folds obliquely in sectional view. These consistent transections of  $F_2$  by  $S_2$  and cross-cutting relationships of  $F_1$  by  $S_2$  produced reliable criteria that were used to differentiate between  $D_1$  and  $D_2$  structures in zones outside of the control of the sub-Cambrian unconformity.

A second objective of this study was to determine whether each of the Proterozoic and Paleozoic rocks were affected by multiple tectonism, a single tectonic event or different phases of a single event. Each  $D_1$  and  $D_2$  showed different styles of deformation under very contrasting tectonic settings. Based on these observations,  $D_1$  was divided into an early  $D_{1a}$  block faulting phase and a late  $D_{1b}$  conjugate kink band contractional phase of the 575-550 Ma tectonostratigraphic event.  $D_2$  was divided into a distinctive  $D_{2a}$   $S_2$  contractional event and a  $D_{2b}$  post- $S_2$  block faulting extensional event.  $D_{1a}$ ,  $D_{1b}$ ,  $D_{2a}$  and  $D_{2b}$  were incorporated into a structural evolution model of the study site and Avalon Peninsula and tested in zones outside the study site.

This study showed that after the emplacement of the Holyrood Intrusive Suite, two phases of the 575-550 Ma tectonostratigraphic event affected late Proterozoic rocks. They include an early  $D_{1a}$  block faulting phase which initiated with the emplacement of the Swift Current granite and vulcanism of the Bull Arm Formation, and a late  $D_{1b}$  conjugate kink band set contractional phase, associated with the progressive and diachronous Avalonian Orogeny.

$D_{2b}$  produced the regional  $F_1$  Trinity Bay synclinorium,  $F_1$  Holyrood Anticline and  $F_1$  Blackhead syncline. If the 575-550 Ma tectonostratigraphic event is associated with the Avalonian Orogeny, then

$D_{2a}$  was interpreted to be associated with the development of the regional  $S_2$  cleavage and open, sub-cylindrical and large wavelength  $F_2$  folds and associated thrusts across the Avalon Peninsula. These folds include the regional  $F_2$  Baccalieu Peninsula anticline and the  $F_2$  Conception Bay syncline, east of the  $F_2$  Trinity Bay syncline. Cambrian rocks are commonly preserved in the core of  $F_2$  synclines and in  $D_{2a}$  inverted  $D_{1a}$  horsts.  $D_{2a}$  may be related to the mid-Paleozoic Salinic and/or Acadian orogenies in the Avalon Zone.

$D_{2b}$  was interpreted to be associated with block faulting and the commensurate rotation of  $S_2$  and Cambrian and older rocks.  $D_{2a}$  block faulting has preserved Cambrian rocks in down-faulted blocks along reactivated  $D_{1a}$  and/or  $D_{2a}$  faults, including the  $D_{2b}$  inverted  $D_{1a}$  Holyrood Horst.  $D_{2b}$  is a post- $S_2$  extensional event which may represent transtension in a strike-slip system of the mid-Devonian to early Permian Alleghenian-Hercynian Orogeny and/or Mesozoic vertical tectonics.

## LITERATURE CITED

- Alsop, G.I., 1992. Progressive deformation and the rotation of contemporary fold axes in the Ballybofey Nappe, north-west Ireland. *Geol. J.* 27, 271-283.
- Anderson, M.M., Brückner, W.D., King, A.F. and Maher, J.B., 1975. The late Proterozoic "H. D. Lilly unconformity" at Red Head, Northeastern Avalon Peninsula, Newfoundland. *Am. J. Sci.*, 275:1012-1027.
- Ayrton, W.G., Birnie, D.E., Swift, J.H., Wellman, H.R., Stevulak, J.F., Waylett, D.C., Wilkinson, R.A.F., Hamilton, J.D. and Harriston, D.B., 1974. Regional Geology of Grand Banks. The American Association of Petroleum Geologists Bulletin, v. 58, no. 6, 1109-1123.
- Biot, M.A., 1965. Similar folding of the first and second kinds. *Geol. Soc. Am. Bull.* 72, 1595-1620.
- Blackwood, R.F. and Kennedy, M.J., 1975. The Dover Fault: western boundary of the Avalon Zone in northeastern Newfoundland. *Can. J. Earth Sci.* 12, 320-325.
- Blackwood, R.F. and O'Driscoll, C.F., 1976. The Gander-Avalon boundary in northeastern Newfoundland. *Can. J. Earth Sci.*, 13, 1155-1159.
- Blewett, R.S., and Pickering, K.T., 1988. Sinistral shear during Acadian deformation in north-central Newfoundland, based on transecting cleavage. *J. Struct. Geol.*, 10, 125-127.
- Borradaile, G.J., 1978. Transected folds: a study illustrated with examples from Canada and Scotland. *Geol. Soc. Am. Bull.*, 89, 481-493.
- Brückner, W.D., 1969. Geology of eastern part of Avalon Peninsula, Newfoundland--summary. North Atlantic-Geology and Continental Drift, Memoir 12, Am. Assoc. of Petroleum Geologists Avalonian Orogeny, 130-138.
- Brun, J.P., and Bale, P., 1990. Cadomian tectonics in northern Brittany. *In* The Cadomian Orogeny, D'Lemos, R.S., Strachan, R.A. and Topley, C.G. (eds), Geological Soc. Special Pub, 51, 95-114.
- Burchfield, B.C. and Royden, L.H., 1995. Extension within an intracontinental region of oblique shear: the Longmen Shan region, eastern Tibetan Plateau, Sichuan, China. Abstract with programs. *Geol. Soc. Am.* 27; 6, 121.
- Chinnery, M.A., 1966. Secondary Faulting. *Can. J. Earth Sci.*, 3, 163-190.
- Cobbold, P.R., 1976. Mechanical effect of anisotropy during large finite deformations. *Bull. Soc. Geol. France*, 18, 1497-510.
- Cutt, B.J. and Laving, J.G., 1977. Tectonic elements and geologic history of the south Labrador and Newfoundland continental shelf, eastern Canada. *Bulletin of Canadian Petroleum Geology*, 25, 1037-1058.
- Dallmeyer, R.D., Blackwood, R.F. and Odom, A.L., 1981. Age and origin of the Dover Fault: tectonic boundary between the Gander and Avalon Zones of the northeast Newfoundland Appalachians. *Can. J. Earth Sci.*, 18, 1431-1442.

- Dallmeyer, R.D., Hussey, E.M., O'Brien, S.J. and O'Driscoll, C.F., 1983. Chronology of tectonothermal activity in the western Avalon zone of the Newfoundland Appalachians. *Can. J. Earth Sci.*, 20, 355-363.
- Dec. T., O'Brien, S.J. and Knight, I., 1992. Late Precambrian volcanoclastic deposits of the Avalonian Eastport Basin (Newfoundland Appalachians): Petrofacies, detrital clinopyroxene geochemistry and paleotectonic implications. *Precambrian Research*, 59, 243-262.
- D'Lemos, R.S., Strachan, R.A. and Topley, C.G., 1990. The Cadomian Orogeny in the North Armorican Massif: a brief review. *In* The Cadomian Orogeny. D'Lemos, R.S., Strachan, R.A. and Topley, C.G. (eds), Geological Soc. Special Publication 51, 3-12.
- Doig, R., Nance, R.D., Murphy, J.B. and Casseday, R.P., 1990. Evidence for Silurian sinistral accretion of Avalon composite terrane in Canada. *J. Geol. Soc.*, London, 147, 927-930.
- Duncan, A.C., 1985. Transected fold: a re-evaluation, with examples from the 'type area' at Sulphur Creek, Tasmania. *J. Struct. Geol.*, 7, 409-419.
- Dunning, G.R., O'Brien, S.J., Colman-Sadd, S.P., Blackwood, R.F., Dickson, W.L., O'Neill, P.P. and Krogh, T.E., 1990. Silurian Orogeny in the Newfoundland Appalachians. *J. of Geol.*, 98, 895-913.
- Durling, P.W., Bell, J.S. and Fader, G.B.J., 1987. The geological structure and distribution of Paleozoic rocks on the Avalon Platform, offshore Newfoundland. *Can. J. Earth Sci.*, 24:1412-1420.
- Espina, R.G., Juan, L. A. and Pulgar, J.A., 1996. Growth and propagation of buckle folds determined from syntectonic sediments (the Ubierna Fold Belt, Cantabrian Mountains, N Spain). *J. Struct. Geol.*, 4: 431-441.
- Fletcher, T.P., 1972. Geology and Lower to Middle Cambrian trilobite faunas of the southwest Avalon, Newfoundland. Ph.D. Thesis, Cambridge University, Cambridge, England, 530 pp.
- Freund, R., 1974. Kinematics of transform and transcurrent faults. *Tectonophysics*, 21, 93-134.
- Gardiner, S. And Hiscott, R.N., 1988. Deep-water facies and depositional setting of the lower Conception Group (Hadrynian), southern Avalon Peninsula, Newfoundland. *Can. J. Earth Sci.*, 25, 1579-1594.
- Gay, N.C. and Weiss, L.E., 1974. The relationship between principal stress directions and the geometry of kinks in foliated rocks. *Tectonophysics*, 21, 287-300.
- Ghosh, S.K., 1966. Experimental tests of buckling folds in relation to strain ellipsoid in simple shear deformation. *Tectonophysics*, 3, 169-185.
- Gibbons, W., 1990. Transcurrent ductile shear zones and the dispersal of the Avalon superterrane. *In* The Cadomian Orogeny. D'Lemos, R.S., Strachan, R.A. and Topley, C.G. (eds), Geological Soc. Special Publication 51, 407-423.
- Rice, R. T., 1996. Structure of the Flat Rock thrust zone, Avalon Peninsula, Newfoundland Appalachians. B.Sc. Thesis. Memorial University of Newfoundland, St. John's, Newfoundland. 117 pp.

- Goscombe, B.D., Findlay, R.H., McClenaghan, M.P. and Everard, J., 1994. Multiscale kinking in northeast Tasmania: crustal shortening at shallow crustal levels. *J. Struct. Geol.* 16, 1077-1092.
- Grant, A.C., 1987. Inversion tectonics on the continental margin east of Newfoundland. *Geology*, 15, 845-848.
- Greene, B.A., 1973. Geology of the Marystown and St. Lawrence study sites, Newfoundland, Mineral Development Division, Newfoundland Department of Mines and Energy, 30 pp.
- Greenough, J.D., 1995. Mesozoic rocks; Chapter 6 in *Geology of the Appalachian-Caledonian Orogen in Canada and Greenland*, (ed.) H. Williams; Geological Survey of Canada, *Geology of Canada*, no. 6, 567-600.
- Greenough, J.D. and Papezik, V.S., 1985. Petrology and geochemistry of Cambrian volcanic rocks from the Avalon Peninsula, Newfoundland. *Can. J. Earth Sci.*, 22, 1594-1601.
- Greenough, J.D., Kamo, S.L. and Krogh, T.E., 1993. A Silurian U-Pb age for the Cape St. Mary's sills, Avalon Peninsula, Newfoundland, Canada: implications for Silurian orogenesis in the Avalon Zone. *Can. J. Earth Sci.*, 30, 1607-1612.
- Harding, T.P., 1976. Tectonic significance and hydrocarbon trapping consequence of sequential folding synchronous with San Andreas faulting, San Joaquin Valley, California. *Am. Assoc. Pet. Geol. Bull.*, 60, 356-378.
- Harland, W.B., 1971. Tectonic transpression in Caledonian Spitsbergen. *Geol. Mag.* 108, 27-42.
- Haworth, R.T. and Lefort J.P., 1979. Geophysical evidence for the extent of the Avalon zone in Atlantic Canada. *Can. J. Earth Sci.*, 16, 552-567.
- Hayes, J.P. and O'Driscoll, C.F., 1990. Regional geological setting and alteration within the eastern Avalon high-alumina belt, Avalon Peninsula, Newfoundland. *Current Research, Newfoundland Dept. of Mines and Energy, Geological Survey Branch, Report 90-1:145-155.*
- Hodych, J.P. and Hayatsu, A., 1988. Paleomagnetism and K-Ar isochron dates of Early Jurassic basaltic flows and dykes of Atlantic Canada. *Can. J. Earth. Sci.*, 25, 1972-1989.
- Honea, E. and Johnson, A.M., 1976. A theory of concentric, kink and sinusoidal folding and of monoclinical flexuring of compressible elastic multilayers, IV. Development of sinusoidal and kink folds in multilayers confined by rigid boundaries. *Tectonophysics*, 30, 197-239.
- Hudleston, P. J. and Lan, L., 1993. Information from fold shapes. *J. Struct. Geol.* 15, 253-264.
- Hughes, C.J., 1970. The late Proterozoic Avalonian Orogeny in Avalon, southeast Newfoundland. *Am. J. Sci.*, 269, 183-190.
- Hughes, C.J., 1971. Anatomy of a granophyre intrusion. *Lithos*, 4, 403-415.
- Hughes, C.J. and Brückner, W.D., 1971. Late Proterozoic rocks of eastern Avalon Peninsula, Newfoundland — a volcanic island complex. *Can. J. Earth Sci.*, 8, 899-915.
- Hutchinson, R.D., 1953. *Geology of Harbour Grace map area, Newfoundland. Geological Survey of Canada, Memoir 275, 43 pp.*



- Hutchinson, R.D., 1962. Cambrian stratigraphy and Trilobite faunas of southeastern Newfoundland. Geological Survey of Canada, Bulletin 88, 56 pp.
- Irving, E., 1979. Paleopoles and paleolatitudes of North America and speculations about displaced terranes. *Can. J. Earth Sci.*, 16, 669-694.
- Jamison, W.R., 1991. Kinematics of compressional fold development in convergent wrench terranes. *Tectonophysics*, 190, 209-232.
- Jenness S.E., 1963. Terra Nova and Bonavista Bay study sites (2D E 1/2 and 2C), Newfoundland. Geological Survey of Canada, Memoir 327, 184 pp.
- Kamber, B.S., Blenkinsop, T.G., Villa, I.M. and Dahl, P.S., 1995. Proterozoic transpressive deformation in the Northern Marginal Zone, Limpopo Belt, Zimbabwe. *J. Geol.*, 103, 493-508.
- Kennedy, M.J., Blackwood, R.F., Colman-Sadd, S.P., O'Driscoll, C.F., and Dickson, W.L., 1982. The Dover-Hermitage Bay Fault: Boundary between the Gander and Avalon zones, eastern Newfoundland. *In* Major Structural Zones and Faults of the Northern Appalachians, St. Julien, P., and Beland, J. (eds.), Geological Association of Canada Special Publication, 24, 231-248.
- Keppie, J.D., 1985. The Appalachian collage. *In* The Caledonide Orogen-Scandinavia and related areas, Part 2. (ed.) D.G. Gee and B.A. Sturt. John Wiley and Sons Ltd., 1217-1226.
- Kidan, T.W. and Cosgrove, J.W., 1996. The deformation of multilayers by layer-normal compression; an experimental investigation. *J. Struct. Geol.* 4, 461-474.
- King, A.F., 1979. The birth of the Caledonides: Late Precambrian rocks of the Avalon Peninsula, Newfoundland, and their correlatives in the Appalachian-Orogen. *In* The Caledonides in the U.S.A., I.G.C.P., Blacksburg, Virginia.
- King, A.F., 1986. Geology of the St. John's area, Newfoundland. *In* Current Research, Newfoundland Department of Mines and Energy, Mineral Development Division, Report 86-1, 209-218.
- King, A.F., 1988. Geology of the Avalon Peninsula, Newfoundland. (Parts of 1K, 1L, 1M, 1N and 2C). Newfoundland Department of Mines, Mineral Development Division, Map 88-01.
- King, A.F., 1990. Geology of the St. John's area. Newfoundland Department of Mines, Mineral Development Division, Report 90-2, 88 pp.
- King, A.F., Brückner, Anderson, M.M. and Fletcher, T., 1974. Late Proterozoic and Cambrian sedimentary sequences of eastern Newfoundland. GAC/MAC, Fieldtrip Manual B-6.
- Knight, I. and O'Brien, S.J., 1988. Stratigraphy and sedimentological studies of the Connecting Point Group, portions of the Eastport (2C/12) and St. Brendans (2C/13) study sites, Bonavista Bay, Newfoundland. Department of Mines and Energy, Mineral Development Division, Report 88-1, 207-228.
- Kontak, D.J., Tuach, J., Strong, D.F., Archibald, D.A., Farrar, E., 1988. Plutonic and hydrothermal events in the Ackley Granite, southeast, Newfoundland, as indicated by total-fusion  $^{40}\text{Ar}/^{39}\text{Ar}$  geochronology. *Can. J. Earth Sci.*, 25, 8, 1151-1160.

- Krabbendam, M. and Leslie, A.G., 1996. Folds with vergence opposite to the sense of shear. *J. Struct. Geol.*, 6, 777-781.
- Krantz, R.W., 1995. The transpressional strain model applied to strike-slip, oblique-convergent and oblique-divergent deformation. *J. Struct. Geol.*, 8, 1125-1137.
- Krogh, T.E., Strong, D.F. and Papezik, V.S., 1983. Precise U-Pb ages of zircons from volcanic and plutonic units in the Avalon Peninsula. *Northeastern Section, Geol. Soc. Am., Abstracts with Programs*, v. 15.
- Krogh, T.E., Strong, D.F., O'Brien, S.J. and Papezik, V.S. 1988. Precise U-Pb zircon dates from the Avalon Terrane in Newfoundland. *Can. J. Earth Sci.*, 25, 442-453.
- LeBlanc, M., 1981. The late Proterozoic ophiolites at Bou Azzer, Morocco; evidence for Pan-African plate tectonics. *In Proterozoic Plate Tectonics*, Kroner, A. (ed.), Elsevier, Amsterdam, 435-441.
- Lilly, H.D., 1966. Late Proterozoic and Appalachian tectonics in the light of submarine exploration on the great bank of Newfoundland and in the Gulf of St. Lawrence. Preliminary views. *Am. J. Sci.*, 264, 569-574.
- Marillier, F., Keen, C.E., Stockmal, G.S., Quinlan, G., Williams, H., Colman-Sadd, S.P., and O'Brien, S.J., 1989. Crustal structure and surface zonation of the Canadian Appalachians: implications of deep seismic reflection data. *Can. J. Earth Sci.*, 26, 305-321.
- McCartney, W.D., 1967. Whitbourne study site, Newfoundland. Geological Survey of Canada, Memoir 341, 133 pp.
- McCartney, W.D., 1969. Geology of the Avalon Peninsula southeast Newfoundland. *In North Atlantic-geology and continental drift*. Am. Assoc. Petroleum Geologists. Memoir 12, 115-129.
- Miller, H.G., 1983. A geophysical interpretation of the geology of Conception Bay, Newfoundland. *Can. J. Earth Sci.*, 20, 1421-1433.
- Miller, H.G., 1985. Offshore extensions of the Avalon Zone of Newfoundland. *Can. J. Earth Sci.*, 22, 1163-1170.
- Nautiyal, A.C., 1967. The Cambro-Ordovician sequence in the southeastern part of the Conception Bay area, eastern Newfoundland. M.Sc. Thesis. Memorial University of Newfoundland, St. John's, Nfld., 334 pp.
- Nixon, G.T., 1975. Late Proterozoic (Hadrynian) ash-flow tuffs and associated rocks of the Harbour Main Group near Colliers, Avalon Peninsula, southeast Newfoundland. M.Sc. Thesis, Memorial University of Newfoundland, St. John's, Nfld., 301 pp.
- Nixon, G.T. and Papezik, V.S. 1979. Late Proterozoic ash-flow tuffs and associated rocks of the Harbour Main Group near Colliers, eastern Newfoundland: chemistry and magmatic affinities. *Can. J. Earth Sci.*, 16, 167-181.
- O'Brien, B.H. 1972. Geology of the area between North Arm, Holyrood Bay and Harbour Main. Unpublished B.Sc. thesis, Memorial University of Newfoundland, 77 pp.
- O'Brien, B.H. and O'Brien, S.J., 1990. Re-investigation and re-interpretation of the Silurian La Poile Group of southwestern Newfoundland. Current Research, Newfoundland Department of Mines and Energy, Geological Survey Branch, Report 90-1:305-316.

- O'Brien, B.H., O'Brien, S.J. and Dunning, G.R., 1991. Silurian cover, late Proterozoic-early Ordovician basement and the chronology of Silurian orogenesis in the Hermitage Flexure (Newfoundland Appalachians). *Am. J. Sci.*, 291, 760-799.
- O'Brien, S.J., 1987. Geology of the Eastport (west half) study site, Bonavista Bay, Newfoundland. *In* Current Research, Blackwood, R.F. and Gibbons, R.V. (eds). Newfoundland Department of Mines and Energy, Mineral Development Division, Report 87-1, 257-270.
- O'Brien, S.J., and Taylor, S.W., 1983. Geology of the Baine Harbour (1M/7) and Point Enragee (1M/6) study sites, southeast Newfoundland. Newfoundland Department of Mines and Energy, Mineral Development Division, Report 88-01, 193-206.
- O'Brien, S.J., Wardle, R.J. and King, A.F., 1983. The Avalon zone: A Pan-African terrane in the Appalachian orogen in Canada. *Geological Journal*, 18, 195-222.
- O'Brien, S.J. and Knight, I., 1988. The Avalonian geology of southwest Bonavista Bay: portion of the St. Brendan's (2C/13) and Eastport (2C/12) study sites. *In* Current Research. Newfoundland Department of Mines, Mineral Development Division, Report 88-1, 193-205.
- O'Brien, S.J., Strong, D.F. and King, A.F., 1990. The Avalon Zone type area: southeastern Newfoundland Appalachians. *In* Avalonian and Cadomian Geology of the North Atlantic. Strachan, R.A. and Taylor, G.K. (eds.), 166-194.
- O'Brien, S.J., O'Driscoll, C.F. and Tucker, R.D., 1992. A reinterpretation of the geology of parts of the Hermitage Peninsula, southwestern Avalon Zone, Newfoundland. *In* Current research. Newfoundland Department of Mines and Energy, Geological Survey Branch, Report 92-1; 185-194.
- O'Brien, S.J., O'Brien, B.H., Dunning, G.R. and Tucker, R.D., 1996. Late Neoproterozoic Avalonian and related peri-Gondwanan rocks of the Newfoundland Appalachians, *in* Nance, R.D. and Thompson, M.D., eds., *Avalonian and Related Peri-Gondwanan Terranes of the Circum-North Atlantic*. Boulder, Colorado, Geol. Soc. Am., Special Paper 304.
- O'Brien, S.J., King, A.F. and O'Driscoll, C.F. 1997. Late Neoproterozoic geology of the central Avalon Peninsula, Newfoundland, with an overview of mineralization and hydrothermal alteration. Newfoundland Department of Mines and Energy, Geological Survey Branch, Report 97-1, 257-282.
- O'Driscoll, C.F. and Strong, D.F., 1979. Geology and geochemistry of late Proterozoic volcanic and intrusive rocks of southwestern Avalon Zone in Newfoundland. *Precambrian Research*, 8, 19-48.
- Papezik, V.S., 1970. Petrochemistry of volcanic rocks of the Harbour Main Group, Avalon Peninsula, Newfoundland. *Can. J. Earth Sci.*, 7, 1485-1498.
- Papezik, V.S. and Barr, S.M., 1981. The Shelburne Dyke, an Early Mesozoic diabase dyke in Nova Scotia: mineralogy, chemistry and regional significance. *Can. J. Earth. Sci.* 18: 1346-1355.
- Poole, W.H., 1967. Tectonic evolution of the Appalachian region of Canada. *Geological Association of Canada Special Paper* 4, 9-51.

- Powell, C.McA., 1974. Timing of slaty cleavage during folding of Proterozoic rocks, northwest Tasmania. *Bull. Geol. Soc. Am.*, 85, 1045-1060.
- Ramsay, J.G. and Graham, R.H., 1970. Strain-variation in shear-belts. *Can. J. Earth Sci.*, 7, 786-813.
- Ramsay, J.G., Casey, M. and Kligfield, R. 1983. Role of shear in development of the Helvetic fold-thrust belt in Switzerland. *Geology*. 11, 439-442.
- Rast, N., Kennedy, M.J. and Blackwood, R.F., 1976. Comparison of some tectonostratigraphic zones in the Appalachians of Newfoundland and New Brunswick. *Can. J. Earth. Sci.*, 13, 868-875.
- Rast, N. and Skehan, S.J., J.W., 1983. The evolution of the Avalonian Plate. *In* M. Friedman and M.N. Toksoz (eds), *Continental Tectonics: Structure, Kinematics and Dynamics*, Tectonophysics, 100, 257-286.
- Roberts, W. and Williams, P.F., 1993. Evidence for early Mesozoic extensional faulting in Carboniferous rocks, southern New Brunswick, Canada. *Can. J. Earth Sci.* 30: 1324-1331.
- Rodgers, J., 1967. Chronology of tectonic movements in the Appalachian region of eastern North America, *Am. J. Sci.*, 265, 408-427.
- Rodgers, J., and Neale, E.R.W., 1963. Possible Taconic klippen in western Newfoundland. *Am. J. Sci.*, 261, 713-730.
- Rose, E.R., 1952. Torbay study site, Newfoundland. Geological Survey of Canada, Memoir 165, 64 pp.
- Sanderson, D.J., Anderson, J.R., Philips, W.E.A. and Hutton, D.H.W., 1980. Deformation studies in the Irish Caledonides. *J. Geol. Soc. London*, 137, 289-302.
- Sanderson, D.J., and Marchini, D., 1984. Transpression. *J. Struct. Geol.*, 6, 449-458.
- Smith, R. A., 1987. Evolution of the Portugal Cove area, northeastern Avalon Zone, Newfoundland. B.Sc. Honours Thesis. Memorial University of Newfoundland, St. John's, Newfoundland. 113 pp.
- Smith, S.A. and Hiscott, R.N., 1984. Latest Proterozoic to Early Cambrian basin evolution, Fortune Bay, Newfoundland: Fault-bounded basin to platform. *Can. J. Earth Sci.*, 21:1379-1392.
- Soper, N.J., 1986. Geometry of transecting, anastomosing solution cleavage in transpression zones. *J. Struct. Geol.*, 8, 937-940.
- Soper, N.J. and Hutton, D.H.W., 1984. Late Caledonian sinistral displacements in Britain: implication of a three-plate collision model. *Tectonics*, 3, 781-794.
- Stringer, P. and Treagus, J.E., 1980. Non-axial planar  $S_1$  cleavage in Hawick Rocks of the Galloway area, Southern Uplands, Scotland. *J. Struct. Geol.*, 2, 317-331.
- Strong, D.F., O'Brien, S.J., Taylor, S.W., Strong, P.G. and Wilton, D.H., 1978a. Geology of the Marystown and St. Lawrence study sites, Newfoundland. Mineral Development Division, Newfoundland Department of Mines and Energy, 81 pp.

- Strong, D.F., O'Brien, S.J., Taylor, S.W., Strong, P.G. and Wilton, D.H., 1978b. Aborted Proterozoic rifting in eastern Newfoundland. *Can. J. Earth Sci.*, 15, 117-131.
- Stubley, M.P., 1989. Fault and kink-band relationships at Mystery Bay, Australia. *Tectonophysics*, 158, 75-92.
- Stubley, M.P., 1990. The geometry and kinematics of a suite of conjugate kink bands, southeastern Australia. *J. Struct. Geol.*, 12, 1019-1031.
- Suppe, J., Chou, G. T. and Hook, S. C., 1992. Rates of folding and faulting determined from growth strata. *In Thrust Tectonics* (editor, McClay, K.R.). Chapman and Hall, London, 105-121.
- Sylvester, A.G., 1988. Strike-slip faults. *Geol. Soc. Am. Bull.*, 100, 1666-1703.
- Treagus, J.E. and Treagus, S.H., 1981. Folds and the strain ellipsoid: a general model. *J. Struct. Geol.* 3, 1-17.
- van der Pluijm, B., 1990. Synchroneity of folding and cross-cutting cleavage in the Newfoundland Appalachians. *J. Struct. Geol.*, 12, 1073-1076.
- van der Voo, R., French, A.N. and French, R.B., 1979. A paleomagnetic pole position from the unfolded upper Devonian Catskill red beds, and its tectonic implications. *Geology*, 7, 345-348.
- van Everdingen, D., 1992. QuickPlot v.3 for Windows: A program for plotting and manipulation of orientation data.
- Wilcox, R.E., Harding, T.P. and Seely, D.R., 1973. Basic wrench tectonics. *Am. Assoc. Pet. Geol. Bull.*, 57, 74-96.
- Williams, H. 1976. Tectonostratigraphic subdivisions of the Appalachian Orogen. *Geol. Soc. Am.*, Abstracts with Programs, vol. 8, No. 2.
- Williams, H., 1978. Tectonic lithofacies map of the Appalachian Orogen. Memorial University Map No. 1, Dept. of Geology, Memorial University of Newfoundland, Canada.
- Williams, H., 1993. Acadian Orogeny in Newfoundland. *In The Acadian Orogeny: Recent Studies in New England, Maritime Canada, and the Autochthonous Foreland*: Boulder, Colorado, *Geol. Soc. Am. Special Paper 275*, Roy, D.C. and Skehan, J.W. (eds).
- Williams, H. and King, A.F., 1979. Trepassey study site, Newfoundland. *Geological Survey of Canada, Memoir 389*, 24 pp.
- Williams, H. and Hatcher, R.D., 1982. Suspect terranes and accretionary history of the Appalachian Orogen. *Geology*, v. 10, 530-536.
- Williams, H., O'Brien, S.J., King, A.F. and Anderson, M.M., 1995. Newfoundland (Avalon Zone). *In Chapter 3 of Geology of the Appalachian-Caledonian Orogen in Canada and Greenland*, Williams, H. (ed.), Geological Survey of Canada, *Geology of Canada*, no. 6, 223-237.
- Williams, P.F. and Price, G.P., 1990. Origin of kink bands and shear-band cleavage in shear zones: an experimental study. *J. Struct. Geol.*, 12, 145-164.

- Wyn, R., and Williams, P.F., 1993. Evidence for early Mesozoic extensional faulting in Carboniferous rocks, southern New Brunswick, Canada. *Can. J Earth Sci.*, 30, 1324-1331.
- Woodcock, N.H., 1990. Transpressive Acadian deformation across the Central Wales Lineament. *J. Struct. Geol.*, 12, 329-337.
- Woodcock, N.H., Awan, M.A., Johnson, T.E., Mackie, A.H. and Smith, R.D.A., 1988. Acadian tectonics in Wales during Avalonia/Laurentia convergence. *Tectonics*, 7, 483-495.
- Yang, Q. and Nielsen, K. C., 1995. Rotation of fold-hinge lines associated with simple shear during southerly directed thrusting, Quachita Mountains, southeastern Oklahoma. *J. Struct. Geol.*, 6, 803-817.
- Younce, G.B., 1970. Structural geology and stratigraphy of the Bonavista Bay region, Newfoundland. Ph.D. Thesis. Cornell University, Ithica, NY. 188 pp.

